Spin gap in doped ladder systems

Von der Fakultät für Mathematik und Physik
der Universität Stuttgart
zur Erlangung der Würde eines
Doktors der Naturwissenschaften (Dr. rer. nat.)
genehmigte Abhandlung

Vorgelegt von
Lorenzo Campos Venuti
aus Bologna (Italien)

Hauptberichter:	Prof. Dr. Alejandro Muramatsu
Mitberichter:	Prof. Dr. Günter Mahler
Tag der mündlichen Prüfung:	15. Dezember 2003

Institut für Theoretische Physik der Universität Stuttgart
2004

Contents

4

Abstract

A proper theoretical description of doped antiferromagnets is until now an unresolved issue. In this work we study chain and ladder systems, and in particularly we focus on the physically most interesting two leg ladder.

Our starting point is the Spin Fermion model in which an antiferromagnetic background of localized spins interacts with mobile holes via a rotation invariant Kondo-like term. The interesting region of the phase diagram is that close to the Mott-insulator transition where the doping δ is zero. At zero doping in fact the system is an insulator and the spins organize themselves in a spin liquid, a rotational invariant state characterized by a finite correlation length and an energy gap (a spin gap) above the ground state. Such a state is also the ground state of a field theory, the non linear sigma model (NLσM) which is recognized as the low energy effective theory for antiferromagnetic spin ladder.

The first question we answer is how such a spin state evolves as one moves off from the Mott phase by increasing the doping. Integrating out the fermions in our model we obtain an effective theory for the spins which we are able to evaluate in the continuum limit. The effective theory is again a NLσM with coupling constants which depend on the concentration of dopant holes. In contrast to existing mean field calculation our theory predicts a lowering of the spin gap with doping and a consequent increase in the correlation length. Indeed a lowering of the spin gap due to doping is also observed in numerical simulation and on NMR experiments on $Sr_{14-x}Ca_xCu_{24}O_{41}$ with which we obtain very good agreement.

Secondly we concentrated on the behavior of the fermions. The general

paradigm of interacting fermions in one dimension is that of the Luttinger Liquid characterized by bosonic excitations and spin charge separation. By generalizing our approach we are able to access the one particle fermion propagator as a quantity averaged over the NLσM which controls the spin background. We see that in the limit of zero doping the quasiparticle weight Z is non-zero in a neighborhood of the Fermi energy. This in turn implies that the Luttinger liquid parameter K_ρ goes to one as the doping δ goes to zero as was first argued by Schulz. Our stronger result allows us to assert that in the very low doping regime the fermions constitute a Fermi liquid.

Introduction

In the late 60's, thanks to the successes of Landau's Fermi liquid (FL) theory (dated 1956) [1, 2, 3] and BCS theory of superconductivity (dated 1957) [4, 5], most researchers in the field of solid state physics thought that their discipline was a very settled one and a very general framework was given once and for all. The situation changed radically during the 80's with the discovery of high temperature superconductivity (1986) [6], heavy fermions (80's) [7] and quantum Hall effect (early 80's) [8, 9]. The common feature of all these systems is the constrained motion of the electrons as a result of restricted dimensionality and/or the strong inter-electron interactions. These constraints induce complicated correlations in the motion of the electrons, and hence the term which is used to describe them collectively: 'Strongly Correlated Electron Systems'.

Emblematic of the interplay between dimensionality and correlation is the different degree of success experienced by Landau's FL theory with decreasing dimensionality. In the Fermi liquid theory the low energy spectrum of the fully interacting many body system, is in one to one correspondence with the (low energy part of) the spectrum of the free Fermi gas. Hence, in terms of the quasiparticles –the quanta of collective excitations of the many body system– the Fermi liquid is essentially a free theory. Although this theory was originally formulated to provide a description of the energy levels of ^{3}He, it was later extended to treat electrons in a metal and nuclear matter and basically it applies to most metals in three spatial dimension –and at low temperature–. In two dimensions the anomalous characteristics of the normal (i.e. not superconducting) state of the copper-oxide superconductors (see

e.g. [10]), have motivated many researchers to look for theories alternative to the FL one. Still the Fermi liquid state is quite robust in two dimensions and to obtain a breakdown of it one must resort to particular situations like the presence of (unscreened) long range forces, singularities in the free propagator or very strong coupling [11]. In these cases one then speaks of non-Fermi liquid (NFL) or marginal-Fermi liquid (MFL), a particular case of NFL.

Instead the situation in one dimension is much more clear and it is now well known that a breakdown of the FL picture in one dimension is the rule rather then the exception. Quantum fluctuation are so strong in 1D that a whatever small interaction in a Fermi (-Dirac) gas, drives the system to a completely new state, the Luttinger liquid (LL) (see e.g. the original paper [12] and the review [13]). This novel[1] state of matter is characterized by the absence of quasiparticle excitations manifested as a vanishing of the renormalization constant Z, and a separation of the charge and spin degrees of freedom. The Luttinger liquid only support bosonic excitations with either charge (charge-density waves) or spin (spin-density waves).

Thus it becomes clear that 1D systems represent a "playground" for the study of strongly correlated systems, where many concepts (like the breakdown of the FL) can be developed and/or tested. In fact in 1D more theoretical methods are available or more powerful than in higher dimensionality. To cite only the most important, exact Bethe ansatz results are available for some models and/or for particular couplings, bosonization techniques with the help of which the concept of LL has been set on a clear grounds, and numerical simulations which are superior in low dimension in that larger lattices can be studied.

The study of low dimensional systems is not only interesting for theorists. Chemists have long been aware that in many organic compounds anisotropy[2] can be as large as 10^3 so that these systems can be regarded as quasi one

[1] Tomonaga, already in 1950, was the first to identify bosonic excitations in 1D systems [14].

[2] Anisotropy can be characterized by the ratio of the conductivities measured parallel and perpendicular to the chain direction.

dimensional for most practical purposes (TTF-TCNQ is one of the most famous member of this group, see e.g. [15]). Later, also triggered by the appearance of an antiferromagnetic state in the phase diagram of the high-T_c cuprates, and by a theoretical conjecture made by Haldane [16], quantum spin chains have been synthesized and studied. In these materials, localized ions act as fixed spins which can interact via a variety of exchange terms. The original form of Haldane's conjecture [16] (1983), asserts that antiferromagnetic spin chains behave differently according to whether the spin per site S is integer or half-odd integer. Chains with half-odd-integer values of the spin fall in the universality class of the spin-1/2 chain, have arbitrarily low energy excitations and present spin-spin correlations which decay algebraically with the distance. On the contrary chains with integer spin present a ground state separated by a gap from the elementary excitations and the correlations fall off exponentially. Ten years later a similar conjecture was put forward by Rice *et al.* [17] in the study of "ladders" system (a collection of M interacting chains is commonly called, after the $M = 2$ case, an M-leg ladder). A spin S, M-leg ladder is in the universality class of the spin-1/2 or the spin-1 chain according to whether the product SM is an half-odd integer or an integer. Besides the numerous numerical simulations which confirmed this "generalized Haldane's conjecture" [18, 19, 20, 21, 22], the motivation provided by the theorists triggered an enormous effort on the experimental front to synthesize chain and ladder materials searching for the predictions made by the theorists, namely the presence of spin gap features in spin-1 chains [23, 24] and spin-1/2 two-leg ladders [25, 26, 27, 28]. Hence the conjecture have been "proved" also on experimental basis. The joint result of these efforts is that the physics of pure spin ladder and chain systems is under reasonable theoretical control.

It is then natural to ask how carrier doping affects these low dimensional spin states. Starting from the mid 90's experimentalists managed to synthesize chains and ladders based on the same Cu-O unit of the high-T_c superconductors [27]. In some of these compounds –namely $La_{1-x}Sr_xCuO_{2.5}$ and $Sr_{14-x}Ca_xCu_{24}O_{41}$– the number of mobile holes can be varied through doping. This allows to study a situation analogous to that of the high-T_c

superconductors, in the restricted dimensionality of chains or ladders. It is hoped that the study of doped Cu-O ladders can provide insight for the understanding of the more complex two-dimensional high-T_c materials. Indeed some similarities have been observed between one and two dimensional system. The most striking fact is surely the achievement of superconductivity in a (two-leg) ladder compound under high pressure [29]. On the other hand the study of one dimensional electron systems, has unveiled quite challenging and interesting physics that adds to the rich behavior of transition-metal-oxides.

A variety of theoretical methods are available for the study of strongly correlated systems. In weak or strong coupling perturbative treatments, roughly speaking, the interaction energy is assumed to be small, respectively, large, with respect to the kinetic energy. Unfortunately in many physical cases, the interaction energy is more or less of the same order of the kinetic energy and a truly small parameter is lacking. Mean-field approaches are, in general, more accurate in large space dimension and for long-range interaction. Bosonization, as we have seen, is very powerful in 1D but is better suited to treat, in weak coupling, systems close to that with gapless excitations –which, as we will see, will not belong to our situation in most cases –. Numerical methods –such as exact diagonalization (ED), density matrix renormalization group (DMRG), and quantum Monte Carlo (QMC)– are also very effective in one dimension, and have indeed provided valuable insight in the study of 1D strongly correlated systems. Nonetheless, besides being limited to finite systems, which means that extrapolation to the thermodynamic limit is often problematic, the numerical approach does not provide, generally, a unifying picture which only analytical approaches can give.

A powerful tool for the quantitative investigation of microscopic models is provided by the study of effective continuum theories. If one is able to single out the most relevant low-energy configurations, the lattice spacing can indeed be considered a small parameter, and a continuum limit effective theory – a Quantum Field Theory (QFT) – can be extracted from the microscopic lattice Hamiltonian. This approach has two major benefits which are in fact interrelated: on the one hand the continuum model is often simpler than

the starting Hamiltonian. This is largely due to the fact that, based on the achievements of Renormalization Group Theory, only relevant and marginal operators need to be accounted for in the continuum theory. This implies that the number of possible QFTs for a given microscopic model, is "small" –at least in the renormalizable case– and largely constrained by symmetries. On the other hand such an approach permits to find universality in different physical phenomena; different model Hamiltonians may have the same low energy effective theory, and hence share the same – low energy – physics. A number of quantum field theories have become increasingly important in solid state physics. To cite only some examples: the free bosonic Gaussian model in (1+1) dimensions, which, via bosonization is related to one dimensional interacting Fermi systems. The sine Gordon model, which is related to the XY model of magnetism, two dimensional classical plasma and describes the Berezin-Kosterlitz-Thouless transition. A QFT with which we will deal directly is the Non Linear Sigma Model (NLσM). Although the NLσM was first studied in high energy physics as a toy model of Quantum Chromodynamics, it is now one of the most important theories in condensed matter as it provides a unifying picture for quantum antiferromagnets [16, 30, 31, 32].

To sum up, in this short introduction we tried to motivate the interest for (a) one dimensional systems and in particular for (b) for 1D doped antiferromagnet. At the same time we introduced our approach which rotates around the effective field theory for antiferromagnets, the non linear sigma model. In this work we take advantage of the achievements of this theory and/or extend it to the more complex and interesting doped case.

In the first chapter of this work we will give motivations for the different microscopic models used to describe doped antiferromagnets in both one and two dimension. Experimental results confirmed that the three band Hubbard model correctly describes the relevant degrees of freedom of materials formed by the Copper-Oxygen plaquette. The range of parameters which Quantum Monte Carlo simulations and experiments provided for this model, gave rise to the possibility to map the model to a simpler one, the Spin Fermion model. A further simplification lead to the so called $t - J$ model. Although simpler

than the Spin Fermion model in that it contains a smaller number of degrees of freedom, the $t-J$ model presents great difficulty from the analytical point of view – mainly because of the constraint that double occupancy is forbidden at any site. For this reason our starting point will be the Spin Fermion model or variants of it. Finally we comment on the all important undoped case. The non linear sigma model in (D+1) dimension is recognised as the low energy effective action of the D dimensional antiferromagnetic Heisenberg model. The different behavior of spin S, M-leg ladders with SM integer or half-odd-integer is to be ascribed to the presence, in the effective action of the model, of an additional term, normally referred to as the topological term.

In the second chapter we derive a continuum field theory for doped antiferromagnets both for chains and for ladders with arbitrary number of rods. A similar field theory in (2+1) dimensions was presented in the past on pure phenomenological grounds, as a possible description for high-T_c superconductors. Here we show that such a Lagrangian, or better an extension of it, naturally shows up in the continuum, low-energy limit of a microscopic model for cuprates chains and ladders.

In chapter three we focus on the case of a two leg ladder. Integrating out the charge degrees of freedom at first we obtain an action which describes the dynamics of the spins under a finite hole concentration. This action can be evaluated explicitly in the continuum limit and is seen to be a non linear sigma model with coupling constants which depend on the concentration of the dopant holes. As a number of numerical simulations [33, 34] and experiments [35, 36, 37, 38] confirmed, the spin liquid state which characterize the undoped ladder, is not destroyed by a minimal concentration of holes. Our approach enables us to calculate explicitly the way the spin liquid parameters evolve with doping. We obtain good agreement with existing measurements on $Sr_{14-x}A_xCu_{24}O_{41}$.

In chapter four we extend the techniques introduces in chapter three, in order to obtain the one particle propagator for the holes. Inserting current coupled to the fermions, thereby promoting the partition function to generating

functional, the one particle propagator is formally obtained through differentiation. An expansion for the vertex function is found in term of a small parameter, the lattice constant. Stopping at first order we obtain an explicit expression for the propagator which is consistent with a free fermionic description for very small momenta and frequency.

Finally we summarize our conclusions.

Chapter 1

Models for Copper-Oxide materials

In the high critical-temperature (high-T_c) superconductors the relevant physics takes place in planes which consist of a lattice formed by Copper and Oxygen atoms[1]. Since the first times of the discovery of high-T_c superconductivity a lot of effort was put in finding the most appropriate and simple model. Soon a microscopical model for the Cu-O planes was proposed – the $d-p$, Emery, three-band Hubbard model [41] – and analysis were carried on. Quantum Monte Carlo simulations [42, 43, 44, 45] and experiments [46] have indicated that the physically relevant parameter set for the three-band Hubbard model lies in the strong coupling regime. This fact gave rise to the possibility of mapping the Hamiltonian to a simpler one, the Spin-Fermion (SF) model [47, 48]. Here "simpler" means basically that the dimension of the Hilbert space goes from 64^N to 32^N where N is the number of Copper sites. A further simplification was proposed by Zhang and Rice [49] which leads to the so called $t-J$ model and brings the dimension of the Hilbert space down to 3^N.[2] Both the Spin Fermion and the $t-J$ model reduce, at zero doping, to

[1] An exception is the surface compound WO_3 doped with Na which exhibits a $T_c \simeq 90\,K$ i.e. in the range of the cuprates High Tc compounds [39, 40], but does not contain the CuO planes.

[2] This brief summary does not reflect completely the historical developments. Anderson had already proposed a one band Hubbard model [50, 51] to explain high-T_c before Zhang

an antiferromagnetic Heisenberg model and hence posses antiferromagnetic correlation at zero temperature (see e. g. [52, 53]). This is comforting as a flood of experimental data on undoped compounds (such like La_2CuO_4 or $YBa_2Cu_3O_6$) has found evidence of two-dimensional antiferromagnetic correlation [54, 55]. Nonetheless the antiferromagnetic phase remains the only region of the phase diagram of the high-T_c superconductors which has been explained in terms of a microscopic model. Adding holes to the system we come to the situation where an antiferromagnetic spin background interacts with mobile charge carriers. This is why high-T_c superconductors are sometimes termed as doped antiferromagnets. Is precisely the doped region of the phase diagram which remain largely unclear.

In more recent times there has been an increasing interest in the study of the problem of a doped antiferromagnet in one dimensional systems and more specifically in chains and collections of interacting chains normally termed ladders (a system of N interacting chains is commonly called, after the $N = 2$ case, an N-leg ladder). There are a number of reasons that have triggered the present enthusiasm on the subject. First one dimensional systems provides a "playground" for studies of high-T_c superconductors. Indeed the first theoretical investigations showed that cuprates ladders posses at least two important similarities with their two-dimensional counterparts. One is the clear evidence of a spin gap in undoped two-leg ladders[3] [21]. Another one is the possibility –revealed first by computational techniques [56]– that upon doping the ground state becomes dominated by superconducting correlations. On the other hand, the motivations provided by the theorists triggered an enormous effort on the experimental side to synthesize ladder materials, searching for the two main predictions made by the theorists, namely the existence of a spin gap and superconductivity. While many experiments on two-leg ladder materials revealed undoubtedly the presence of

and Rice succeeded in their mapping to the $t-J$ model. Nowadays it is generally accepted that both a one band Hubbard model and a $t-J$ model minimally incorporate the essential ingredients to explain high-T_c. An explanation has not yet been found though.

[3] In Chapter three we will explicitly address –and answer– the question of the behavior of the spin gap with doping. We reference the reader to that chapter for a discussion on this point.

a spin gap [35, 36, 37, 57, 58, 38], the observation of superconductivity found in the ladder materials $Sr_{14-x}Ca_xCu_{24}O_{41}$ [59] is more controversial, as we will discuss in section 1.1.2.

The $p-d$, three band Hubbard model used to describe the two dimensional high-T_c Copper-Oxides apply equally well to chain and ladder materials which are based on the same Cu-O unity. Given the similarity in the Cu-O-Cu bonds on ladders and planes, the actual coupling constants of the model are very similar as in the two-dimensional case and a reduction to a Spin-Fermion model is possible also for ladders. Similarly to the high-T_c case the SF model can be further reduced to a $t-J$ model and we will show explicitly in section 1.2.3 where small modifications are needed.

Undoped ladders, in which only the spin degrees of freedom remain, are described by a Heisenberg antiferromagnet on the appropriate lattice. Here an interesting phenomenon occurs. The crossover from the chain to the plane is not at all smooth but shows a strong even-odd effect. Ladders with an odd number of legs fall in the universality class of the single chain. Excitations with arbitrarily small energy exist above the ground state and the equal time spin correlations decay to zero only algebraically (a phenomenon called quasi long range order -QLRO-). On the other hand, ladders with an even number of legs fall in a different universality class. The ground states is in this case a spin liquid: a rotational invariant state separated by a finite gap Δ from the first excitations with spin-spin correlation which decay exponentially with the distance. Hence a correlation length ξ of the order of the inverse gap $\xi \sim 1/\Delta$ can be defined.

1.1 Doped antiferromagnetic materials

1.1.1 The two dimensional high-T_c superconductors

In figure 1.1 (a) and (b) we can see the structure of typical high-T_c superconductors (HTcSC): in (a) $La_{2-x}Sr_xCuO_4$ (x is the doping fraction) the first discovered HTcSC [6] which has its highest critical temperature $T_c \simeq 39\,K$

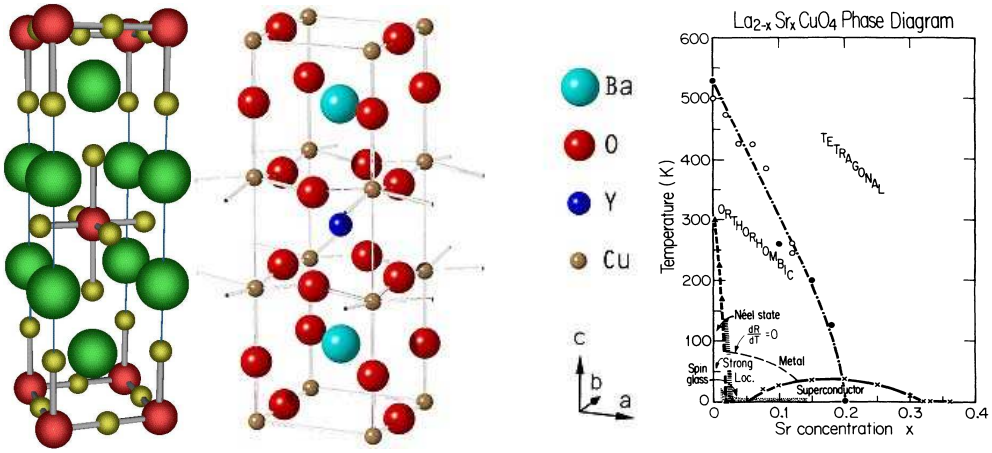

(a) (b) (c)

Figure 1.1: (a) Structure of $(La, Sr)_2\, CuO_4$. Cu atoms are in red and O atoms in yellow, the green dots represent weather La or Sr. In (b) schematic structure of YBCO. (c) Phase diagram of $La_{2-x}Sr_xCuO_4$ taken from [60].

at $x = 0.15$. In (b) $YBa_2Cu_3O_{6+x}$ (YBCO) with a T_c as high as $T_c \simeq 92\,K$ at $x = 1$. Thanks to a critical temperature higher then the ebullition point of nitrogen $(77\,K)$, its non-toxicity, and the relative simplicity of its preparation, YBCO has already found applications in the industry. As can also be inferred from fig. 1.1 (a) and (b), in the high-T_c compounds the CuO_2 planes are organized in the lattice of figure 1.2. In the crystal Copper is in a configuration Cu: $[Ar]\,(3d)^9$ and the Oxygen is O: $[He]\,(2s)^2\,(2p)^6$. This means that the oxygen is in a O^{2-} configuration which completes its p-orbitals, and Copper is Cu^{2+} and since an electron is missing to complete the $(3d)^{10}$ orbitals, on the copper sites sits effectively a hole with spin 1/2. The phase diagram of $La_{2-x}Sr_xCuO_4$ is shown in figure 1.1 (c) and is typical of all the cuprates superconductors. Neutron scattering experiments have shown that in absence of doping, the parent compounds of the high-T_c cuprates, such as La_2CuO_4 or $YBa_2Cu_3O_6$, are insulators with three dimensional antiferromagnetic long-range order below Néel temperatures of $T_N \approx 200 - 500\,\mathrm{K}$ [61, 62, 63]. The magnetic moments are associated with the Cu^{2+} ions, which interact via a

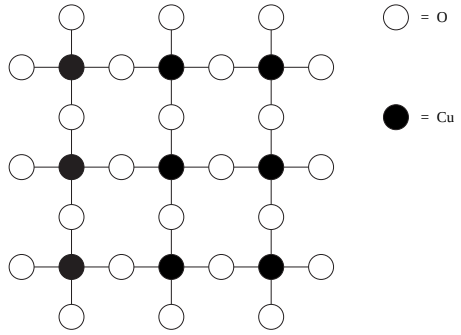

Figure 1.2: CuO_2 lattice presents in the high-T_c superconductors.

nearest-neighbor superexchange coupling mediated by the oxygen ions. The existence of a weak antiferromagnetic interplane coupling [64, 65] is responsible for the observation of a finite Néel temperature. As is well known, in a purely two dimensional system a continuous symmetry cannot be broken at a finite temperature [66]. Upon doping, the long-range antiferromagnetic order is destroyed and ultimately superconductivity is stabilized below the critical temperature as in figure 1.1 (c). The "normal" state (i.e. not superconducting) region of the phase diagram also exhibits a number of unusual proprieties (for a review see [10]). To cite only the most striking, first, at optimal doping (when the critical temperature is highest), the resistivity $\rho(T)$ is linear in temperature over a wide temperature range from just above T_c to nearly 1000 K [67]. This is in contrast with conventional low-temperature superconductors where it is experimentally observed that $\rho \approx a + bT^5$, at low T (but larger than T_c) [68]. Second, and more important for us, in the normal state, a spin gap in the energy spectrum has been observed, namely it costs a finite amount of energy to create a spin excitation above the ground state [69]. Actually the name "pseudogap" is more appropriate since neutron scattering experiments reveal, in fact, low-energy spin excitation, although with a very low spectral wight [70, 65]. As we will see, a number of theoretical work on undoped antiferromagnetic spin ladders have shown unambiguously that these systems possess a real spin gap. Such a similarity with the high-T_c superconductors, among others, certainly greatly stimulated the study of ladders material, in the hope of understanding the more complex 2D systems.

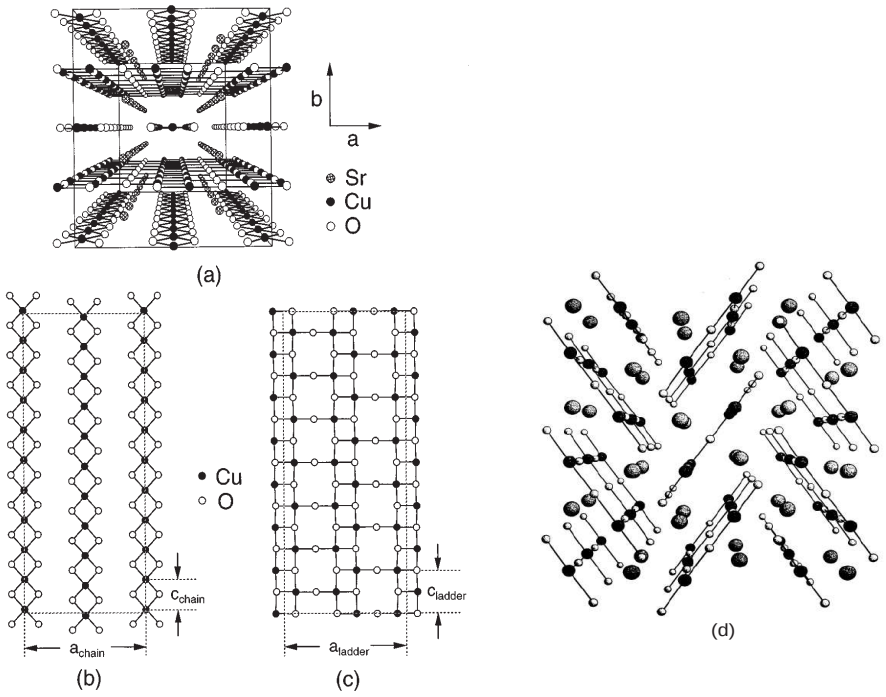

Figure 1.3: Structure of $Sr_{14-x}Ca_xCu_{24}O_{41}$(a) which contains both chains (b) and two-leg ladders (c). In (d) structure of $LaCuO_{2.5}$ along the c axis, which has also chains and ladders. Large, medium and small balls represent La, Cu, O atoms respectively.

1.1.2 One dimensional chains and ladders

Experimentalist have long tried to synthesize ladder system based on the same Cu-O cell present in the high-T_c superconductors (figure 1.4). In 1994 Azuma et al. [27] reported the preparation of a copper-oxide $S = 1/2$ ladder whose chemical composition is $SrCu_2O_3$. Unfortunately in this compound – which is well described by an antiferromagnetic Heisenberg model – carriers remain localized after substitution of Sr by La. Instead doping is possible in two other compounds which contain ladders, $La_{1-x}Sr_xCuO_{2.5}$ and $Sr_{14-x}Ca_xCu_{24}O_{41}$ (see fig. 1.3 (c) and (d)). This latter material has moreover attracted much attention as superconductivity at a pressure of 3 Gpa was discovered in 1996 by Uehara et al. [29] at a doping concentration $x = 13.6$. Later superconductivity was found at $x = 11.5$ and $x = 12$. On

top of that Mayaffre et al. [59] on the basis of NMR experiment, argued that the spin gap collapse to zero as high pressure of 3.1 Gpa (31 Kilobar) is applied (at $x = 12$). Hence, according to these authors, since the spin gap goes to zero as superconductivity is stabilized, they argue that the ladder is responsible for the superconducting phase. This is in analogy to what happens in the 2D high-T_c materials, where the pseudogap also disappears when superconductivity is stabilized. This conclusions are still under debate, as other experiments [71] at a smaller pressure of 1.7 Gpa revealed a robust spin gap very similar to that measured at ambient pressure. It is difficult to understand how this gap disappear so abruptly as pressure goes up to 3 Gpa as claimed by Mayaffre et al. [59]. See also the recent ref. [72] for a discussion on this point.

$Sr_{14-x}Ca_xCu_{24}O_{41}$ (also known as [14-24-41] or "phone number" compound) contains 1D CuO_2 chains, (Sr,Ca) layers and two leg Cu_2O_3 ladder as shown in figure 1.3 (a-c). The nominal valence of Cu is +2.25 which arises from [2×41 (Oxygens) - 2×14 (Sr)]/ 24(Cu) instead of just +2.0. This means that holes are already doped into the structure leading to a so called "self-doped" system.

1.2 Microscopic models for doped antiferromagnets

1.2.1 The three-band Hubbard model

Less than one year after the first high-T_c compound has been synthesized, Emery [41] proposed a model for the Copper-Oxide planes which incorporates minimally the relevant degrees of freedom. Although it was originally proposed for the planes in the high-T_c superconductors, it equally applies to any geometry based one the Copper-Oxide cell of figure 1.4 such as the chains or ladders that we discussed in paragraph 1.1.2.

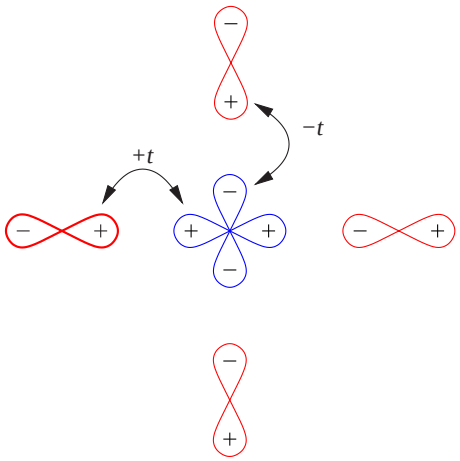

Figure 1.4: Schematic picture of Cu-O unit and the hybridization between copper and oxygen atoms. In red are depicted the $\left(2p^5\right)$ orbital for the O hole and in blue the $(3d)^9$ one for the Cu hole. The signs + and - represent the phase of the orbitals, t is the wavefunctions overlap indicated as t_{pd} in the text.

The Emery, $d-p$, three band Hubbard model is defined as following:

$$\begin{aligned} H_{dp} &= \epsilon_d \sum_{i,\sigma} d^\dagger_{i,\sigma} d_{i,\sigma} + \epsilon_p \sum_{l,\sigma} p^\dagger_{l,\sigma} p_{l,\sigma} \\ &\quad + U \sum_i d^\dagger_{i,\uparrow} d_{i,\uparrow} d^\dagger_{i,\downarrow} d_{i,\downarrow} + H' \end{aligned} \tag{1.1}$$

where the hybridization term is

$$H' = \sum_{i,\sigma} \sum_{l \in \{i\}} V_{i,l} \left(d^\dagger_{i,\sigma} p_{l,\sigma} + \text{h.c.} \right), \tag{1.2}$$

here the sum over l runs over the four O sites around a given Cu site i. In Eq. (1.1) the vacuum is defined as filled Cu $(3d)^{10}$ and O $(2p)^6$ states. The operators $d^\dagger_{i,\sigma}$ crate Cu $(3d_{x^2-y^2})$ holes at site i, and $p^\dagger_{l,\sigma}$ create O $(2p_x, 2p_y)$ holes at site l. U is a positive constant and correspond to the (screened) Coulomb repulsion between holes when they are in the same orbital. The hybridization matrix V_{il} is assumed to be proportional to the wave-function overlap of the Cu and O holes. Because of the form and relative phases of

the $p_{x,y}$ and $d_{x^2-y^2}$ orbitals (see figure 1.4) one can write

$$V_{i,l} = (-1)^{\alpha_{i,l}}\, t_{pd} \tag{1.3}$$

where t_{pd} is the amplitude of the hybridization, and

$$\alpha_{i,l} = \begin{cases} 2 & \text{if} \quad l = i - \frac{a}{2}\hat{x} \text{ or } l = i - \frac{a}{2}\hat{y} \\ 1 & \text{if} \quad l = i + \frac{a}{2}\hat{x} \text{ or } l = i + \frac{a}{2}\hat{y} \end{cases} \tag{1.4}$$

and a is the Cu-Cu distance.

In undoped high-T_c materials the picture where all the Cu sites are singly occupied and all the O sites are empty, is consistent with Hamiltonian (1.1) if $\Delta \equiv \epsilon_p - \epsilon_d > 0$ and $U > 0$; at least in the atomic limit where the hybridization term $V_{i,l}$ is zero. Upon doping, an important question which arise is whether the holes will go on the copper or on the oxygen sites. In the first case, the hybridization term may be included by eliminating the O sites to give an effective Hamiltonian for the motion of the Cu sites alone. This is a one band Hubbard model, i.e. there is only one site per unit cell. In the second case, Zhang and Rice [49], as we will see in section 1.2.3, have shown that a reduction to single band model is also possible.

Indeed electron-energy-loss experiments [46, 73] have shown that the second possibility is realized in the 2D cuprates and the great majority of the holes sit on the oxygen sites. This is consistent with band structure calculations [42] and more recent Quantum Monte Carlo simulation compared with experiments [44, 45]. The estimated actual values of the parameter in Hamiltonian (1.1) from [43, 44, 45] together with the value $t_{pd} = 1.3$ eV obtained in [42] give:

$$U \;=\; 7.8, \;\; \epsilon_p - \epsilon_d \equiv \Delta = 5.2, \;\; t_{pd} = 1.3 \quad \text{(eV)}. \tag{1.5}$$

In fact, according to (1.1) again in the limit where the hybridization is zero, holes will sit on O sites when $\Delta < U$ and on copper sites otherwise. For a comparison between prediction for these parameters obtained by different

groups, see [74].

In the case of the ladders present in [12-24-41] the situation is more complicated as this compound contains also chains and experiments must be able to separate the contribution of the ladders from those of the chains. Moreover, as we have seen, holes are already present in the undoped compound. However it has been shown in [75] and [76] that isovalent substitution of Sr by Ca (both in a 2+ valence state) result in a reorganization of carriers and holes are transferred from the chains to the ladders increasing the conductivity of the latter. More recently Nücker et al. [77] have somehow mitigated the previous results, but they also agree that the number of holes in the ladders increase with doping, although in a less pronounced way. Motivated by these experiments we will consider the ladders present in [12-24-41] as a realization of a doped antiferromagnet.

As the elementary cell for the cuprates chains and ladders is very similar (when not exactly the same) to that of the 2D high-T_c material, the three band Hubbard model Eq. (1.1) is also a valid model in these cases. The actual value of the constants is expected to be similar to that for the 2D material Eq (1.5) and hence a reduction to a spin fermion or $t-J$ model is also possible for ladders.

1.2.2 Mapping to a Spin Fermion model

As we have seen, in the doped cuprates compounds (ladders or 2D planes), the Copper are always singly occupied. Moreover the hybridization term t_{pd} is clearly the smallest parameter of the theory (cf. Eq. (1.5)). It is then reasonable to apply the formalism of degenerate perturbation theory with a model space formed by the singly occupied copper sites, and the full fermionic Hilbert space for the oxygen sites. Using a Schrieffer-Wolff transformation Zaanen and Oleś [48] calculated the effective Hamiltonian in this subspace with contribution up to fourth order in the hybridization t_{pd}. The result is the so called spin-fermion (SF) Hamiltonian:

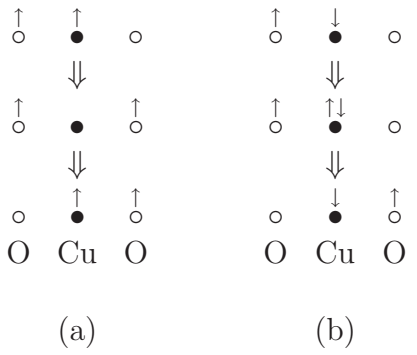

(a) (b)

Figure 1.5: Cartoons of the two channels involved in second order processes. In (a) the energy denominator is Δ, in (b) is $U-\Delta$. Only the carrier-spin conserving processes are indicated.

$$
\begin{aligned}
H_{SF} &= \tilde{t}\sum_{ijj',\sigma} V_{ij}V_{ij'}p^{\dagger}_{j,\sigma}p_{j',\sigma} + J_K\sum_i \mathbf{S}_i\cdot\sum_{jj',\alpha,\beta} V_{ij}V_{ij'}p^{\dagger}_{j,\alpha}\boldsymbol{\sigma}_{\alpha,\beta}p_{j',\beta} \\
&\quad + \frac{J_H}{2}\sum_{\langle i,i'\rangle}\mathbf{S}_i\cdot\mathbf{S}_{i'} \qquad (1.6)
\end{aligned}
$$

where the constants are given by [48]

$$\tilde{t} = \frac{1}{2}\left(\frac{1}{\Delta}-\frac{1}{U-\Delta}\right)t_{pd}^2 \qquad (1.7)$$

$$J_K = \left(\frac{1}{\Delta}+\frac{1}{U-\Delta}\right)t_{pd}^2 \qquad (1.8)$$

$$J_H = \left(\frac{4}{\Delta}+\frac{3U-4\Delta}{(U-\Delta)^2}\right)\frac{t_{pd}^4}{\Delta^2} \qquad (1.9)$$

and the indexes i, i' (j, j') run over the copper (oxygen) sites. As the calculation involve actually only three sites, this result is valid for any geometry, chain, ladder or plane. In figure 1.5 we can see the second order process of perturbation theory which differently contribute to $\tilde{t}$ and J_K. Superexchange spin-spin interaction among the coppers arise only at fourth order, the two

different process are shown in figure 1.6.

According to Zhang and Rice, one can define symmetrical combination of oxygen orbital, centered around a copper site as

$$P_{i,\sigma} = \frac{1}{2}\sum_j V_{ij} p_{j,\sigma}. \tag{1.10}$$

These states are non-orthogonal, since two neighboring states share a common oxygen; they have nonetheless a very high overlap with their orthogonal counterpart, the Wannier states. The commutation relations are in fact

$$\left\{P_{i,\alpha}, P^\dagger_{i',\beta}\right\} = \delta_{\alpha,\beta}\left(\delta_{i,i'} - \frac{1}{4}\delta_{\langle i,i'\rangle}\right) \tag{1.11}$$

where $\delta_{\langle i,i'\rangle}$ is one whenever i and i' are nearest neighbors from the point of view of the copper lattice, zero otherwise.

The Hamiltonian is readily rewritten as

$$\begin{aligned} H_{SF} &= 4\tilde{t}\sum_{i,\sigma} P^\dagger_{i,\sigma} P_{i,\sigma} + 4J_K \sum_{i,\alpha,\beta} \mathbf{S}_i \cdot P^\dagger_{i,\alpha} \boldsymbol{\sigma}_{\alpha,\beta} P_{i,\beta} \\ &\quad + \frac{J_H}{2}\sum_{\langle i,i'\rangle} \mathbf{S}_i \cdot \mathbf{S}_{i'} \end{aligned} \tag{1.12}$$

For physical values of the parameters (cf. Eq. (1.5)), it results $J_K > 0$ and $J_H > 0$, i.e. all the coupling are antiferromagnetic.

1.2.3 Mapping to a $t - J$ model: the Zhang-Rice approach

Writing the SF Hamiltonian in terms of the $P_{i,\alpha}$ states, we actually neglected antisymmetrical combination of oxygen orbitals, i.e. we neglected half of the total O states. In fact the hybridization term involve only the coppers and the symmetric states $P_{i,\alpha}$:

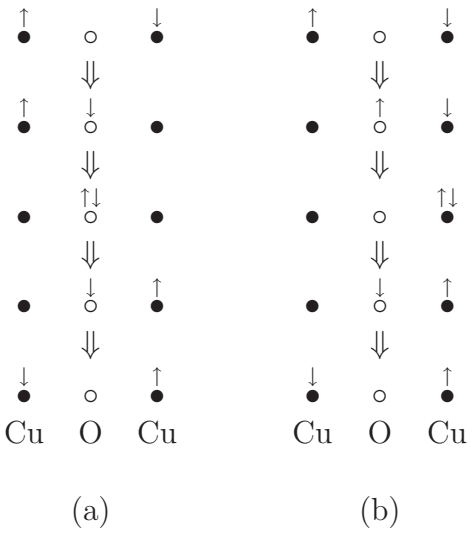

(a) (b)

Figure 1.6: The two fourth-order channels giving rise to spin-spin superexchange: (a) charge transfer only $(1/\Delta)$; (b) charge transfer $(1/\Delta)$ and $1/(U-\Delta)$.

$$H' = 2t_{pd} \sum_{i,\sigma} d^{\dagger}_{i,\sigma} P_{i,\sigma} + \text{h.c.}. \tag{1.13}$$

therefore, only the symmetric O states (which is one half the number of the total O states) couple to the Cu ions. The other half of the O states are nonbonding and are hence irrelevant to the low energy physics [49, 78]. The next step is to find orthogonal states for the carriers. Wannier states $f_{l,\sigma}$ are easily found via

$$P_{i,\sigma} = \sum_{l} \Gamma(i-l) f_{l,\sigma} \tag{1.14}$$

with

$$\Gamma(d) = \frac{1}{N} \sum_{k} e^{ikd} \sqrt{\beta_k} \tag{1.15}$$

Here β_k is the norm square of the wavefunction created by the Fourier transform of $P^{\dagger}_{i,\sigma}$. Equation (1.15) should be interpreted differently according to different lattice structures e. g. 1D, 2D, two-leg ladder. In two dimension it

means

$$\Gamma\left(d_x, d_y\right) = \frac{1}{\left(2\pi\right)^2} \int_{-\pi}^{\pi} dk_x \int_{-\pi}^{\pi} dk_y \, e^{ikd} \left(1 - \frac{\cos\left(k_x d_x\right) + \cos\left(k_y d_y\right)}{2}\right)^{\frac{1}{2}}$$

for a single chain takes the form

$$\Gamma\left(d\right) = \frac{1}{\left(2\pi\right)} \int_{-\pi}^{\pi} dk \, e^{ikd} \left(1 - \frac{\cos\left(kd\right)}{2}\right)^{\frac{1}{2}}.$$

A two-leg ladder with open boundary condition along the rungs is equivalent to a the same system with periodic boundary condition, with the constants in the perpendicular direction being halved. The momentum in the perpendicular dimension assumes only two values, $k_y = 0$ for the symmetrical channel and $k_y = \pi$ for the antisymmetrical one. Hence for the two-leg ladder case we have

$$\Gamma\left(d, \lambda\right) = \frac{1}{2} \sum_{k_y = 0, \pi} \frac{1}{\left(2\pi\right)} \int_{-\pi}^{\pi} dk \, e^{ikd} \left(1 - \frac{\cos\left(kd\right) + \cos\left(k_y \lambda\right)/2}{2}\right)^{\frac{1}{2}} \tag{1.16}$$

and $\lambda = 1, 2$ distinguishes the two chain whereas d runs along the chains direction.

Now in any geometry, the function Γ decreases exponentially with the distance. Since the Kondo coupling is the biggest energy in the system, the most relevant contribution to the Hamiltonian (1.12) is

$$4\Gamma\left(0\right)^2 J_K \sum_i \mathbf{S}_i \cdot \mathbf{s}_i \tag{1.17}$$

where $\mathbf{s}_i$ is an effective spin 1/2 half operator constructed upon the Wannier orbitals for the for the oxygen sites $f_{l,\sigma}$:

$$\mathbf{s}_i = \frac{1}{2} f^{\dagger}_{i,\alpha} \boldsymbol{\sigma}_{\alpha,\beta} f_{i,\beta} \tag{1.18}$$

As the coupling J_K is of antiferromagnetic nature, the spins on the Copper will form singlets with the spins $\mathbf{s}_i$ representing the carriers

$$S_i^\dagger |0\rangle = \frac{1}{\sqrt{2}} \left(f_{i\uparrow}^\dagger d_{i\downarrow}^\dagger - f_{i\downarrow}^\dagger d_{i\uparrow}^\dagger \right) |0\rangle \tag{1.19}$$

Since the O holes are created in a background of singly occupied Cu holes, when the singlet S moves from site i to j a Cu hole moves simultaneously from site j to i. This motion is represented by the process $S_i d_{j\sigma} \rightarrow S_j d_{i\sigma}$ with kinetic energy represented by the effective hopping Hamiltonian

$$H_t = \sum_{i \neq j,\sigma} \left\langle 0 | d_{j\sigma} S_i H_{\tilde{t}+J_K} S_j^\dagger d_{i\sigma}^\dagger | 0 \right\rangle S_i^\dagger d_{j\sigma}^\dagger d_{i\sigma} S_j. \tag{1.20}$$

From this equation we see that, when a Cu d hole is created at site j, the singlet state is destroyed at the same site. Therefore the state $S_i^\dagger |0\rangle$ is equivalent to the empty state of the d holes at site i. Projecting the Hamiltonian (1.12) onto the subspace of the singlet we obtain a $t-J$ model. Restricting the interaction to nearest neighbor only, we obtain in the 2D and pure 1D (i.e. single chain) case:

$$H_{t-J} = -t \sum_{\langle i,j \rangle} c_{i,\sigma}^\dagger c_{j,\sigma} + \frac{J}{2} \sum_{\langle i,j \rangle} \mathbf{S}_i \cdot \mathbf{S}_j \tag{1.21}$$

where i and j run now on the Cu sites only. As the Cu holes were half filled, now at each site we can have either a spin up or down or a hole (the singlet) but not a double occupied site. Hence the $c_{i,\sigma}$ operators actually represent constrained $d_{i,\sigma}$ holes i.e. $d_{i,\sigma}$ operators projected on the Hilbert space of no double occupancy:

$$c_{i,\sigma} = d_{i,\sigma} \left(1 - n_{i,\bar{\sigma}} \right).$$

In the two-dimensional case, the parameters are given case by (see also [79])

$$t = -0.81\tilde{t} + 0.80 J_K \tag{1.22}$$
$$J = J_H \tag{1.23}$$

whereas for the chain we obtain

$$t = -0.5\tilde{t} + 0.76 J_K \tag{1.24}$$
$$J = J_H \tag{1.25}$$

In the case of the two-leg ladder we have instead

$$\begin{aligned} H_{t-J} &= -t_{||} \sum_{\langle ij \rangle} \left(c_i^{1\dagger} c_j^1 + c_i^{2\dagger} c_j^2 \right) - t_\perp \sum_i \left(c_i^{1\dagger} c_i^2 + c_i^{2\dagger} c_i^1 \right) \\ &\quad + J \sum_{i,\lambda} \mathbf{S}_i^\lambda \cdot \mathbf{S}_{i+1}^\lambda + J \sum_i \mathbf{S}_i^1 \cdot \mathbf{S}_i^2 \end{aligned} \tag{1.26}$$

with constants given by

$$t_{||} = -0.5\tilde{t} + 0.76 J_K \tag{1.27}$$
$$t_\perp = \tilde{t} - 1.58 J_K \tag{1.28}$$
$$J = J_H \tag{1.29}$$

1.3 The undoped case: Non Linear Sigma Model approach

The mapping of the $d-p$ model for the cuprates material to a single band $t-J$ model greatly reduces the dimension of the Hilbert space making possible

(especially in the case of single chain systems or two-leg ladders) to resort to numerical solution. From the analytic point of view though the $t-J$ model presents an additional difficulty represented by the constraint of having no double occupancy. The original spin fermion model does not present this problem and this is the reason why we will work with this model in the sequel. In any case the situation for the undoped compound is much more clear. The model describing undoped cuprates is the Heisenberg model on the appropriate lattice. The properties of the single chain for spin one half, are know from the exact Bethe's solution [80], bosonization approach and conformal field theory [81]. In all other cases much of the understanding is due to a mapping to a continuum field theory realized first in 1983 by Haldane [16, 82] for the 1D case, and later extended to other geometries. This mapping is also valid in the disordered phase which is known to take place at $T=0$ and D=1 in contrast to spin waves approaches which assume an ordered ground state. The (low energy sector of the) D dimensional Heisenberg antiferromagnet is mapped onto the D+1 non linear sigma model plus eventually a term of topological nature on which we will come shortly. The action of the non linear sigma model in (D+1) dimension is

$$S_{NL\sigma M}=\frac{1}{2g}\int d^{D}\mathbf{x}\int d\tau\left(\partial_{\mu}\mathbf{N}\cdot\partial_{\mu}\mathbf{N}\right) \tag{1.30}$$

where we set the velocity of light equal to one, g is the coupling constant and $\mathbf{N}$ is a three-dimensional vector field subjected to the constraint $|\mathbf{N}|^{2}=1$. The field $\mathbf{N}$ describe antiferromagnetic fluctuations. This means that, at leading order, the original spin-spin correlation are described by

$$(-1)^{i}\left\langle \mathbf{S}_{0}\cdot\mathbf{S}_{i}\right\rangle _{Heisenberg}\sim\left\langle \mathbf{N}\left(0\right)\cdot\mathbf{N}\left(x\right)\right\rangle _{NL\sigma M} \tag{1.31}$$

at least asymptotically that is when $ai=x\gg a$ (a is the lattice spacing). This field theory also describes (when the inverse temperature $\beta=\infty$) the long wave-length limit of the classical Heisenberg magnet in (D+1) dimensions (there is no difference between ferromagnet and antiferromagnet classically).

In one spatial dimension (i.e. D+1=2) the requirement that the action is finite (infinite action configurations have zero weight in the partition function) implies that the field $\mathbf{N}$ must go to a fixed value, say $\mathbf{N}_0$, when $|(\mathbf{x}, \tau)| \to \infty$. This means that the physical space $\mathbb{R}^2$ is essentially compactified into a spherical surface $\mathbb{S}^2$ i.e. the circle at infinity reduces to, say, the north pole of the sphere. On the other hand, the 'internal space', i.e. the space of the field $\mathbf{N}$, subject to the constraint $|\mathbf{N}|^2 = 1$, is precisely the two dimensional sphere $\mathbb{S}^2$. Then, any finite action configuration $\mathbf{N}(\mathbf{x}, \tau)$ is a mapping of $\mathbb{S}^2$ into $\mathbb{S}^2$.

It turns out that any non singular mapping of $\mathbb{S}^2$ into $\mathbb{S}^2$, can be classified into homotopy sectors[4]. Mappings within one sector can be continuously deformed into one another, whereas mappings from two different sectors cannot. Furthermore there is a denumerable infinity of such sectors or classes, which can be characterized by the set of integers. More precisely, these homotopy classes themselves form a group which is isomorphic to the group of integers. Formally all this is written in the compact form

$$\pi_2\left(\mathbb{S}^2\right) = \mathbb{Z} \tag{1.32}$$

where $\pi_n(\mathbb{S}^m)$ stands for the homotopy group associated with mappings $\mathbb{S}^n \to \mathbb{S}^m$, and $\mathbb{Z}$ is the group of integers. A precise proof of this statement together with the proper definition of homotopy classes can be found in [83]. In summary each physical configuration $\mathbf{N}(x)$ can be classified into homotopy sectors, characterized by some integer which we label Q. The signed integer Q can be represented as an integral over the fields in the following way:

$$Q[\mathbf{N}] = \frac{1}{4\pi} \int dx \int d\tau \mathbf{N} \cdot (\partial_\tau \mathbf{N} \times \partial_x \mathbf{N}) \tag{1.33}$$

This functional is indeed a topological invariant, i..e. does not change under a smooth deformation of the map $\mathbf{N}$. Indeed, by varying $\mathbf{N}(x)$ infinitesimally:

[4]Two maps are homotopic if they can be smoothly deformed one into the other. An equivalent class of maps under homotopy transformation defines an homotopy sector.

$$\mathbf{N} \to \mathbf{N} + \delta\mathbf{N} \tag{1.34}$$

we find, neglecting boundary terms:

$$\delta Q = \frac{3}{4\pi} \int dx \int d\tau \delta\mathbf{N} \cdot (\partial_\tau \mathbf{N} \times \partial_x \mathbf{N}) \,. \tag{1.35}$$

But, by virtue of the constraint on $\mathbf{N}$:

$$\mathbf{N} \cdot \delta\mathbf{N} = \mathbf{N} \cdot \partial_\mu \mathbf{N} = 0 \;\; \forall \mu \tag{1.36}$$

Therefore, $\delta\mathbf{N}$ and the partial derivatives $\partial_\mu \mathbf{N}$ are complanar, and the triple product in (1.35) vanishes. So $\delta Q = 0$ and Q is indeed a topological (homotopy) invariant. Moreover one can show (see again [83]) that the functional Q can be cast into the from

$$Q\left[\mathbf{N}\right] = \frac{1}{4\pi} \int_{\mathbf{N}(\mathbb{S}^2)} d\Omega, \tag{1.37}$$

where $d\Omega$ is the solid angle on the two sphere and $\mathbf{N}\left(\mathbb{S}^2\right)$ is the image of the sphere $\mathbb{S}^2$ upon the action of the mapping $\mathbf{N}$. Then expression (1.37) is nothing but the number of times the map $\mathbf{N}$ winds around the target space $\mathbb{S}^2$ and so the topological term (1.33) is indeed a (signed) integer.

Haldane's original mapping of spin S one dimensional Heisenberg chains [16] together with the generalization to M-leg ladder [32, 84], showed that indeed the topological term is present in the low energy effective action, when the spin per site S is half-odd-integer and the number of interacting chains M is odd ($M = 1$ identifies the single chain). More precisely, for a spin S, M-leg ladder Heisenberg model the effective theory is the non linear sigma model in (1+1) dimension equation (1.30) plus a term:

$$\begin{aligned} S' &= i\vartheta Q\left[\mathbf{N}\right] \\ \vartheta &= 2\pi S \delta_{M,\text{odd}} \,. \end{aligned} \tag{1.38}$$

We note here that $Q[\mathbf{N}]$ given by equation (1.33) changes sign under a parity (or time reversal) transformation. Hence the topological term break explicitly parity (or time reversal) unless $\vartheta = 0 \,\text{or}\, \pi \,(\text{mod} 2\pi)$, which are indeed the values allowed by the mapping. The contribution to the partition function given by the topological term is the phase $\exp(-i\vartheta Q[\mathbf{N}])$ where $Q[\mathbf{N}]$ is an integer that depends on the configuration $\mathbf{N}$. For SM integer, this phase is equal to 1 for any path $\mathbf{N}$ and the topological term can be ignored. On the contrary when S is half odd integer, and M is odd, the phase can be 1 or -1 and can generate interference effect between different paths in the functional integral.

At this point we add a brief comment on the two dimensional case. Again the requirement that a configuration $\mathbf{N}(x)$ has finite action implies that the physical space $\mathbb{R}^3$ is compactified into the sphere $\mathbb{S}^3$. Hence the configurations are maps from $\mathbb{S}^3$ to $\mathbb{S}^2$. The homotopy classes of maps from $\mathbb{S}^3$ to $\mathbb{S}^2$ are also indexed by an integer, i.e. one also has $\pi_3(\mathbb{S}^2) = \mathbb{Z}$. This integer is called the Hopf invariant. However there is no simple expression of the Hopf invariant as an integral over the field $\mathbf{N}$, as for the topological term in (1+1) dimension. In section 2.1.3.1 we will see an explicit mapping from $\mathbb{S}^3$ to $\mathbb{S}^2$, called the Hopf map, with the help of which is possible to write the Hopf invariant as an integral over the appropriate manifold $\mathbb{S}^3$. As this is outside the scope of this thesis we reference the reader again to the book [83] for a discussion on this point. However Haldane's mapping in D=2 dimension does not give rise to any topological term [30] although the possibility of its existence was conjectured following other routes [85]. In any case we will concentrate on the one dimensional case.

In (1+1) dimension the theory (1.30) without topological term has been studied for quite some time in particle physics, mainly because it possesses some properties analogue to those of quantum chromodynamic, for being an asymptotic free theory (that is, the coupling constant runs down to zero as we move up to higher and higher energy scales) [86], because it presents dynamical mass generation and because admits the existence of instantons [87]. Being a theory with a gap, static correlation functions decay to zero at long

Haldane's Conjecture & LSM Theorem	SM Half-odd integer	$\Rightarrow$	No Haldane Phase Single S=1/2 chain Universality class
Haldane's Conjecture	SM integer	$\Rightarrow$	Haldane Phase

Table 1.1: Results of Haldane's mapping and LSM theorem for the antiferromagnetic Heisenberg model defined on an M-leg ladder. S is the spin per site.

distances. The prediction that this should also hold for the single antiferromagnetic Heisenberg chain with general integer spin S, was conjectured by Haldane in 1983, and bears the name "Haldane's conjecture".

At the times of the first Haldane's works, it was not clear what to expect from the theory with the topological term. Hence the mapping was rather used backward. From the known analytical solution of the spin 1/2 Heisenberg antiferromagnetic chain, it was for long time known, that this system presents gapless excitations [88, 89] and have algebraically decaying correlation functions [90]. Thanks to Haldane's mapping these properties must hold also for the non linear sigma model with topological term, – and hence, backward again, must be valid for all cases where SM is an half-odd integer.

In more recent times, Shankar and Read [91] were able to show, independently from Haldane's construction, that the non linear σ model with topological term does not have a gap above the ground state, hence consolidating the original "proof" about the absence of a gap in Heisenberg ladders for SM half-odd integer.

As we already said, absence of a gap for the spin 1/2 Heisenberg chain was know for long time. In 1961 Lieb Schultz and Mattis [88] proved rigorously that the spin 1/2 chain must have gapless excitations[5]. Later this result was extended to all half integer spin S [94] and can also be trivially extended to

[5]Actually, the possibility that the ground state will be degenerate in the thermodynamic limit, is also left open. That the ground state is unique for any finite size was proved in [92, 93], and is normally considered as an exotic possibility that the ground state will be degenerate in the thermodynamic limit.

ladder with S half-odd integer and M odd, where M is the number of legs (see i.e. [95]). Lieb, Schultz and Mattis (LSM) theorem hence proves one part of "Haldane's conjecture". Nowadays, the results of Haldane's conjecture have received such a great amount of confirmations, through numerical simulations [18, 96, 22], and even through a number of experiments on ladders material [23, 27], that the validity of the conjecture is nowadays not brought into question anymore.

A spin state with a gap and exponentially decaying correlation is sometimes called, not by chance, an Haldane state or Haldane phase. The property of the antiferromagnetic M-leg ladder ($M = 1$ is the single chain) are then clear. For integer values of SM, the ground state is in an Haldane phase, weather for half integer values, the system is in the universality class of the single chain and has a gapless ground state with quasi long ranged correlations. The different behavior for SM integer or half integer is to be attributed to the presence of a topological term in the effective action of the model. These result are summed up in table 1.1.

Chapter 2

Effective theories for doped chains and ladders

In this section we will derive effective, continuum, action for the problem of holes interacting in an antiferromagnetic spin background. To reach this goal we will employ the following general strategy:

- Integrate out the high energy modes.
- Send the lattice spacing to zero, i.e. find the long wavelength (continuum) theory.

This procedure will be repeated both for spins and fermionic degrees freedom (see for instance the book of Popov [97] where such a strategy is widely used).

For what regard the spin degrees of freedom we follow the now well established (Haldane's) mapping of the antiferromagnetic Heisenberg model onto the non linear sigma model (NLσM) field theory, which we already anticipated in the previous chapter. Haldane's mapping holds when the continuum approximation is justified i.e. when the -spin- correlation length of the system extends over several lattice spacing: $\xi \gg a$. Several numerical studies have clarified this point. The mapping is surely satisfied in the $S = 1/2$ chain and three-leg ladder as these systems posses antiferromagnetic QLRO and the correlation length is infinity [90, 22, 21]. In the $S = 1/2$ two-leg ladder the

numerically determined correlation length is only $\xi \simeq 3.24a$ [22, 21]. Haldane's mapping for the two leg ladder is surely satisfied for high value of the spin S, since the correlation length grows exponentially with S. The fact the the predictions of the non linear sigma model –namely a spin liquid ground state– apply very well also to the spin $1/2$ two leg ladder, indicates that the mapping is valid down to the value $S = 1/2$. A similar situation happens for the single chain for integer values of the spin.

This general picture remains essentially unaltered even if a small fraction of doping is allowed and this motivated us to generalize Haldane's mapping in case of lightly doped antiferromagnet. Again, numerical simulation on the $t - J$ model on chains [98, 99] and three-leg ladders [100] have confirmed the presence of QLRO of antiferromagnetic nature. In the two leg-ladder also, the introduction of a small amount of holes does not destroy the spin liquid state [34].

To recognize the high energy modes for the fermions we take advantage of a result that we will show in the following chapter. There, using other techniques, it will be shown that, in the continuum limit, the holes feel primarily an antiferromagnetic spin background. It will be then useful to expand around this configuration, but without breaking explicitly spin rotational symmetry, which in one dimension is never broken. This will be achieved rotating the spin quantization axis of the holes. At the same time this procedure is at the basis of the so called one-dimensional complex projective -$\mathbb{CP}^1$- representation of the non linear sigma model, which enable a large N expansion and is very effective in explaining the property of the NLσM. A very similar approach was presented in [101, 102] to obtain an affective theory for the two dimensional planes forming high-T_c superconductors. Here we treat instead single chains and ladders.

2.1 The chain

We will explain all the steps in detail for the case of the single chain, and only give the results and the few necessary modification, for the two- and

three-leg ladder case.

As a starting point we use a slightly modified version of the spin fermion Hamiltonian, sometimes called Heisenberg-Kondo lattice (HKL) (see e. g. [103]). The difference lies in the fact that in the HKL model, a band of fermions interacts with localized spins through a Kondo coupling which is *local* both in the spins and in the fermions. As for the Spin-Fermion model the spin dynamic is given by a nearest neighbor Heisenberg model. The Hamiltonian is:

$$H_{HKL} = -t \sum_{i,\alpha} \left(c^{\dagger}_{i,\alpha} c_{i+1,\alpha} + \text{h.c.} \right) + J_K \sum_{i,\alpha,\beta} c^{\dagger}_{i,\alpha} \boldsymbol{\sigma}_{\alpha,\beta} c_{i,\beta} \cdot \mathbf{S}_i + J_H \sum_i \mathbf{S}_i \cdot \mathbf{S}_{i+1}. \tag{2.1}$$

By expressing the states $P_{i,\alpha}$ in terms of orthogonal Wanniers operator we can establish a simple correspondence between the constants of the two models:

SF	HKL
t	$2g_0 \left\vert g_1 \right\vert t \approx 0.25t$
J_K	$g_0^2 J_K \approx 0.97 J_K$

where

$$g_m = \frac{1}{2\pi} \int_{-\pi}^{\pi} dk \cos\left(km\right) \sqrt{1 - \frac{\cos\left(k\right)}{2}}. \tag{2.2}$$

The function g_m decays exponentially to zero which makes reasonable to stop to the very first relevant terms and hence obtain model (2.1) from the equation (1.12) of the preceding chapter.

Next we write the partition function as a coherent state path integral both for fermions and spins:

$$\begin{aligned} Z &= \text{tr} e^{-\beta H_{HKL}} \\ &= \int D\left[c, c^{\dagger}\right] D\hat{\Omega} e^{-S_{HKL}}, \end{aligned} \tag{2.3}$$

where the action is

$$\begin{aligned} S_{HKL} &= \sum_i \int_0^\beta d\tau \left\{ c^*_{i,\alpha} \partial_\tau c_{i,\alpha} - t \left(c^*_{i,\alpha} c_{i+1,\alpha} + c^*_{i+1,\alpha} c_{i,\alpha} \right) + S J_K \mathbf{R}_i \cdot \hat{\mathbf{\Omega}}_i \right. \\ &\left. + S^2 J_H \hat{\mathbf{\Omega}}_i \cdot \hat{\mathbf{\Omega}}_{i+1} - iS\omega_B \left[\hat{\mathbf{\Omega}}_i (\tau) \right] \right\}, \end{aligned} \tag{2.4}$$

and we introduced the shorthand

$$\mathbf{R}_i (\tau) = c^*_{i,\alpha} (\tau) \boldsymbol{\sigma}_{\alpha,\beta} c_{i,\beta} (\tau) . \tag{2.5}$$

The c_i ($\hat{\mathbf{\Omega}}_i$) are now time (imaginary time actually) dependent Grassmann (complex) variables with antiperiodic (periodic) boundary conditions at $\tau = 0$ and $\tau = \beta$. The last term $\int d\tau \omega_B \left[\hat{\mathbf{\Omega}} (\tau) \right]$ is the Berry term which measures the solid angle enclosed by the path γ described by the vector $\hat{\mathbf{\Omega}} (\tau)$ as it moves from zero to β. Following Haldane [82] it can be written in an explicitly rotational invariant way:

$$\int_0^\beta d\tau \omega_B \left[\hat{\mathbf{\Omega}} (\tau) \right] = \int_0^\beta d\tau \mathbf{A} \left(\hat{\mathbf{\Omega}} \right) \cdot \frac{\partial \hat{\mathbf{\Omega}}}{\partial \tau}, \tag{2.6}$$

where the vector $\mathbf{A}$ is the potential of a Dirac monopole i.e. satisfies

$$\epsilon^{abc} \frac{\partial \mathbf{A}^b}{\partial \Omega^c} = \Omega^a . \tag{2.7}$$

Expressing $\hat{\Omega}$ in spherical coordinates it reads

$$\int_0^\beta (1 - \cos (\vartheta)) \dot{\phi} d\tau \tag{2.8}$$

Before passing to our actual calculation, we want to make a comment on the spin coherent path integral. The derivation of the spin coherent path integral is strictly valid only in the large-S limit. For instance it is known that the

partition function for a free spin in magnetic field, calculated via coherent state path integral differs from the exact one by a factor $\left(1+\frac{1}{2S}\right)^N$ where N is the number of time slices [104]. Such a factor, although diverging, is however unimportant as all the quantities we are interested in are expressed as ratios. Nonetheless this imprecision has led many authors to find alternative path integral description for the spin as using an Hubbard-Stratonovich field [105], or a fermion representation for the spins, and the corresponding path integral, as in [106]. However in the spirit of the mapping to a non linear sigma model, all these different approach give exactly the same result. Here we use the coherent states approach. For a thorough review on Haldane's mapping via coherent states on undoped systems see for instance [107] chapter 12.

2.1.1 Parametrization

Even if, in one dimension, quantum fluctuations make the system disordered, we expect that antiferromagnetic order survives at least at short distances. Hence we decompose the dynamical field $\hat{\Omega}$ into an antiferromagnetic part plus a ferromagnetic fluctuation (see e. g. [108]):

$$\hat{\mathbf{\Omega}}_i(\tau) = (-1)^i \mathbf{n}_i(\tau) \sqrt{1 - a^2 \left|\frac{\mathbf{l}_i(\tau)}{S}\right|^2} + a\frac{\mathbf{l}_i(\tau)}{S} \tag{2.9}$$

In the above equation $\mathbf{n}_i(\tau)$ keeps track of slow variations from antiferromagnetic order and $\mathbf{l}_i(\tau)$ represent fluctuations at short wave-length. The lattice constant a in front of $\mathbf{l}_i(\tau)$in eq. (2.9) makes explicit the fact that $\mathbf{l}_i(\tau)$ is proportional to a generator of rotations of $\mathbf{n}_i(\tau)$, namely to a first-order derivative of $\mathbf{n}_i(\tau)$ (see [31] for a discussion on this point). The constraint $\left|\hat{\Omega}\right|^2 = 1$ is resolved imposing

$$\left|\mathbf{n}_i(\tau)\right|^2 = 1, \text{ and } \mathbf{l}_i(\tau)\cdot\mathbf{n}_i(\tau) = 0. \tag{2.10}$$

Having found high and low energy modes we can now pass to the actual continuum limit. Being our new new field slowly varying, we can use the

following gradient expansion:

$$\mathbf{n}_{i+1} = \mathbf{n}_i + a\partial_x \mathbf{n}_i + \frac{a^2}{2}\partial_x^2 \mathbf{n}_i + \dots \tag{2.11}$$

and proceed similarly for the field $\mathbf{l}$. The expansion above is valid if the correlation length of the system is much larger than the lattice spacing:

$$\xi \gg a. \tag{2.12}$$

In case of the undoped spin 1/2 chain (and more generally for half integer spin) this is surely satisfied as we know from Bethe solution (see the definitive result [90]) that spin-spin correlations fall off algebraically and hence the correlation length is infinite. For spin 1, numerical simulation on the Heisenberg model reported a correlation length $\xi \simeq 6a$ [109, 110]. In case of spin 2 one already has $\xi \simeq 49a$ [111] and generally the correlation length grows exponentially with the spin and the inequality (2.12) is better and better satisfied as the spin S increases. As we already mentioned, numerical investigation on the spin 1/2, $t-J$ chain [98, 99], revealed that antiferromagnetic QLRO survives at small doping. For the spin one case, neutron scattering experiments on a spin one antiferromagnetic doped material ($Y_{2-x}Ca_xBaNiO_5$) have shown that the gap which identifies the spin liquid state of the undoped parent compound is essentially un-affected by the introduction of holes [112]. On top of that, quasi long ranged antiferromagnetic correlations seem to appear, a fact that can only reinforce the validity of the continuous approximation.

A reasonable question which now poses itself is how many terms must we keep in the expansion (2.11)? One usual argument is: $\mathbf{n}$ is slowly varying, so we keep up to $(\partial_\mu \mathbf{n})^2$, $\mathbf{l}$ contains already a derivative so we keep up to $\mathbf{l}^2$. One can make this argument more precise using "power counting". Let's say we keep all the terms. The first terms will be something like

$$\sim (\partial_\mu \mathbf{n})^2 + a\,|\mathbf{l}|^2 + b\mathbf{l} \tag{2.13}$$

very naturally, we want these terms to survive in the continuum limit ($a \to 0$). So we will rescale the fields in order to have these quantity integrated over $dxd\tau$ to be dimensionless. In d=(1+1)=2 this implies that $\mathbf{n}$ is dimensionless and $[\mathbf{l}] = L^{-1}$. This in turn implies that if we encounter a term like

$$\gamma_{r,m} \int d^2x \left(\partial_\mu\right)^m \mathbf{l}^r, \tag{2.14}$$

dimensional analysis tells us that the dimension of the constant will be

$$[\gamma_{r,m}] = L^{m-2+r}, \tag{2.15}$$

such terms will be relevant or marginal for $m+r \leq 2$. Terms with $m+r > 2$ are irrelevant and may be safely discarded. Similarly for the $\mathbf{n}$ field we have

$$\lambda_{r,m} \int d^2x \left(\partial_\mu\right)^m \mathbf{n}^r \Rightarrow [\lambda_{r,m}] = L^{m-2}, \tag{2.16}$$

so for $\mathbf{n}$ we must keep up to $m \leq 2$. All in all this amount to keep terms up to a^2.

Now we insert equation (2.9) in the action (2.4), perform the gradient expansion (2.11) and keep term up to $O\left(a^2\right)$.

The Berry's phase term require some little extra care. It is at the origin of the topological term responsible for the already mentioned even-odd effect for spin chains and ladder. Substituting (2.9) into the expression for the Berry's phase, we obtain

$$\sum_i \omega_B\left(\hat{\Omega}_i\right) \;=\; \sum_i \left(-1\right)^i \omega_B\left(\mathbf{n}_i\right) + a \sum_i \int_0^\beta d\tau \left(\mathbf{n}_i \times \partial_\tau \mathbf{n}_i\right) \cdot \mathbf{l}_i, \tag{2.17}$$

and we used the formula for the variation of the Berry's phase:

$$\omega_B\left(\phi + \delta\phi\right) = \omega_B\left(\phi\right) + \int_0^\beta d\tau \left(\phi \times \partial_\tau \phi\right) \cdot \delta\phi. \tag{2.18}$$

The first term of the RHS of Eq. (2.17) gives rise, in the continuum limit, to the topological term[1]:

$$\begin{aligned}\sum_i (-1)^i \omega_B(\mathbf{n}_i) &= \sum_i \omega_B(\mathbf{n}_{2i}) - \omega_B(\mathbf{n}_{2i+1}) \\ &\overset{a\to 0}{=} \frac{1}{2}\int dx \int_0^\beta d\tau \frac{\delta\omega}{\delta\mathbf{n}} \cdot \partial_x \mathbf{n} \\ &= \frac{1}{2}\int dx \int_0^\beta d\tau \left(\partial_\tau \mathbf{n} \times \partial_x \mathbf{n}\right) \cdot \mathbf{n} \end{aligned} \tag{2.19}$$

Which is the term we already encountered at the end of the last chapter.

Finally we summarize all the contribution coming from the spins

$$\begin{aligned} S_s = \sum_i \int_0^\beta d\tau \Big\{ &\frac{a^2 S^2 J_H}{2} \left|\partial_x \mathbf{n}_i(\tau)\right|^2 + S J_K (-1)^i \mathbf{R}_i(\tau) \cdot \mathbf{n}_i(\tau) + \\ &a^2 J_H \left[\mathbf{l}_i(\tau) \cdot \mathbf{l}_i(\tau) + \mathbf{l}_i(\tau) \cdot \mathbf{l}_{i+1}(\tau)\right] - a^2 \frac{J_K}{2S} (-1)^i \mathbf{R}_i(\tau) \cdot \mathbf{n}_i(\tau) \left|\mathbf{l}_i(\tau)\right|^2 \\ &- ia \mathbf{l}_i(\tau) \cdot \mathbf{n}_i(\tau) \times \partial_\tau \mathbf{n}_i(\tau) + a J_K \mathbf{R}_i(\tau) \cdot \mathbf{l}_i(\tau) \Big\} + i 2\pi S \omega_T[\mathbf{n}] \ . \end{aligned} \tag{2.20}$$

2.1.2 Integration of the spin fluctuations

We still cannot integrate out the fluctuations because of the constraint $\mathbf{l}_i(\tau) \cdot \mathbf{n}_i(\tau) = 0$. We re-write then the functional delta function through its Fourier representation:

$$\delta\left(\mathbf{n}_i(\tau) \cdot \mathbf{l}_i(\tau)\right) = \int D\lambda \exp\left[ia \sum_i \int_0^\beta d\tau \lambda_i(\tau)\, \mathbf{n}_i(\tau) \cdot \mathbf{l}_i(\tau)\right], \tag{2.21}$$

[1] There is an ambiguity in the sign of the following formula as we do not know on which sites $(-1)^i$ is plus. Obviously a change of sign in the topological term has no relevance.

at this point the $\mathbf{l}$ field is Gaussian and can be integrated out. Next we also integrate out the λ field which is also Gaussian. The two determinants which emerge from the Gaussian integration cancel one another apart from constant terms. We also discard contributions which are more than quadratic in the fermions as we consider the low doping regime. The result is

$$\begin{aligned} S_{eff} &= S_F + S_{NL\sigma M} + i\vartheta\omega_T \\ S_F &= \sum_i \int_0^\beta d\tau \left\{ c^*_{i,\alpha}\partial_\tau c_{i,\alpha} + t\left(c^*_{i,\alpha}c_{i+1,\alpha} + c^*_{i+1,\alpha}c_{i,\alpha}\right) + SJ_K\left(-1\right)^i \mathbf{R}_i\cdot\mathbf{n}_i \right. \\ &\quad \left. + i\frac{J_K}{4J_H}\mathbf{R}_i\cdot\left[\mathbf{n}_i\times\partial_\tau\mathbf{n}_i\right]\right\}, \end{aligned} \tag{2.22}$$

where the non linear sigma model action and topological term are respectively

$$S_{NL\sigma M} = \frac{1}{2g}\int dx\int_0^\beta d\tau\left[v_s\left|\partial_x\mathbf{n}\right|^2 + \frac{1}{v_s}\left|\partial_\tau\mathbf{n}\right|^2\right] \tag{2.23}$$

$$\omega_T = \frac{1}{4\pi}\int dx\int_0^\beta d\tau\mathbf{n}\cdot\left(\partial_\tau\mathbf{n}\times\partial_x\mathbf{n}\right), \tag{2.24}$$

and the constants are

$$g = \frac{2}{S},\ v_s = 2SJa,\ \vartheta = 2\pi S\,. \tag{2.25}$$

2.1.3 Integration of the fermionic high energy modes

Up to now we did only half of the job, we still have to find the high energy modes for the holes which we will then integrate out. We also want to take advantage of the fact the J_K is the biggest parameter of our theory. As already mentioned, in the next chapter we will see that the holes are primarily influenced by an exactly staggered configuration for the spin. A decomposition like

$$\mathbf{n}_i = \hat{\mathbf{z}} + \delta\mathbf{n}_i \tag{2.26}$$

would indeed give rise to a free term representing holes in an exactly staggered spin background plus a fluctuating term proportional to $\delta\mathbf{n}_i$. Unfortunately we know that such a spin waves approach fails in one dimension i.e. the assumption of an antiferromagnetically ordered ground state is wrong (see e.g. chapter 11 of [107]). We want to keep rotational symmetry as we know that, in D=1, it will never be broken, even at zero temperature.

2.1.3.1 Rotating reference frame

A solution is to rotate the quantization axis of the fermions, i.e. to pass to new states $\psi_{i,\beta}$ defined by

$$c_{i,\alpha}(\tau) \;=\; [U_i(\tau)]_{\alpha,\beta}\,\psi_{i,\beta}(\tau)\,, \tag{2.27}$$

where U is a 2×2 matrix which belongs to the group SU(2) i.e. $U^\dagger U = \mathbf{I}$ (now on we employ matrix convention for the SU(2) indexes, unless explicitly otherwise specified). If we choose the matrix U so as to align the vector $\mathbf{n}$ in the 'z' direction:

$$U_i^\dagger(\tau)\,\mathbf{n}_i(\tau)\cdot\boldsymbol{\sigma}U_i(\tau) = \sigma^z, \tag{2.28}$$

then a free term which is exactly what we were looking for, appears in the action (2.22). Before passing further in the calculations we want comment on the significance of transformations (2.27) and (2.28).

It is to be pointed out that Eq. (2.28) does not determine $U_i(\tau)$ uniquely, but only up to a rotation around the 'z' axis. Indeed if $U_i(\tau)$ satisfies equation (2.28) the matrix $U_i'(\tau) = U_i(\tau)\,e^{i\phi_i(\tau)\sigma^z}$, where $\phi_i(\tau)$ is a scalar function, satisfies the same equation as well. The two matrices U, U' must correspond

to the same spinor $c_i(\tau)$ which knows nothing about the transformation. Hence to a transformation

$$U_i(\tau) \to U_i'(\tau) = U_i(\tau)\, e^{i\phi_i(\tau)\sigma^z} \tag{2.29}$$

must correspond an analogous transformation on the states $\psi_i(\tau)$:

$$\psi_i(\tau) \to \psi_i'(\tau) = e^{-i\phi_i(\tau)\sigma^z}\psi_i(\tau) \tag{2.30}$$

A consequence of this is that the fermionic action S_F in terms of the new variables ψ and U must be invariant under the following local (gauge) transformation:

$$U_i(\tau) \to U_i(\tau)\, e^{i\phi_i(\tau)\sigma^z}, \qquad \psi_i(\tau) \to e^{-i\phi_i(\tau)\sigma^z}\psi_i(\tau)\,. \tag{2.31}$$

This symmetry, originally not present in the model, is due to the fact the we are expressing the two free parameters of the unimodular vector $\mathbf{n}$, with the three parameters which suffice to fix an SU(2) matrix.

The gauge freedom associated with equation (2.28) tells us that any two SU(2) matrices U, U' which are related by a U(1) transformation as in equation (2.29) must be considered equivalent. Hence we are constructing the coset group SU(2)/U(1). It turns out that the coset group SU(2)/U(1) can be identified with the two dimensional complex projective space $\mathbb{CP}^1$, i.e. the space of all equivalent classes $[Z]$ of complex vectors $Z = (z_1, z_2) \neq 0$, two of which Z and Z' are equivalent if

$$Z = \lambda Z', \quad \lambda \in \mathbb{C} \tag{2.32}$$

(see e.g. ref. [113], p. 159). The transformation (2.28) can also be represented in term of $\mathbb{CP}^1$ fields Z. We can think of $\mathbb{CP}^1$ as the unit sphere in $\mathbb{C}^2$, that is, instead of fields $[Z]$, we may equally well consider fields of complex unit vectors

$$Z_i(\tau) = (z_1(i,\tau), z_2(i,\tau)), \quad |Z|^2 = |z_1|^2 + |z_2|^2 = 1, \ z_1, z_2 \in \mathbb{C}, \quad (2.33)$$

keeping in mind, however, that fields related by a gauge transformation

$$Z_i(\tau) \to Z_i'(\tau) = e^{i\phi_i(\tau)} Z_i(\tau) \quad (2.34)$$

should be considered equivalent. In other words, $Z_i(\tau)$ is one of the unit length representatives of the class $[Z](i,\tau)$ and eq. (2.34) simply reflects the ambiguity involved, when choosing $Z_i(\tau)$ out of $[Z](i,\tau)$. We also note in passing that because of the constraint $|Z|^2 = 1$ of eq. (2.33), this space has the topology of the sphere $\mathbb{S}^3$.

Now, with such a field Z we can write any SU(2) matrix as

$$U = \begin{pmatrix} z_1 & -\bar{z}_2 \\ z_2 & \bar{z}_1 \end{pmatrix}, \quad (2.35)$$

(here we dropped for simplicity site and time dependence). The constraint $U^\dagger U = \mathbb{1}$ is assured by $|Z|^2 = 1$. One sees immediately that the transformation (2.34) corresponds to the transformation (2.29). Moreover, by using

$$\mathbf{n}^a = \frac{1}{2}\mathrm{tr}\left(U\sigma^z U^\dagger \sigma^a\right), \quad (2.36)$$

one can convince himself that equation (2.28) is equivalent to

$$\mathbf{n} = Z^\dagger \boldsymbol{\sigma} Z. \quad (2.37)$$

This equation defines also the so called Hopf map (see e. g. [114] chapter 5), a mapping between the sphere $\mathbb{S}^3$ defined by $|Z|^2 = 1$, and the sphere $\mathbb{S}^2$ given by $|\mathbf{n}|^2 = 1$. Equation (2.37) is the starting point of the $\mathbb{CP}^1$ representation of the non linear sigma model. The usefulness of this formulation is that the space $\mathbb{CP}^1$ is easily generalized to $\mathbb{CP}^{N-1}$ by extending the number of complex fields from 2 to N:

$$Z = (z_1, z_2, \dots z_N)\,, \quad N \geq 2, \tag{2.38}$$

and generalizing the constraint $|Z|^2 = 1$ to

$$|Z|^2 = \sum_{m=1}^{N} |z_m|^2 = \frac{N}{2}. \tag{2.39}$$

In this way one can use the number of complex components N as an expansion parameter and obtain a controlled expansion of the non linear sigma model. It is possible to reformulate the action in a power series of $1/\sqrt{N}$, the lowest order term of which reproduces already very well the known properties of the non linear sigma model [115, 116].

As is customary in the $\mathbb{CP}^1$ language we define

$$U^\dagger \partial_\mu U = i\sigma^z a_\mu + K_\mu\,, \tag{2.40}$$

where K_μ is completely off diagonal 2×2 matrix and a_μ is real scalar. In terms of the Z field we have

$$a_\mu = -iZ^\dagger \partial_\mu Z, \;\; K_\mu = \begin{pmatrix} 0 & \bar{z}_2 \partial_\mu \bar{z}_1 - \bar{z}_1 \partial_\mu \bar{z}_2 \\ z_1 \partial_\mu z_2 - z_2 \partial_\mu z_1 & 0 \end{pmatrix}. \tag{2.41}$$

Finally we plug equation (2.27) into the fermionic part of the action (2.22), as a result we obtain a free term and an interaction one:

$$
\begin{aligned}
S_F &= S_0 + S_1 && (2.42)\\
S_0 &= \sum_i \int_0^\beta d\tau \left\{ \psi_i^* \partial_\tau \psi_i + t \left(\psi_{i,\alpha}^* \psi_{i+1,\alpha} + \text{h.c.} \right) \right. \\
&\quad \left. + S J_K \left(-1\right)^i \psi_i^* \sigma^z \psi_i \right\} && (2.43)\\
S_1 &= \sum_i \int_0^\beta d\tau \left\{ \psi_{i,\alpha}^* U_i^\dagger \partial_\tau U_i \psi_{i,\alpha} + t \left(\psi_i^* \left(U_i^\dagger U_{i+1} - \mathbb{1} \right) \psi_{i+1} + \text{h.c.} \right) \right. \\
&\quad \left. - \frac{J_K}{2J_H} \psi_i^* K_\tau \psi_i \right\}, && (2.44)
\end{aligned}
$$

and we also used

$$
U_i^\dagger \boldsymbol{\sigma} \cdot \left(\mathbf{n}_i \times \partial_\mu \mathbf{n}_i \right) U_i = 2 i K_\mu . \tag{2.45}
$$

We note here that the free action S_0 does not contain the small parameter 'a', the lattice spacing, whereas the interaction term S_1 is at least of order of a – or equivalently contains at least one derivative of the fields. In fact we can use the gradient expansion and realize

$$
\left(U_i^\dagger U_{i+1} - \mathbb{1} \right) = a U_i^\dagger \partial_x U_i + \frac{a^2}{2} U_i^\dagger \partial_x^2 U_i + \ldots \tag{2.46}
$$

Hence we achieved to write the action as a free term plus a interacting one controlled by a small parameter. For small values of the lattice constant a the high energy modes of the interacting model equation (2.42) coincide with the high energy modes of the free term (2.43). We will proceed than to individuate and then integrate out such states. At the same time the transformation given by equations (2.27) and (2.28) allowed us to rewrite the NLσM in the $\mathbb{CP}^1$ representation which is enabled of a powerful large N expansion.

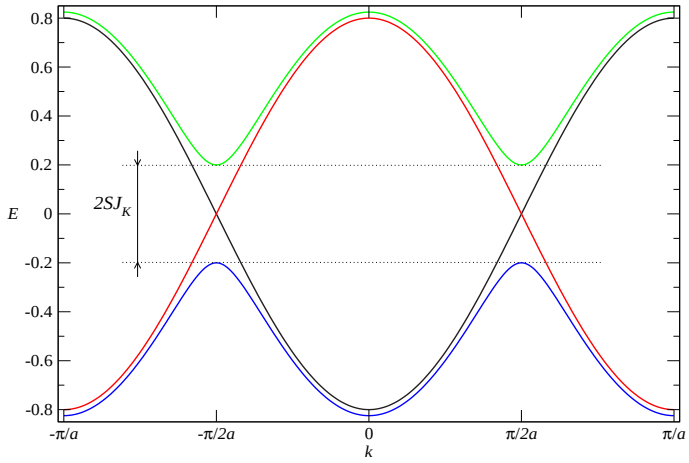

Figure 2.1: The black and red curves are the free band $e(k) = -2t\cos(ka)$ and the free-shifted $e(k+\pi/a)$ respectively. Blue and green curves are the bands in presence of the staggerization factor SJ_k indicated respectively with $\epsilon_1(k)$ and $\epsilon_2(k)$ in the text. Constants are $t = J_K = 0.4$, spin one half.

2.1.3.2 The free action

At this point it is worth studying the free action eq. (2.43), which correspond to the case where, in the original model, the spins are frozen in a perfectly antiferromagnetic (Nèel) configuration. The staggerization factor $(-1)^i$ breaks translation invariance by one site which remains by two sites. The action is readily diagonalized by going to the reduced Brillouin zone $RBZ = [-\pi/2a, \pi, 2a]$.

We obtain two bands in the RBZ separated by a gap $2J_K S$ which opens up at the Bragg points $(\pm\pi/2a)$. Passing to fermionic Matsubara frequency, the free action in the new states looks[2]

$$S_0 = \sum_{k,\omega_n} \sum_{\lambda,\alpha} \left(i\omega_n + \epsilon_\lambda(k)\right) \chi^{*\lambda}_{k,\omega_n,\alpha} \chi^{\lambda}_{k,\omega_n,\alpha}\,, \tag{2.47}$$

[2]For the sign convention on the Fourier transform for fermionic variables see eq. (3.7) on page 70.

where $\lambda = 1, 2$ is the band index and the energy bands are given by

$$\epsilon_\lambda (k) = (-1)^\lambda \sqrt{4t^2 \cos (ka)^2 + S^2 J_K^2}, \tag{2.48}$$

and are shown in figure 2.1. Now we see that we achieved also the last goal. The states χ^2 are separated —at least at the free level— by an energy of the order $2SJ_K$ from the states χ^1. Hence we recognize in χ^2 the high energy modes. We want then to integrate out these states and at the same time to pass to the continuum limit in the fermionic variables. These are the different steps of our procedure:

1. Express the action S_F in the reduced Brillouin zone.
2. Pass to the new states χ^λ which diagonalize the free problem.
3. Find the "continuum limit" of the theory. As we want to study the limit in which the doping (δ) goes to zero, the chemical potential will be very close to the minimum of the lowest band. The important k points are those close to such a minimum attained at a certain wave-vector k_0. We will then expand quadratically around such a minimum. In fact, the standard procedure of expanding linearly around the Fermi momenta $\pm k_F$, does not work since the Fermi velocity goes to zero as $\delta \to 0$.
   At this stage the free action for the lowest band assume the familiar form:
   $$S_{0,L} = \int dx \int_0^\beta d\tau \left(\chi^* \partial_\tau \chi + \frac{1}{2m} \partial \chi_x^* \partial_x \chi \right). \tag{2.49}$$
4. Finally we can integrate out the highest band states.

We note in passing, that steps 3) and 4) in fact commute. Performing first step 4) and then step 3) is perhaps more satisfying from a logical point of view. We verified that integrating first the high energy modes and then passing to the continuum limit produce the same result. Here we follow steps 3) and 4) in this order as in this case calculations are simplified.

A comment on gauge symmetry is due here. The action we started with, Eq. (2.42) possessed a gauge symmetry given by equation (2.31). The final result, which represent the low energy part of the theory, must also satisfies gauge invariance. So in the new states χ we must also have invariance through following transformations:

$$\chi \to e^{-i\phi\sigma^z}\chi, \quad Z \to e^{+i\phi}Z\,. \tag{2.50}$$

Following [117], we call the charge associated with the above gauge transformation Z charge. Then χ_1 has Z charge -1 χ_2 has charge +1 and the boson field Z has also charge +1.[3] As we want the final Lagrangian – function of the χ and Z fields – to be invariant after the transformation (2.50), it must contain only objects of Z charge zero. It is then possible to write such a Lagrangian with this only symmetry requirement. This phenomenological approach has indeed been followed by Wen in [117] where he presented a phenomenological effective action for the 2D cuprates materials. Here we substitute intuition by the actual calculation and show explicitly that the effective action has indeed the form suggested by Wen.[4] Moreover we are able to link the parameter of that theory with those of a microscopical model for the doped antiferromagnets.

2.1.3.3 Action in the Reduced Brillouin Zone

In the reduced Brillouin zone we call the states $\left(\psi^1_{k,\alpha}, \psi^2_{k,\alpha}\right) = \left(\psi_{k,\alpha}, \psi_{k+Q,\alpha}\right)$, then we have

$$\begin{aligned} S_0 \;=\; & \sum_{k,\alpha,\gamma,\lambda} \psi^{*\gamma}_{k,\alpha} \Big[\left(i\omega_n\right)\delta^{\gamma,\lambda} - 2t\cos\left(ak\right)\left(\tau^z\right)^{\gamma,\lambda} \\ & + \alpha S J_K \left(\tau^x\right)^{\gamma,\lambda} \Big] \psi^{\lambda}_{k,\alpha}, \end{aligned} \tag{2.51}$$

[3] We call the two components of the spinor $\chi = (\chi_1, \chi_2)$ and not "up" and "down", as, after the transformation (2.27) the spin degree of freedom is coupled to the field $\mathbf{n}$ and makes no sense anymore to talk about a χ hole with spin up/down.

[4] Actually Wen completely discard the K_μ field, arguing that these terms are insignificant and can be ignored in the leading order approximation [117].

$$S_1 = \sum_{k,q} \sum_{\alpha,\beta,\gamma,\lambda} \psi^{*\gamma}_{k,\alpha} \left\{ \left[\left(U^\dagger \partial_\tau U\right)^{\alpha,\beta}_{k-q} - \frac{J_K}{2J_H} \left(K_\tau\right)^{\alpha,\beta}_{k-q} \right] \delta^{\gamma,\lambda} - t \left(e^{iqa} \Omega^{\alpha,\beta}_{k-q} \left(\tau^x\right)^{\gamma,\lambda} + \text{h.c.} \right) \right\} \psi^{\lambda}_{q,\beta} \,, \tag{2.52}$$

where $\tau^{x,y,z}$ are Pauli matrices in the internal "band space", and momentum sums extend over the the reduced Brillouin zone.

With the spin dependent rotation $M_{k,\alpha}$ we diagonalize S_0: $\psi^{\gamma}_{k,\alpha} = \sum_\lambda M^{\gamma,\lambda}_{k,\alpha} \chi^{\lambda}_{k,\alpha}$. In this basis the zeroth order action has the form (2.47).

2.1.3.4 Continuum limit

For small doping fraction, the most important k points are those close to the minimum of the lowest band. From the explicit from of the bands Eq. (2.48) we see that this minimum falls at $k = 0$ for all the values of the parameters. So in S_0 we can expand the k sum around this point. In the fluctuating part S_1 the presence of the matrix field U constrains $k \approx q$. In fact as we supposed ($\mathbf{n}_i$ and hence) U_i slowly varying, its Fourier transform U_k has only small momentum transfer. Exploiting also the following property of the U matrices

$$\frac{1}{2} \left[U^\dagger \partial^2_\mu U + \left(U^\dagger \partial^2_\mu U\right)^\dagger \right] = \left(K_\mu\right)^2 - \mathbb{1} \left(a_\mu\right)^2 , \tag{2.53}$$

we obtain

$$S_1 = \sum \chi^{*\gamma}_{k,\alpha} \left\{ \left[\left(U^\dagger \partial_\tau U\right)^{\alpha,\beta}_{k-q} - \frac{J_K}{2J_H} \left(K_\tau\right)^{\alpha,\beta}_{k-q} \right] \left(M^\dagger_{k,\alpha} M_{q,\beta} \right)^{\gamma,\lambda} - t \left[(iqa + ika) \left(U^\dagger \partial_x U\right)^{\alpha,\beta}_{k-q} + \left(-a^2_x + K^2_x\right)^{\alpha,\beta}_{k-q} \right] \times \left(M^\dagger_{k,\alpha} \tau^x M_{q,\beta} \right)^{\gamma,\lambda} \right\} \chi^{\lambda}_{q,\beta} \tag{2.54}$$

2.1.3.5 Gaussian integration

At this point we may integrate out the highest states χ^2. In an obvious notation, the Gaussian integration of the highest band is

$$\int D\left[\chi^{*2}\chi^2\right] e^{-\left[\chi^{*2}F_{22}\chi^2+\chi^{*2}F_{21}\chi^1+\chi^{*1}F_{12}\chi^2+\chi^{*1}F_{11}\chi^1\right]} = \exp\left[\mathrm{tr}\ln\left(F_{22}\right)+\chi^{*1}F_{12}\left(F_{22}\right)^{-1}F_{21}\chi^1-\chi^{*1}F_{11}\chi^1\right] \quad (2.55)$$

The tr ln term can be expanded again in power of a. The zero order term is the free energy of the fermions in the highest band and being a constant, can be discarded. The first order term is proportional to

$$\sum_{\omega_n} g_{20}\left(\omega_n\right) = n\left(e_2\right), \quad (2.56)$$

where g_{20} is the Green's function for the highest band. But at zero temperature this will always be zero, as we are considering very low doping which will never excite the high energy band e_2. Similarly the term of order $O\left(a^2\right)$ is proportional to

$$\sum_{\omega_n} g_{20}\left(\omega_n\right) g_{20}\left(\omega_n\right) = n\left(e_2\right)\left(n\left(e_2\right)-1\right), \quad (2.57)$$

which is again zero at zero temperature.

The second and third term of equation (2.55) sum up to give the following effective Lagrangian

$$\begin{aligned}\mathcal{L}_{F,eff} &= \chi^*\left(\partial_\tau + ia_\tau\sigma^z\right)\chi + \frac{1}{2m}\left[\left(\partial_x + ia_x\sigma^z\right)\chi\right]^\dagger\left[\left(\partial_x + ia_x\sigma^z\right)\chi\right] \\ &\quad -\frac{1}{2m}K_x^2\chi^*\chi - |t|\left(\chi^*K_x(\partial_x\chi) - (\partial_x\chi)^*K_x\chi\right) \\ &\quad +\left(1-\frac{J_K}{2J_H}\right)\frac{1}{|t|\,m}\chi^*K_\tau\chi \\ &\quad -\left(1-\frac{J_K}{2J_H}\right)^2\frac{\left(J_KS\right)^2}{2\left(4t^2+J_K^2S^2\right)^{3/2}}\left(K_\tau\right)^2\chi^*\chi \end{aligned} \quad (2.58)$$

where the band curvature is

$$\frac{1}{2m} = \frac{2t^2}{\sqrt{4t^2 + S^2 J_K^2}} a^2. \tag{2.59}$$

We note here that the sign appearing in front of the terms linear in K_μ, i. e. the third and fourth term in eq. (2.58), is conventional[5]. In fact it depends on the phases of the eigenvectors of the free problem, which is arbitrary. Indeed one can perform a rigid rotation $\chi \to \sigma^z \chi$ and see that all the terms remains invariant except the ones linear in the K_μs which gain a minus sign. The field Z is described by the non linear model action plus topological term. The total effective Lagrangian is then

$$\mathcal{L}_{eff} = \mathcal{L}_{F,eff} + \mathcal{L}_{NL\sigma M} + i\vartheta \mathcal{L}_{\text{top. term}}, \tag{2.60}$$

where the ϑ angle is $2\pi S$ as defined in equation (2.25). For completeness we rewrite also the NLσM Lagrangian in the $\mathbb{CP}^1$ representation:

$$\mathcal{L}_{NL\sigma M} = \frac{2}{g}\left[v_s \left|(\partial_x - a_x) Z\right|^2 + \frac{1}{v_s}\left|(\partial_\tau - a_\tau) Z\right|^2\right] \tag{2.61}$$

$$\mathcal{L}_{\text{top. term}} = \frac{1}{2\pi}\left(\partial_\tau a_x - \partial_x a_\tau\right). \tag{2.62}$$

The effective Lagrangian for the fermions Eq. (2.58) can be rewritten in terms of the original vector field $\mathbf{n}$ by going to a global reference frame:

$$\tilde{\chi} = U\chi. \tag{2.63}$$

In terms of these states the Lagrangian is

[5] Of course the *relative* sign is not conventional but fixed by the mapping.

$$\begin{aligned}\mathcal{L}_{F,eff} &= \tilde{\chi}^*\partial_\tau\tilde{\chi} + \frac{1}{2m}\left|\partial_x\tilde{\chi}\right|^2 + i\left(\frac{1}{4m} - \frac{|t|}{2}\right)(\mathbf{n}\times\partial_x\mathbf{n})\cdot\left[\left(\partial_x\tilde{\chi}\right)^*\boldsymbol{\sigma}\tilde{\chi} - \tilde{\chi}^*\boldsymbol{\sigma}\partial_x\tilde{\chi}\right] \\ &+ \left(\frac{1}{4m} - \frac{|t|}{2}\right)\left|\partial_x\mathbf{n}\right|^2\tilde{\chi}^*\tilde{\chi} + \frac{i}{2}\left[1 - \left(1 - \frac{J_K}{2J_H}\right)\frac{1}{|t|\,m}\right]\tilde{\chi}^*\boldsymbol{\sigma}\cdot(\mathbf{n}\times\partial_\tau\mathbf{n})\,\tilde{\chi} \\ &+ \left(1 - \frac{J_K}{2J_H}\right)^2\frac{\left(J_K S\right)^2}{8\left(4t^2 + J_K^2 S^2\right)^{3/2}}\left|\partial_\tau\mathbf{n}\right|^2\tilde{\chi}^*\tilde{\chi}. \end{aligned} \tag{2.64}$$

This Lagrangian describes fermions interacting with an antiferromagnetic spin background via a current-current coupling. In fact we can easily recast the Lagrangian (2.64) in the following form

$$\mathcal{L}_{F,eff} = \tilde{\chi}^*\partial_\tau\tilde{\chi} + \frac{1}{2m}\left|\partial_x\tilde{\chi}\right|^2 + \sum_{\mu=x,\tau}\left(c_\mu\left|\partial_\mu\mathbf{n}\right|^2\tilde{\chi}^*\tilde{\chi} + \gamma_\mu\mathbf{J}_\mu^S\cdot\mathbf{J}_\mu^F\right),$$

with appropriate real constants c_μ, γ_μ. The current-current coupling is similar to the one obtain by Shraiman and Siggia for the two dimensional $t-J$ model [118, 119]. For the temporal component we have a coupling between the local spin-density of the fermions $\mathbf{J}_\tau^F = \tilde{\chi}^*\boldsymbol{\sigma}\tilde{\chi}$ and the background magnetization $\mathbf{J}_\tau^S = i\mathbf{n}\times\partial_\tau\mathbf{n}$. The spatial component, instead, denotes a coupling between the spin-current of the holes $\mathbf{J}_x^F = i\left[\left(\partial_x\tilde{\chi}\right)^*\boldsymbol{\sigma}\tilde{\chi} - \tilde{\chi}^*\boldsymbol{\sigma}\partial_x\tilde{\chi}\right]$ and the magnetization current of the background $\mathbf{J}_x^S = \mathbf{n}\times\partial_x\mathbf{n}$. We would like to stress that the coupling constants as well as the masses in equation (2.64), were directly derived from the microscopic underlying HKL model, in contrast to phenomenological hydrodynamical descriptions like the one proposed by Shraiman and Siggia for the two dimensional $t-J$ model [118, 119].

2.2 Ladder case

The same procedure can be generalized to ladders. In case of an M-leg ladder, the HKL action for holes interacting with an antiferromagnetic spin

background is

$$\begin{aligned} S &= \int_0^\beta d\tau \left\{ \sum_{i=1}^{N}\sum_{j=1}^{M} c_{i,j}^* \partial_\tau c_{i,j} - t_{||} \left(c_{i,j}^* c_{i+1,j} + \text{h.c.} \right) \right. \\ &\quad -t_\perp \sum_{i=1}^{N}\sum_{j=1}^{M-1} \left(c_{i,j}^* c_{i,j+1} + \text{h.c.} \right) + \\ &\quad +SJ_K \sum_{i=1}^{N}\sum_{j=1}^{M} \mathbf{R}_{i,j} \cdot \hat{\Omega}_{i,j} + S^2 J_\perp \sum_{i=1}^{N}\sum_{j=1}^{M-1} \hat{\Omega}_{i,j} \cdot \hat{\Omega}_{i,j+1} + \\ &\quad \left. +S^2 J_{||} \sum_{i=1}^{N}\sum_{j=1}^{M} \left(\hat{\Omega}_{i,j} \cdot \hat{\Omega}_{i+1,j} + i\omega_B \left[\hat{\Omega}_{i,j}(\tau) \right] \right) \right\} \end{aligned} \tag{2.65}$$

The label j refers to the perpendicular direction and we allowed for an anisotropy between the parallel and perpendicular direction, to account for generalizations.

In mapping an antiferromagnetic ladder to a non linear sigma model, there is some arbitrariness in how one chooses the order parameter. This was made clear by Sierra in [84, 120]. The physical conclusions are in all cases the same and are, as the now vast literature on the subject confirms:

- A spin gap exist when SM is an integer
- For integer spin, the spin gap goes to zero exponentially with the number of legs

In all cases one maps the Heisenberg antiferromagnetic ladder onto a non linear sigma model, but the coupling constant and the spin wave velocity which characterize this model can be slightly different renormalized. Here we follow the most natural choice of [32] and parametrize the field as follows

$$\hat{\Omega}_{i,j} = (-1)^{i+j} \mathbf{n}_i \sqrt{1 - \frac{a^2}{S^2} |\mathbf{l}_{i,j}|^2} + \frac{a}{S} \mathbf{l}_{i,j} \tag{2.66}$$

As for the chain we have the constraints $|\mathbf{n}_i|^2 = 1$ and $\mathbf{n}_i \cdot \mathbf{l}_{i,j} = 0$. We see that in the parametrization (2.66) we assumed that the slow varying field $\mathbf{n}$

depends only on the index i along the chain, but not on the index j which label the various chains. This assumption is justified if the correlation length ξ is much greater then the total width of the ladder: $\xi \gg Ma$. Under this hypothesis in fact, the variation of $\hat{\Omega}$ from chain to chain are described by the small fluctuations $\mathbf{l}$, for which we admit a dependence on the index j.

The validity of such hypothesis is confirmed, in the isotropic case $J_{||} = J_{\perp}$, from numerical studies on spin 1/2 ladders [21, 22]. At zero temperature, for an even number of chains, one finds, for instance $\xi = 3.24a$ for two chains and $\xi = 10.3a$ for four chains, and, in general that increasing the number of chains, the hypothesis $\xi \gg Ma$ is better and better verified. On the other hand, for an odd number of chains and half integer spin, the correlation length diverges and hence the hypothesis is surely verified. Finally for half-integer spin, the assumption $\xi \gg Ma$, is better obeyed for small $J_{\perp}/J_{||}$. In the limit $J_{\perp}/J_{||} \to 0$ in fact, the correlation length diverges as one would expect in the case of decoupled chains.

We substitute then formula (2.66) in the action (2.65). The steps are again similar as in the chain case. We perform the gradient expansion of the dynamical fields in the direction parallel to the chain but not in the perpendicular one. After integrating out the fluctuating field $\mathbf{l}$ the final result for the action is:

$$S = S_F + S_{NL\sigma M} + i\vartheta\omega_T, \tag{2.67}$$

where

$$\begin{aligned} S_F \;=\; & \int_0^{\beta} d\tau \left\{ \sum_{i=1}^{N}\sum_{j=1}^{M} c^*_{i,j}\partial_\tau c_{i,j} - t_{||}\left(c^*_{i,j}c_{i+1,j} + \text{h.c.}\right) \right. \\ & -t_{\perp}\sum_{i=1}^{N}\sum_{j=1}^{M-1}\left(c^*_{i,j}c_{i,j+1} + \text{h.c.}\right) + SJ_K\sum_{i=1}^{N}\sum_{j=1}^{M}(-1)^{i+j}\,\mathbf{R}_{i,j}\cdot\mathbf{n}_i \\ & \left. + i\frac{J_K}{4J_{||}}M\sum_{i=1}^{N}\sum_{j=1}^{M} C_j\left(J_{\perp}/J_{||}\right)\mathbf{R}_{i,j}\cdot[\mathbf{n}_i\times\partial_\tau\mathbf{n}_i]\right\}, \end{aligned} \tag{2.68}$$

where the parameters of the NLσM are now

$$g = \frac{2}{SM\sqrt{f_M\left(J_\perp/J_{||}\right)}},\ v_s = 2J_{||}Sa\frac{1}{\sqrt{f_M\left(J_\perp/J_{||}\right)}}\ \theta = 2\pi S\delta_{M,\text{odd}}\,. \quad (2.69)$$

Hence we see that the topological term is effective only for M odd and S half odd integer. The function $f_M(z)$ appearing in eq. (2.69) is related to the following $M \times M$ matrix A_{ab}

$$A = \begin{pmatrix} 4J_{||}+J_\perp & J_\perp & & & & \\ J_\perp & 4J_{||}+2J_\perp & J_\perp & & & \\ & J_\perp & \ddots & \ddots & & \\ & & \ddots & 4J_{||}+2J_\perp & J_\perp & \\ & & & J_\perp & 4J_{||}+J_\perp \end{pmatrix}, \quad (2.70)$$

with the help of which the function $f_M\left(J_\perp/J_{||}\right)$ is

$$f_M\left(\frac{J_\perp}{J_{||}}\right) = \frac{4J_{||}}{M}\sum_{ab}\left(A^{-1}\right)_{ab}\,, \quad (2.71)$$

whereas the vector C_a $(M \times 1)$ is

$$C_a = \frac{4J_{||}}{M}\sum_{b}\left(A^{-1}\right)_{ab}\,. \quad (2.72)$$

We note here that the function $f_M(z)$ can be calculated exactly for general number of legs M [84], but as we deal only with the two and three leg ladder, it suffices for us know:

$$\begin{aligned} f_2(z) &= \tfrac{1}{1+\frac{1}{2}z} &&=|_{z=1} \quad \tfrac{2}{3} = 0.6666\ldots \\ f_3(z) &= \tfrac{\left(1+\frac{1}{12}z\right)}{\left(1+\frac{3}{4}z\right)} &&=|_{z=1} \quad \tfrac{13}{21} = 0.6190\ldots \end{aligned} \quad (2.73)$$

and

$$\begin{aligned} C_2^{\top}(z) &= \tfrac{1/2}{1+z/2}[1,1] &&=|_{z=1} \quad \tfrac{1}{3}[1,1] \\ C_3^{\top}(z) &= \tfrac{1}{3}\tfrac{1}{\left(1+\frac{3}{4}z\right)}\left[\left(1+\tfrac{z}{4}\right),\left(1-\tfrac{z}{4}\right),\left(1+\tfrac{z}{4}\right)\right] &&=|_{z=1} \quad \tfrac{1}{3}\tfrac{1}{7}[5,3,5]\ . \end{aligned} \tag{2.74}$$

Again we rotate the quantization axis of the spin along the direction of the field $\mathbf{n}_i$:

$$c_{i,j,\alpha}(\tau) = \left[U_i(\tau)\right]_{\alpha,\beta}\psi_{i,j,\beta}(\tau)\ , \tag{2.75}$$

where the matrix U_i again satisfies equation (2.28). Plugging Eq. (2.75) into (2.68) and performing the gradient expansion of the matrix field U_i in the direction along the chain, we can again recognize a free term S_0 plus a fluctuating one S_1. Now we will show in detail for the two- and three-leg ladder what kind of low energy action arise.

2.2.1 Two-leg ladder

A two-leg ladder with open boundary conditions in the direction of the rungs (say the 'y' direction), is equivalent to the same system with periodic boundary conditions and constant halved in the same direction. The momentum in the perpendicular direction assumes only two values and distinguish between symmetric ($k_y = 0$) and antisymmetric ($k_y = \pi$) states. The free action S_0 is readily diagonalized in the reduced Brillouin zone and we find therefore four states, two low and two high energy ones separated by a gap of the order J_K. Since the Kondo coupling is the highest energy scale we can integrate out these high states. The two lowest states are instead separated by a gap of the order of $t_{||}t_{\perp}/J_K$ which does not need to be big. So at first we keep also these states. The result is

$$\begin{aligned}\mathcal{L}_{eff} &= \sum_{\lambda=s,a}\Bigg\{\chi^*_\lambda\left(\partial_\tau + ia_\tau\sigma^z\right)\chi_\lambda + \frac{1}{2m_\lambda}\left[\left(\partial_x + ia_x\sigma^z\right)\chi_\lambda\right]^\dagger\left[\left(\partial_x + ia_x\sigma^z\right)\chi_\lambda\right] \\ &\quad -\frac{1}{2m_\lambda}K_x^2\chi^*_\lambda\chi_\lambda - b_\lambda K_\tau^2\chi^*_\lambda\chi_\lambda - |t_{||}|\left(\chi^*_\lambda K_x(\partial_x\chi_\lambda) - (\partial_x\chi_\lambda)^* K_x\chi_\lambda\right) \\ &\quad +\left(1-\frac{J_K}{4J_{||}}f_2\left(J_\perp/J_{||}\right)\right)\frac{1}{|t_{||}|\,m_\lambda}\chi^*_\lambda K_\tau\chi_\lambda + \delta_{\lambda,a}\epsilon_{0,a}\Bigg\}, \qquad (2.76)\end{aligned}$$

As for the chain case, the overall sign of the terms linear in the K_μs is conventional. The constants are given by

$$\frac{1}{2m_s} = \frac{t_{||}\left(2t_{||}+t_\perp\right)}{\sqrt{S^2J_K^2+\left(2t_{||}+t_\perp\right)^2}} \qquad (2.77)$$

$$\frac{1}{2m_a} = \frac{t_{||}\left(2t_{||}-t_\perp\right)}{\sqrt{S^2J_K^2+\left(2t_{||}-t_\perp\right)^2}} \qquad (2.78)$$

$$b_\lambda = \left(1-\frac{J_K}{4J_{||}}f_2\left(J_\perp/J_{||}\right)\right)^2\frac{\left(J_KS\right)^2}{2\left(S^2J_K^2+\left(2t_{||}\pm t_\perp\right)^2\right)^{\frac{3}{2}}} \qquad (2.79)$$

$$\epsilon_{0,a} \approx \frac{4t_{||}t_\perp}{SJ_K} \qquad (2.80)$$

where in equation (2.79) the plus refers to the symmetric states ($\lambda = s$) and the minus to antisymmetric ones. What is important is that, since the original model was symmetric upon interchanging chain one with chain two, and at the same time changing the sign of $\mathbf{n}_i$, we cannot have couplings between symmetric and antisymmetric states. This implies that these two channels behave exactly in the same manner under the influence of the antiferromagnetic spin background.

2.2.2 Three leg ladder

Finally we present the result for the three leg ladder. If we order our states as 1, 2, 3 from top to bottom say, the action is invariant under swapping the extremities: $(1,2,3) \to (3,2,1)$ (and $\mathbf{n}_i$ stays the same). After passing to the reduced Brillouin zone, we have 6 states, two antisymmetric and four symmetric. The symmetric bonding is the lowest in energy in the free part. As for the other cases, half of the states (3) are separated by gap of the order J_K from the other on whereas the lowest three are separated by gaps of order $t_{||}t_\perp/J_K$. After integrating out the highest states and passing to the continuum limit, we obtain

$$\begin{aligned}
\mathcal{L}_{eff} \;=\; & \sum_{\lambda=A,Sb,Sa} \Big\{ \chi^*_\lambda \left(\partial_\tau + i a_\tau \sigma^z\right) \chi_\lambda + \frac{1}{2m_\lambda} \left[\left(\partial_x + i a_x \sigma^z\right) \chi_\lambda\right]^\dagger \left[\left(\partial_x + i a_x \sigma^z\right) \chi_\lambda\right] \\
& - \frac{1}{2m_\lambda} K_x^2 \chi^*_\lambda \chi_\lambda - b_\lambda K_\tau^2 \chi^*_\lambda \chi_\lambda - |t_{||}| \left(\chi^*_\lambda K_x (\partial_x \chi_\lambda) - (\partial_x \chi_\lambda)^* K_x \chi_\lambda\right) \\
& + \left(1 - \frac{J_K}{4J_{||}} c_\lambda \left(J_\perp/J_{||}\right)\right) \frac{1}{\left|t_{||}\right| m_\lambda} \chi^*_\lambda K_\tau \chi_\lambda + \delta_{\lambda,A}\epsilon_{0,A} + \delta_{\lambda,Sa}\epsilon_{0,Sa} \\
& - \frac{J_K}{2J_{||}} \left(\frac{z/4}{1+\frac{3}{4}z}\right) \left(\frac{\sqrt{2}t_\perp}{2SJ_K}\right) \left(\chi^*_{Sb} K_\tau \chi_{Sa} + \chi^*_{Sa} K_\tau \chi_{Sb}\right) \Big\}. \qquad (2.81)
\end{aligned}$$

here the label λ stays for antisymmetric, symmetric-bonding, symmetric-antibonding, z is the anisotropy $z = J_\perp/J_{||}$. The other constants are

$$\frac{1}{2m_{Sb,Sa}} = \frac{t_{||}\left(2t_{||} \pm \sqrt{2}t_\perp\right)}{\sqrt{S^2J_K^2 + \left(2t_{||} \pm \sqrt{2}t_\perp\right)^2}} \equiv \frac{t_{||}\left(2t_{||} \pm \sqrt{2}t_\perp\right)}{d_{Sb,Sa}} \qquad (2.82)$$

$$\frac{1}{2m_A} = \frac{2t_{||}^2}{\sqrt{S^2J_K^2 + 4t_{||}^2}} \equiv \frac{2t_{||}^2}{d_A} \qquad (2.83)$$

$$b_\lambda = \left(1 - \frac{J_K}{4J_{||}} c_\lambda \left(J_\perp/J_{||}\right)\right)^2 \frac{\left(J_K S\right)^2}{2\left(d_\lambda\right)^3} \qquad (2.84)$$

$$\epsilon_{0,A} \approx \frac{t_{||}\left(2\sqrt{2}t_{||} + t_\perp\right)}{SJ_K}, \quad \epsilon_{0,Sa} \approx \frac{4\sqrt{2}t_{||}t_\perp}{SJ_K}. \qquad (2.85)$$

The constants c_λ, ordered as $c = (c_A, c_{,Sb}, c_{Sa})$ are given by ($z = J_\perp / J_{||}$):

$$c(z) = \frac{1}{1 + \frac{3}{4}z}\left(1 + \frac{z}{4}, 1, 1\right) = \left(\frac{5}{7}, \frac{4}{7}, \frac{4}{7}\right), \text{ for } z = 1. \tag{2.86}$$

The last term of equation (2.81), a coupling between the bonding antibonding sates, is the only channel allowed by the symmetry. We can see that, correctly goes to zero both for $J_\perp$ and $t_\perp$ going to zero.

Looking at the Lagrangian (2.81) we can note that, as a result of the interaction between mobile holes and an antiferromagnetic spin background, two fermionic channels (symmetric bonding and antibonding) behaves similarly, whereas a third one, the antisymmetric channel, has a different dynamic.

Chapter 3

Spin gap vs doping in a two-leg ladder

In the previous chapter we have seen that holes in an antiferromagnetic spin background can be described by a non linear sigma model minimally coupled to fermions via a U(1) gauge field plus an interaction term reminiscent of the off-diagonal part of the whole SU(2) group (or better of its algebra). This interaction could be cast into the form of a current-current interaction. If we are only interested in the dynamic of the spins, we can still integrate out the fermions and obtain — by symmetry argument — a non linear sigma model with parameter renormalized by the chemical potential [121]. In this case though, another approach is feasible and more powerful. This will also provide an explanation for some steps we did in the previous chapter (see the discussion in section 3). Most of this chapter is devoted to the description of this technique. Here we can anticipate that the starting point consists in integrating out all the fermion at first. This is always possible since our model is quadratic in the fermions. The result of the Gaussian integration is a fermionic determinant. In seeking for a continuum limit i.e. an expansion in power of the lattice constants, this determinant contains also zero order terms which depend on the dynamical field. This was not so in the approach of the previous chapter where we saw explicitly that the fluctuating action S_1 (Eq. (2.44)) was at least of first order in the lattice constant. The calculation

of this zeroth order term constitutes the major problem.

The result is again a nonlinear sigma model, with parameter renormalized by the hole concentration. In the case of a two leg ladder neither the spin part [32, 84] nor — as we will show explicitly — the fermionic part, contribute, in the continuum limit with a topological term. This is opposed to the case of the single chain where Tsvelik [122] has shown that a similar model, in the opposed limit of half filling, both spin and fermionic part contribute a topological term of equal and opposite magnitude, which hence cancel from the low energy description of the model.

The absence of the topological term allows us to use all the known result on the NLσM, a well studied theory, integrable in the sense that the exact form of the S-matrix is known [123]. This means in particular that the spin liquid state of the undoped system – a state characterized by rotational symmetry and exponentially falling-off correlation – is not destroyed by a minimal concentration of holes, but survives at least up to a finite doping. Moreover we are able to make prediction about the quantities characterizing the spin liquid state interacting with a finite, small, amount of dopant carriers. In particular we are able to study the evolution of the spin gap as a function of the hole concentration.

This problem is not only of theoretical relevance. As we saw in the first chapter, Cu_2O_3 ladders are present in $Sr_{14-x}Ca_xCu_{24}O_{41}$ which constitutes a perfect playground to study the influence of doping on a spin liquid state. In fact, with isovalent Ca^{2+} substitution of Sr^{2+} holes are transferred from the CuO_3 chains to the ladders [76], increasing the conductivity of the latter. Two crucial ingredients signaling a spin liquid state, the presence of a spin gap and a finite correlation length are confirmed from a number of experiments [38, 35, 36, 37, 57, 124]. The spin gap, as measured by various nuclear magnetic resonance (NMR) experiments [35, 36, 37] is seen to diminish with increasing doping concentration.

From the theoretical point of view, a contradiction has arisen between numerical simulation and analytical works. As we already saw, the simplest model which is believed to grasp the physics of the problem is the $t - J$

model on a two leg ladder. It is believed in general that this system evolves continuously from the isotropic case to the limit of strong rung interaction. In this limit some simplifying pictures are at hand: without doping the gap is the energy of promoting a singlet rung to a triplet proportional to $J_\perp$. Interaction among the rungs leads eventually to the usual magnon band. Upon doping the systems shows two different kinds of spin excitations [125, 126]. One is still the singlet-triplet transition as before, the other one corresponds to the splitting of a hole pair into a couple of quasiparticles (formed by a spinon and an holon), each carrying charge $+|e|$ and spin 1/2. The number of possible excitations is proportional to $(1-\delta)$ (for the magnons) and δ (for the quasiparticles), respectively, where δ is the number of holes per copper sites. For this reason, at low doping concentration, the magnon gap will be the most important in influencing the form of the static susceptibility or dynamical structure factor.

First Sigrist *et al.* [127] and more recently Lee *et al.* [128] attacked the problem ultimately with some sort of mean field decoupling. Their results agree in predicting an increase of the magnon gap (Δ_M, originated from the singlet-triplet transition), in clear contradiction to the above mentioned experiments. Lee *et al.* were also able to calculate a decrease of the quasiparticle gap (Δ_{QP} originated from the splitting of a hole pair) for small doping concentrations.
In contrast to the mean-field results above, Ammon *et al.* [34] obtained a decrease of the magnon gap and an almost doping independent Δ_{QP} using temperature density matrix renormalization group (TDMRG). The behavior of the magnon gap observed numerically is consistent with the one observed in several experiments, and hence it is natural to ascribe those experimental observations to Δ_M.

Here we concentrate on the behavior of the magnon gap upon doping. Due to the contradiction above it is imperative to go beyond mean field and include the role of fluctuations in a controlled manner. As we already discussed, the mapping from an AFM Heisenberg model to the non linear σ model, is perfectly suited to include the role of quantum fluctuations and proved

very efficient in describing the magnetic properties of two dimensional spin lattices [129], chains [16], and ladders [32]. This mapping was extended in Ref. [130] to the case of a doped two dimensional AFM using a procedure that we will closely follow.

3.1 Integrate out the fermions

In this section we focus on the two leg ladder (see fig. 3.1). Our method can be applied with a simple trick to the original Spin Fermion model Eq. (1.12). As we want to make contact/compare with experiments, from the one hand we preferred to study the "most microscopical" model and not the Antiferromagnetic Kondo Lattice model which we introduced in section 2.1 (see eq. (2.1)). On the other hand, when comparing to experiments is also preferred to keep the number of parameters as small as possible.

We treat then the Spin Fermion Hamiltonian for a two-leg ladder which we here rewrite for clarity

$$\begin{aligned} H_{SF} &= 4t \sum_{\substack{l=1\ldots N \\ \lambda=1,2,\sigma}} P^{\dagger}_{l,\lambda,\sigma} P_{l,\lambda,\sigma} + 4J_K \sum_{\substack{l=1\ldots N \\ \lambda=1,2,\alpha,\beta}} P^{\dagger}_{l,\lambda,\alpha} \boldsymbol{\sigma}_{\alpha,\beta} P_{l,\lambda,\beta} \cdot \mathbf{S}_{l,\lambda} \\ &\quad + J_{\perp} \sum_{l=1\ldots N} \mathbf{S}_{l,1} \cdot \mathbf{S}_{l,2} + J_{||} \sum_{\substack{l=1\ldots N \\ \lambda=1,2}} \mathbf{S}_{l,\lambda} \cdot \mathbf{S}_{l+1,\lambda}, \end{aligned} \tag{3.1}$$

N is the number of the rungs along the ladder and $\lambda = 1, 2$ distinguishes the two legs. For the sake of generality, an anisotropy in the Heisenberg term is allowed. In fact, from the experimental side, the question of an anisotropy in the Heisenberg part for $Sr_{14-x}Ca_xCu_{24}O_{41}$ is still controversial [57, 124, 38]. In figure 3.1 one can see a pictorial representation of a two-leg ladder based on the Cu-O unit cell common to the High Tc superconductors.

Our starting point is always a path integral representation for the partition function, for which we need orthogonal fermion states to define the fermionic integration measure.

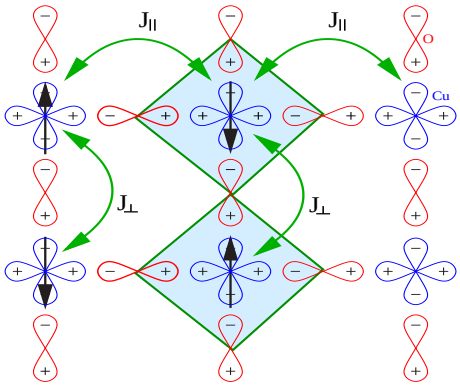

Figure 3.1: Schematic picture of a two leg ladder Copper-Oxide based on the Cu-O cell of the high-T_c superconductors.

Wannier states are easily found via $P_{\mathbf{k},\sigma} = \sqrt{\epsilon(\mathbf{k})} f_{\mathbf{k},\sigma}$where

$$\epsilon\left(\mathbf{k}\right) = \left(1 - \frac{\cos\left(k_x a\right) + \cos\left(k_y a\right)/2}{2}\right). \tag{3.2}$$

Here a is the lattice constant and we used a two dimensional Fourier transform where k_y takes only values 0 and π/a distinguishing between symmetric (bonding) and antisymmetric (antibonding) states. The partition function is expressed as a path integral

$$Z = \int D\left[f^*, f\right] D[\hat{\Omega}] e^{-S_{SF}}, \tag{3.3}$$

where $S_{SF} = S_h + S_s$. The action S_s contains all terms with spins degree of freedoms only [108]:

$$S_s = \int_0^\beta d\tau \left[-iS \sum_{l,\lambda} \mathbf{A}\left(\hat{\Omega}_{l,\lambda}\right) \cdot \frac{\partial \hat{\Omega}_{l,\lambda}}{\partial \tau} + H_{\text{Heis}}\left(S\hat{\Omega}\left(\tau\right)\right)\right], \tag{3.4}$$

We already encountered this action in the previous chapters and we know, in case no holes are presents, how to map it to its low energy effective theory the NLσM. For this reason, here we will deal mainly with the part of the action which contains fermionic degrees of freedom S_h:

$$S_h = \sum_{kq\alpha\beta} f^*_{k,\alpha} \left[\left(i\omega_n + 4t\epsilon\left(\mathbf{k}\right) - \mu \right) \delta_{k,q}\delta_{\alpha,\beta} + g\sqrt{\epsilon\left(\mathbf{k}\right)\epsilon\left(\mathbf{q}\right)}\boldsymbol{\sigma}_{\alpha,\beta} \cdot \hat{\Omega}_{k-q} \right] f_{q,\beta}, \tag{3.5}$$

we adopted the concise notation $k = (k_x, k_y, \omega_n)$ where $\omega_n = \pi\left(2n+1\right)/\beta$ are the fermionic Matsubara frequency and $g = 4J_K S$.

Our conventions for the Fourier transform of fermionic degrees of freedom are

$$f_{i,\lambda}\left(\tau\right) = \frac{1}{\sqrt{2N\beta}} \sum_{k_x \in BZ} \sum_{k_y=0,\frac{\pi}{a}} \sum_{\omega_n} e^{i(x_i k_x + a\lambda k_y + \tau\omega_n)} f_{k_x,k_y,\omega_n} \tag{3.6}$$

$$f^*_{i,\lambda}\left(\tau\right) = \frac{1}{\sqrt{2N\beta}} \sum_{k_x \in BZ} \sum_{k_y=0,\frac{\pi}{a}} \sum_{\omega_n} e^{-i(x_i k_x + a\lambda k_y + \tau\omega_n)} f^*_{k_x,k_y,\omega_n} \tag{3.7}$$

along with inverse

$$f_{k_x,k_y,\omega_n} = \frac{1}{\sqrt{2N\beta}} \sum_{i=1\ldots N} \sum_{\lambda=1,2} \int_0^\beta d\tau e^{-i(x_i k_x + a\lambda k_y + \tau\omega_n)} f_{i,\lambda}\left(\tau\right) \tag{3.8}$$

$$f^*_{k_x,k_y,\omega_n} = \frac{1}{\sqrt{2N\beta}} \sum_{i=1\ldots N} \sum_{\lambda=1,2} \int_0^\beta d\tau e^{i(x_i k_x + a\lambda k_y + \tau\omega_n)} f^*_{i,\lambda}\left(\tau\right). \tag{3.9}$$

For bosonic degrees of freedom we use instead an unconventional normalization which allows us to a avoid a proliferation of factor $1/\sqrt{2N\beta}$:

$$\Omega_{k_x,k_y,\omega_n} = \frac{1}{2N\beta} \sum_{i=1\ldots N} \sum_{\lambda=1,2} \int_0^\beta d\tau e^{-i(x_i k_x + a\lambda k_y + \tau\omega_n)} \Omega_{i,\lambda}\left(\tau\right) \tag{3.10}$$

It is natural to decompose the inverse propagator into $G^{-1} = G_0^{-1} - \Sigma$ where the free part is

$$G_0^{-1} = \left(i\omega_n + 4t\epsilon(\mathbf{k}) - \mu \right) \delta_{k,q}\delta_{\alpha,\beta}, \tag{3.11}$$

and the fluctuating external potential is

$$\Sigma = -g\sqrt{\epsilon(\mathbf{k})\epsilon(\mathbf{q})}\boldsymbol{\sigma}_{\alpha,\beta}\cdot\hat{\Omega}_{k-q}. \tag{3.12}$$

We can now integrate out the fermions f, f^*. As we only have bilinear terms, the Gaussian integration leads to

$$Z = \int D[\hat{\Omega}]e^{-\left(S_s - \mathrm{tr}\ln\left(G^{-1}\right)\right)}. \tag{3.13}$$

Defining the matrix

$$A = \sqrt{\epsilon\left(\mathbf{k}\right)}\delta_{k,q}\delta_{\alpha,\beta}\,, \tag{3.14}$$

and a rescaled propagator $\hat{G}^{-1}$ through

$$\hat{G}^{-1} = \left(A^{\dagger}\right)^{-1}G^{-1}A^{-1}, \tag{3.15}$$

we can write

$$\mathrm{tr}\ln\left(G^{-1}\right) = \mathrm{tr}\ln\left(AA^{\dagger}\right) + \mathrm{tr}\ln\left(\hat{G}^{-1}\right), \tag{3.16}$$

the first term gives just a constant and we can ignore it. Again we decompose the rescaled inverse propagator as $\hat{G}^{-1} = \hat{G}_0^{-1} - \hat{\Sigma}$ which brings us to

$$\hat{G}_0^{-1} = \left(\frac{i\omega_n + 4t\epsilon\left(\mathbf{k}\right) - \mu}{\epsilon\left(\mathbf{k}\right)}\right)\delta_{kq}\delta_{\alpha\beta} \equiv g_0^{-1}\left(k_x, k_y, \omega_n\right)\delta_{k,q}\delta_{\alpha,\beta}, \tag{3.17}$$

$$\hat{\Sigma} = -g\Omega_{\mathbf{k}-\mathbf{q},\omega-\nu}\cdot\boldsymbol{\sigma}_{\alpha\beta}. \tag{3.18}$$

The remaining part of the calculation is devoted to the evaluation of $S_{h\ \mathrm{eff}} = -\mathrm{tr}\ln\left(\hat{G}^{-1}\right)$ in the continuum limit.

3.2 Parametrization

We have already seen how to implement Haldane's mapping in a coherent state path integral. The first step is a parametrization of the fields which separates the antiferromagnetic from the ferromagnetic contributions. In Chapter 2 we gave a parametrization of the fields which admitted a simple generalization to ladders with an arbitrary number of legs. In case of the two leg ladder we can be a bit more precise. In principle we can think of a two leg ladder as two coupled chain. For each chain we can adopt the parametrization (2.9) on page 41. Then we get two antiferromagnetic order parameters $\mathbf{n}_\lambda$. Being the chains coupled, the two chains order parameters $\mathbf{n}_\lambda$ will sum to give rise to an antiferromagnetic configuration, or subtract and form ferromagnetic field $\mathbf{M}$ representing the fluctuations in the perpendicular direction. In the undoped case has already been shown that these additional field do not couple to the other fields, and, being Gaussian, can be integrated out without further consequences [84, 120]. Here we will show explicitly that even in presence of mobile charge carriers the field $\mathbf{M}$ remains uncoupled and can be safely discarded, hence providing further justification for the parameterization (2.66) on page 58.

Hence we parameterize the spin field in the following way

$$\Omega_{i,\lambda}(\tau) = (-1)^{i+\lambda}\,\mathbf{n}_{i,\lambda}\sqrt{1-\left|\frac{a\mathbf{l}_{i,\lambda}}{S}\right|^2} + \frac{a\mathbf{l}_{i,\lambda}}{S}. \tag{3.19}$$

The constraint on the spin field is resolved in the usual way imposing

$$|\mathbf{n}_{i,\lambda}|^2 = 1, \quad \text{and} \quad \mathbf{l}_{i,\lambda}\cdot\mathbf{n}_{i,\lambda} = 0, \tag{3.20}$$

The normalized effective order parameter field $\mathbf{N}$ and the additional fluctuating field $\mathbf{M}$ are then defined via

$$\mathbf{N}_i = \frac{\mathbf{n}_{i,1} + \mathbf{n}_{i,2}}{2\sqrt{1 - a^2 \left|\mathbf{M}_i\right|^2}} \tag{3.21}$$

$$\mathbf{M}_i = \frac{-\mathbf{n}_{i,1} + \mathbf{n}_{i,2}}{2a} \tag{3.22}$$

along with inverse

$$\mathbf{n}_{i,\lambda} = \mathbf{N}_i \sqrt{1 - a^2 \left|\mathbf{M}_i\right|^2} + (-1)^\lambda a \mathbf{M}_i. \tag{3.23}$$

Note that thanks to $\left|\mathbf{n}_{i,\lambda}\right|^2 = 1$, the new fields automatically satisfy $\left|\mathbf{N}_i\right|^2 = 1$ and $\mathbf{N}_i \cdot \mathbf{M}_i = 0$.

The next step is the gradient expansion, or equivalently, in Fourier space, an expansion in powers of k. Again, with the same arguments as on page 42, "dimensional engineering" tells us that in (1+1) dimension, the field $\mathbf{N}$ will get no scaling dimension, whereas the fields $\mathbf{l}$ and $\mathbf{M}$ get scaling dimension -1. Accordingly, in the subsequent expansion we will need to keep terms with up to two derivative and any power of the field $\mathbf{N}$. Terms containing $\mathbf{l}, \mathbf{M}$ are marginal whenever two fields or one field and one derivative are present. Higher order terms are irrelevant and will be discarded. This again correspond to expand all our quantities up to $O\left(a^2\right)$.

Expressing parametrizations (3.19) and (3.23) in Fourier space and inserting them in equation (3.18) we obtain the following expansion for the self energy:

$$\hat{\Sigma} = \Sigma_{00} + \Sigma_{01} + \Sigma_{02} + \Sigma_1 + \Sigma_2 + O\left(a^3\right), \tag{3.24}$$

where the various quantity are

$$\Sigma_{00} = -g\delta_{k_y-q_y,\pi}\,\mathbf{N}_{k_x-q_x+\pi,\omega-\nu}\cdot\boldsymbol{\sigma}_{\alpha\beta}, \tag{3.25}$$

$$\Sigma_{01} = -ag\delta_{k_y-q_y,0}\,\mathbf{M}_{k_x-q_x+\pi,\omega-\nu}\cdot\boldsymbol{\sigma}_{\alpha\beta}, \tag{3.26}$$

$$\Sigma_{02} = \frac{a^2g}{2}\delta_{k_y-q_y,\pi}\left(\mathbf{N}\left|\mathbf{M}\right|^2\right)_{k_x-q_x+\pi,\omega-\nu}\cdot\boldsymbol{\sigma}_{\alpha\beta}, \tag{3.27}$$

$$\Sigma_{1} = -\frac{ag}{S}\mathbf{l}_{\mathbf{k}-\mathbf{q},\omega-\nu}\cdot\boldsymbol{\sigma}_{\alpha\beta}, \tag{3.28}$$

$$\Sigma_{2} = \frac{a^2g}{2S^2}\left(\mathbf{N}\left|\mathbf{l}\right|^2\right)_{\mathbf{k}-\mathbf{q}+\mathbf{Q},\omega-\nu}\cdot\boldsymbol{\sigma}_{\alpha\beta}, \tag{3.29}$$

where $\mathbf{Q} = (\pi/a, \pi/a)$ is the antiferromagnetic modulation vector suitable for a ladder geometry. We also regroup the zero-th order term in $F^{-1} \equiv \hat{G}_0^{-1} - \Sigma_{00}$.

The quantity to be evaluated is

$$S_{h\ \mathrm{eff}} = -\mathrm{tr}\ln\left(F^{-1}\right) - \mathrm{tr}\ln\left(\mathbb{1} - F\left(\Sigma_{01}+\Sigma_{02}+\Sigma_{1}+\Sigma_{2}\right)\right). \tag{3.30}$$

The first term in Eq. (3.30) is the free energy of a system of fermions interacting with an antiferromagnetically modulated slow varying field. The second term instead, contains ferromagnetic and mixed contributions. Since the evaluation of the two terms in the continuum limits proceed along different lines we treat these two terms separately in the following two sections.

3.3 Antiferromagnetic contribution

Expanding the logarithm we rewrite the first term of the RHS of Eq. (3.30) as:

$$\begin{aligned}\mathrm{tr}\ln\left(F^{-1}\right) &= \mathrm{tr}\ln\left(\hat{G}_0^{-1}\right) + \mathrm{tr}\ln\left(\mathbb{1} - \hat{G}_0\Sigma_{00}\right)\\ &= \mathrm{tr}\ln\left(\hat{G}_0^{-1}\right) - \sum_{m=1}^{\infty}\frac{1}{m}\mathrm{tr}\left(\hat{G}_0\Sigma_{00}\right)^m.\end{aligned} \tag{3.31}$$

The first term is the free energy of free fermions and is uninteresting in the following as it is just a constant independent from the dynamical fields. Each term of the sum in Eq. (3.31) has the following expression

$$\begin{aligned}\mathrm{tr}\left(\hat{G}_0\Sigma_{00}\right)^m &= (-g)^m \sum_{k_1,k_2\ldots k_m} g_0(k_1)g_0(k_2)\cdots g_0(k_m)\\ &\times\delta_{k_y^1-k_y^2,\pi}\delta_{k_y^2-k_y^3,\pi}\cdots\delta_{k_y^m-k_y^1,\pi}\\ &\times\mathbf{N}^{a_1}_{k_1-k_2+Q}\mathbf{N}^{a_2}_{k_2-k_3+Q}\cdots\mathbf{N}^{a_m}_{k_m-k_1+Q}\\ &\times\mathrm{tr}\left(\sigma^{a_1}\sigma^{a_2}\cdots\sigma^{a_m}\right). \end{aligned} \tag{3.32}$$

Here we made explicit the presence of Kronecker delta's of the perpendicular momenta which are in fact hidden in the Fourier transformed field:

$$\mathbf{N}_q = \delta_{q_y,0}\mathbf{N}_{q_x,\nu_n}. \tag{3.33}$$

Because of these Kronecker delta's, the sum over the perpendicular momenta k_y^i gives zero whenever m is odd. In case m is even, with a change of variables and introducing the notation

$$\bar{g}_0^{-1}\left(\mathbf{k},\omega_n\right) = g_0^{-1}\left(\mathbf{k}+\mathbf{Q},\omega_n\right), \tag{3.34}$$

we can rewrite equation (3.32) as

$$\begin{aligned}\mathrm{tr}\left(\hat{G}_0\Sigma_{00}\right)^m &= (g)^m \sum_{k,q_2\ldots q_m} g_0(k)\bar{g}_0(k+q_2)g_0(k+q_3)\bar{g}_0(k+q_4)\cdots\\ &\cdots g_0(k+q_{m-1})\bar{g}_0(k+q_m)\\ &\times\mathbf{N}^{a_1}_{-q_2}\mathbf{N}^{a_2}_{q_2-q_3}\cdots\mathbf{N}^{a_m}_{q_m}\mathrm{tr}\left(\sigma^{a_1}\sigma^{a_2}\cdots\sigma^{a_m}\right), \end{aligned} \tag{3.35}$$

where m now denotes an even integer. The calculation is a bit involved and we refer to Appendix A for the details. Roughly speaking the trace over the Pauli matrices can be carried out using a trace reduction formula [131].

Moreover, from equation (3.35) for m even, since each $\mathbf{N}_q$ field has small momentum transfer, the sum over the q_j variables is effectively constrained in a neighborhood of $(q_2, q_3, \ldots, q_m) = (0, 0, \ldots, 0)$. The gradient expansion is then obtained by performing an expansion of the product of propagators $g_0(k) \cdots \bar{g}_0(k + q_m)$ in powers of the variables $q_2, q_3, \ldots q_m$ that appear as argument of the fields $\mathbf{N}$. The result which we obtain is (see also [130])

$$\operatorname{tr} \ln \left(\mathbb{1} - \hat{G}_0 \Sigma_{00} \right) = \int dx d\tau \left[\frac{\bar{\chi}_{xx}}{2} \left| \partial_x \mathbf{N} \right|^2 + \frac{\bar{\chi}_{\tau\tau}}{2} \left| \partial_\tau \mathbf{N} \right|^2 \right], \tag{3.36}$$

with the definition

$$\bar{\chi}_{\alpha\beta} = \frac{\partial^2}{\partial q_\alpha \partial q_\beta} \frac{1}{N\beta} \sum_k \ln \left[1 - g^2 g_0(k) g_0(k + q + Q) \right] \delta_{q_y 0} \Big|_{q=0} \tag{3.37}$$

where the vector Q now include the frequency part i.e. $Q = (\pi/a, \pi/a, 0)$.

3.4 Ferromagnetic and mixed contributions

Here we evaluate the contribution of

$$\operatorname{tr} \ln \left(\mathbb{1} - F \left(\Sigma_{01} + \Sigma_{02} + \Sigma_1 + \Sigma_2 \right) \right). \tag{3.38}$$

We need then to find the inverse of F^{-1} up to $O(a)$. It turns out that (see Appendix B page 134)

$$F = \bar{F} D^{-1} - a \bar{F} D^{-1} R D^{-1} + O\left(a^2\right), \tag{3.39}$$

where the various matrices are

$$\bar{F} = \bar{g}_0^{-1}(\mathbf{k},\omega)\,\delta_{kq}\delta_{\alpha\beta} - g\delta_{k_y-q_y,\pi}\mathbf{N}_{k_x-q_x+\pi}\cdot\boldsymbol{\sigma}_{\alpha\beta}, \tag{3.40}$$

$$D = D(\mathbf{k},\omega)\delta_{kq}\delta_{\alpha\beta}, \tag{3.41}$$

$$R = -g\,\delta_{k_y-q_y,\pi}\sum_{r=x,\tau}\left(k_r - q_r + \delta_{r,x}\frac{\pi}{a}\right)\partial_r g_0^{-1}(\mathbf{k},\omega)\mathbf{N}_{k-q+Q}\cdot\boldsymbol{\sigma}_{\alpha\beta}, \tag{3.42}$$

and we used the shorthand notation

$$\bar{g}_0^{-1}(\mathbf{k},\omega_n) = g_0^{-1}(\mathbf{k}+\mathbf{Q},\omega_n), \tag{3.43}$$

$$D(\mathbf{k},\omega_n) = g_0^{-1}(\mathbf{k},\omega_n)\,\bar{g}_0^{-1}(\mathbf{k},\omega_n) - g^2. \tag{3.44}$$

We can now pass to the evaluation of the second term in eq. (3.30). This does not present particular problems, since after expanding all the quantities, it reduces to the evaluation of a finite number of traces. Again, for the details see Appendix A. The result is

$$\begin{aligned}\operatorname{tr}\ln\left(\mathbb{1} - F\left(\Sigma_{01}+\Sigma_{02}+\Sigma_1+\Sigma_2\right)\right) &= i\frac{g^3}{S}\int dx\,d\tau\hat{\chi}_\tau\left(\mathbf{N}\times\partial_\tau\mathbf{N}\right)\cdot\left(\mathbf{l}_1+\mathbf{l}_2\right)\\ &\quad -\frac{g^2}{4S^2}\int dx\,d\tau\tilde{\chi}\left(|\mathbf{l}_1|^2+|\mathbf{l}_2|^2\right).\end{aligned} \tag{3.45}$$

Here we omitted to write a Gaussian term $\propto \mathbf{M}^2$, completely decoupled, which can be integrated out without further consequences. The quantities $\hat{\chi}_\tau$ and $\tilde{\chi}$ are given by

$$\hat{\chi}_\tau = -\frac{i}{N\beta}\sum_k D^{-1}(k)\partial_\omega g_0^{-1}(k)D^{-1}(k+Q), \tag{3.46}$$

$$\tilde{\chi} = \frac{1}{N\beta}\sum_k\left[D^{-1}(k)\left(g_0^{-1}(k+Q) - g_0^{-1}(k)\right)\right]^2. \tag{3.47}$$

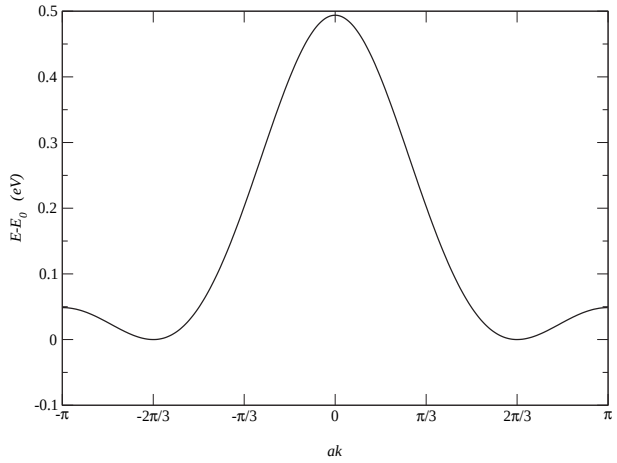

Figure 3.2: Effective holes lowest-band emerging from our theory. Parameters are $t = 0.24, J_K = 1$ eV. The minima fall exactly at $(ak) = \pm 2\pi/3$

3.4.1 The effective bands

The quantities appearing in equations (3.46), (3.47) are generalized susceptibilities of the holes in presence of the long-wavelength spin fields. In particular $\tilde{\chi}$ is the response of free fermions in a staggered field to a ferromagnetic field $\mathbf{l}$. The poles of these susceptibilities – that is, the zeros of $D(k)$– determine the effective dispersion of the holes. The doping concentration is extracted through the dependence of the chemical potential. Not surprisingly, the bands originating in such a way correspond to free holes moving in a staggered magnetic field, a result which we anticipated in the previous chapter and which provides a justification for the approach we used there. A staggered field would break translation invariance by one site and we would obtain four bands in the reduced Brillouin zone. Instead in our procedure we never broke explicitly translation invariance, so that we obtain genuinely two bands in the Brillouin zone. The lowest of these two band is symmetric in character (bonding). In Fig. 3.2 we show it for values of the constants relevant for the Copper-Oxide ladders presents in $Sr_{14-x}Ca_xCu_{24}O_{41}$ i.e. a band-width of ≈ 0.5 eV (Ref. [132]) and $J_K \approx 1$ eV [133, 134, 135]. This

band is in good agreement with accurate calculations on the one hole spectrum of the $t-J$ model. In particular, in the isotropic $t-J$ model, for $t/J \approx 2$ (which is a value relevant for the cuprates ladders) the same qualitative feature are observed: a global maximum at $(ka)=0$, global minima at $(ka) \approx \pm 2\pi/3$ and local maxima at $(ka)=\pm\pi$ [136, 137].

3.5 Result and comments

Now that we calculated the long wavelength contribution coming from the holes, we still have to consider the continuum limit (in the low energy sector) of the pure spin action S_s given by eq. (3.4). The result is

$$\begin{aligned} S_{s\,\mathrm{eff}} &= -i\int dx\,d\tau\,(\mathbf{N}\times\partial_\tau\mathbf{N})\cdot(\mathbf{l}_1+\mathbf{l}_2) + a\left(J_\parallel+\frac{J_\perp}{2}\right)\int dx\,d\tau\,(\mathbf{l}_1+\mathbf{l}_2)^2 \\ &\quad + aJ_\parallel\int dx\,d\tau\,(\mathbf{l}_1-\mathbf{l}_2)^2 + aS^2J_\parallel\int dx\,d\tau\,|\partial_x\mathbf{N}|^2\,. \end{aligned} \tag{3.48}$$

The very last step is the Gaussian integration of the $\mathbf{l}_\perp$ field, leaving us with the effective long-wavelength action for the antiferromagnetic order parameter, a (1+1) NLσM:

$$S_{\mathrm{eff}} = S_{h\,\mathrm{eff}} + S_{s\,\mathrm{eff}} = \frac{1}{2f}\int dx d\tau\left[v\,|\partial_x\mathbf{N}|^2 + \frac{1}{v}\,|\partial_\tau\mathbf{N}|^2\right], \tag{3.49}$$

where the NLσM parameters are given by

$$f = \frac{1}{2}\left[\left(S^2J_\parallel-\frac{\bar\chi_{xx}}{2}\right)\left(\frac{\left(1+\frac{g^3}{S}\hat\chi_\tau\right)^2}{\left[4J_\parallel+2J_\perp+\frac{g^2}{2S^2}\tilde\chi\right]}-\frac{\bar\chi_{\tau\tau}}{2}\right)\right]^{-\frac{1}{2}}, \tag{3.50}$$

$$v = a\left[\frac{\left(S^2J_\parallel-\frac{\bar\chi_{xx}}{2}\right)}{\left(\frac{1+\frac{g^3}{S}\hat\chi_\tau{}^2}{\left[4J_{||}+2J_\perp+\frac{g^2}{2S^2}\tilde\chi\right]}-\frac{\bar\chi_{\tau\tau}}{2}\right)}\right]^{\frac{1}{2}}. \tag{3.51}$$

Hence, the spin-fermion model with mobile holes interacting with an antiferromagnetic background is mapped into an effective NLσM whose coupling constant depend on doping through the generalized susceptibilities in Eqs. (3.37), (3.46), and (3.47).

Now we can immediately transpose to our model of a doped spin liquid, some known result for the NLσM, e. g. mainly the presence of a gap which separates the singlet ground state from a triplet of magnetic excitations. This gap should persist as long as the continuum approximation is valid.

The fact that the NLσM in (1+1) dimension has a gap above the ground state can be established in a variety of ways. Using the two loop beta function [138] one obtains

$$\Delta = v\Lambda e^{-\frac{2\pi}{f}} \left(\frac{2\pi}{f} + 1 \right), \tag{3.52}$$

where Λ is a cutoff of the order of the inverse lattice constant. Now we have an explicit analytic form for the doping dependence of the spin gap in the spin-liquid state of a two leg ladder.

It remains to calculate the doping dependence of the generalized susceptibilities i.e. evaluate the sums and integrals in eqs. (3.37), (3.46), and (3.47). The frequency sums appearing in those expressions can be evaluated exactly with standard contour integration techniques. At zero temperature, the result of the frequency sums are one-dimensional integrals over the Fermi "volume", which are easily evaluated numerically. Here we have to distinguish two regimes according to whether the minimum of the lowest effective band falls either at zero or at $2/3\pi$. For $J_K > 2t$ we have two minima at $\pm 2/3\pi$. In this case all the generalized susceptibilities in Eqs. (3.37), (3.46), and (3.47) contribute to lower f and, since from eq. (3.52) Δ is an increasing function of f, they make the gap smaller for any value of the constants (see Fig. 3.3). This is comforting, since, as we mentioned, for J_K very large the physics of the Spin-Fermion model should be similar to that of the $t - J$ model [49], and for that one, TDMRG simulations show that the gap decreases at least in a strong anisotropic case ($J_\perp = 10 J_\parallel$). When $J_K < 2t$ the band minimum falls in zero and there is one susceptibility, $\tilde{\chi}$, which instead makes f grow.

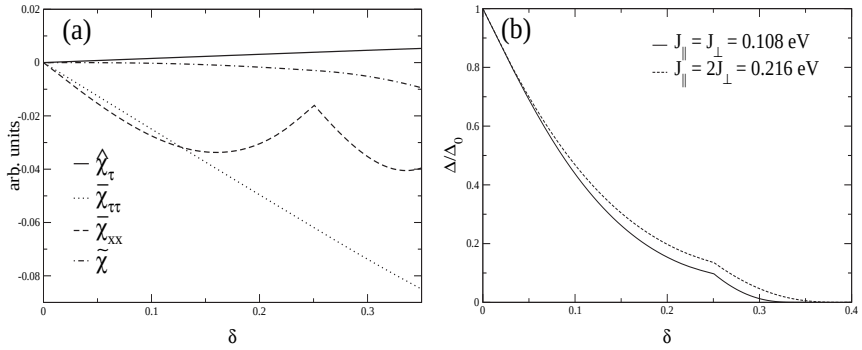

Figure 3.3: $J_K > 2t$. (a) Generalized susceptibilities of Eqs. (3.37), (3.46), and (3.47) for $J_K = 2$, $t = 0.76$ eV. For $J_K > 2t$ all the susceptibilities contribute to lower f hence the gap decreases for small doping for any value of the constants. (b) Normalized gap from eq. (3.52). Here we fixed $J_\perp = 0.108$ eV. The solid line refers to isotropic couplings $J_{||}/J_\perp = 1$. For comparison, an isotropic case with $J_{||}/J_\perp = 2$ is also shown (dashed curve). It can be seen that anisotropy does not influence greatly the gap vs. doping curve.

In this regime there is then a (small) region of parameters where the gap grows with doping (see figure 3.4).

Before passing to a comparison with experiments, we want to comment on a possible simplifying understanding.

A simple picture to explain the observed diminishing of the spin gap with doping in $Sr_{14-x}Ca_xCu_{24}O_{41}$, is that (at least for low doping concentration where speaking of a spin liquid is still feasible) the effect of the holes is that of renormalizing the anisotropy parameter $\lambda = J_\perp/J_\parallel$ for the spin part toward larger values. In many studies on the 2 leg ladder Heisenberg antiferromagnet [139, 140, 22], the spin gap is seen to increase with λ. In fact, the same occurs in the NLσMwithout doping in the range $\lambda \approx 1 \div 2$.

According to equations (3.50,3.51) effective coupling constants $\tilde{J}_\parallel, \tilde{J}_\perp$ can be defined for the doped system such that the form of the NLσM parameters is that for a pure spin system [32] i.e.

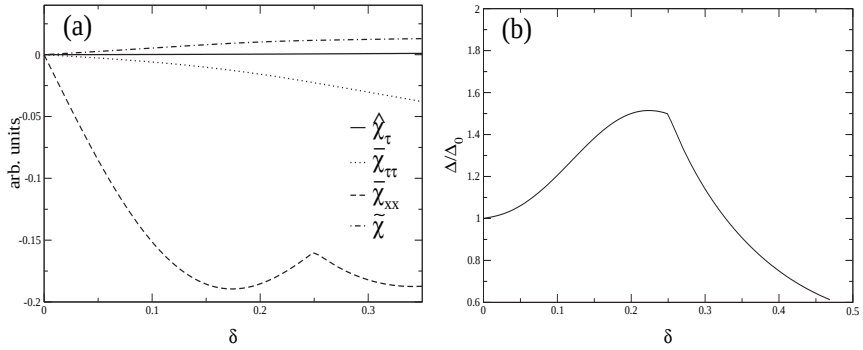

Figure 3.4: $J_K < 2t$. (a) Generalized susceptibilities of Eqs. (3.37), (3.46), and (3.47) for $J_K = 3\,t = 1.8$ eV. For $J_K < 2t$, one susceptibility, $\tilde{\chi}$, grows with doping and contributes to increase f and hence the gap. For $(J_K, t) \gg (J_{\|}, J_{\perp})$ we can have an increasing gap for small doping. (b) Normalized gap of eq. (3.52). Fixing the exchange constants to $J_{\|} = J_{\perp} = 0.108$ eV is enough to have an increasing gap for small doping.

$$f = \frac{1}{S}\sqrt{1+\frac{\tilde{J}_{\perp}}{2\tilde{J}_{\|}}}, \tag{3.53}$$

$$v = 2aS\tilde{J}_{\|}\sqrt{1+\frac{\tilde{J}_{\perp}}{2\tilde{J}_{\|}}}. \tag{3.54}$$

A small doping expansion up to $O(\delta)$ in the regime $J_K > 2t$ leads to

$$\tilde{J}_{||} = J_{||} + \frac{3}{4}\frac{(J_K^2 - 4t^2)}{J_K}\delta, \tag{3.55}$$

$$\tilde{J}_{\perp} = J_{\perp} - \left(\frac{3}{2}\frac{(J_K^2 - 4t^2)}{J_K} + 2\left(4J_{||} + 2J_{\perp}\right) + \frac{\left(4J_{||} + 2J_{\perp}\right)^2}{8J_K}\right)\delta, \tag{3.56}$$

so indeed $\tilde{J}_{\|}$, $\tilde{J}_{\perp}$ are seen respectively to increase, decrease, such that λ decreases. However, such an interpretation breaks down beyond $\delta \approx 0.04$ whereas f, v are still well defined positive constants. This means that beyond such doping, this simplified picture cannot be naïvely applied and holes have a more effective way of lowering the gap.

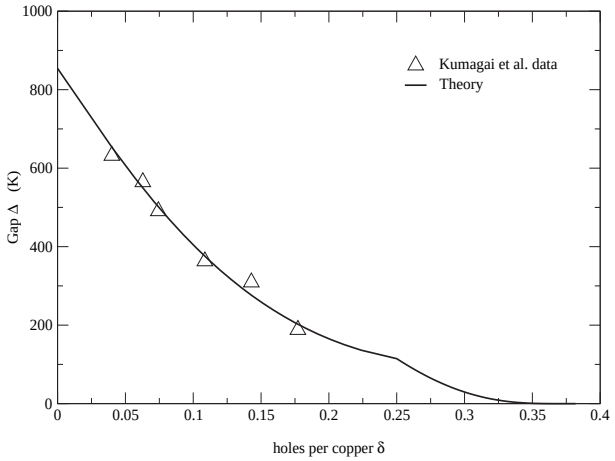

Figure 3.5: Result of our theory and comparison with experiments. The values of the constants used in equation (3.52) are $t = 0.76, J_K = 2$ eV, $J_\parallel/J_\perp = 1$. The momentum cutoff Λ was fixed by fixing the the value of the gap with the one measured in $Sr_{14}Cu_{24}O_{41}$. For anisotropic case $J_\perp/J_\parallel = 0.8$ the curve does not change appreciably.

3.6 Comparison with Experiments

We come now to the comparison with experiments. Our theory depends on four parameters $t, J_K, J_\parallel, J_\perp$ which we now want to fix to physical values. Angle-resolved photoemission (ARPES) measurements on $Sr_{14}Cu_{24}O_{41}$ were performed by Takahashi *et al.* [132] who found a band matching the periodicity of the ladder with a bandwidth of $\sim 0.5 \div 0.4$ eV. Adjusting our lowest band to have such a bandwidth we obtain a relation between t and J_K. On the other hand, experiments on the CuO_2 cell materials and band theory calculation [133, 134, 135] agreed in assuming a value of J_K of the order of $J_K \approx 1 \div 2$ eV. This in turn gives us a value of $t \approx 0.24 \div 0.76$ eV, which is also consistent with the same calculation.

We already mentioned that the debate around an anisotropy of the spin exchange constants in $Sr_{14-x}Ca_xCu_{24}O_{41}$ is not completely settled yet. Recent Raman data [38] give $J_\perp/J_\parallel \approx 0.8$. We adjusted the value of the momentum cutoff Λ by fixing the theoretical gap with the experimental one for the

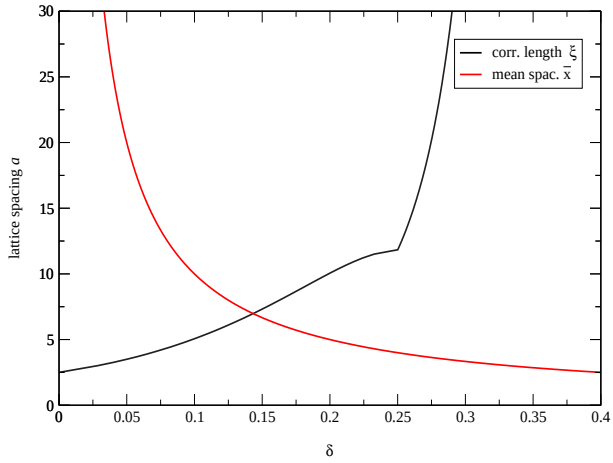

Figure 3.6: In black is the correlation length given by $\xi = v_s/\Delta$ and equation (3.52) for the gap. The red line is the average spacing between the holes approximated by $\bar{x} \simeq a/\delta$ where a is the lattice spacing and δ is the doping. Parameters are the same as for figure 3.5.

undoped compound $Sr_{14}Cu_{24}O_{41}$. Finally, to compare with the measured values of the gap for different doping concentration x in $Sr_{14-x}A_xCu_{24}O_{41}$ (where A can be either divalent Ca^{2+}, Ba^{2+} or trivalent Y^{3+}, La^{3+}), we still need a relation between the A substitution x and the number of holes per copper site present in the ladder δ. This is another unsettled issue of the telephone number compound. In particular Osafune *et al.* [76] studying the optical conductivity spectrum, inferred that with increasing Ca substitution x, holes are transferred from the chain to the ladder. On the other hand Nücker *et al.* [77] argue that in the series compound $Sr_{14-x}Ca_xCu_{24}O_{41}$ the number of holes in the ladder is almost insensitive to Ca substitution x (although a small increase is observed). Here we will assume that $Sr_{14-x}A_xCu_{24}O_{41}$ is an example of doped spin liquid and will use the data from [76]. The result of our theory can be seen in figure 3.5. There we used isotropic exchange constant, but the theoretical curve did not change in a visible way if we used a value $J_\perp/J_{||} \approx 0.8$ and in general is not very sensitive to the anisotropy of the ladder as can also be seen in figure 3.3(b). We see from the figure

that the spin gap becomes zero for $\delta \approx 0.37$, beyond this value the coupling constants f and v would become imaginary signaling that our effective model cease to make sense. This means that for such doping ratios our parameterization (3.19) is no longer valid, in the sense that it does not incorporate the most important spin configurations. However our theory could cease to make sense much before. If one takes the point of view of the $t-J$ model (as we said the Spin-Fermion model should map to it for large J_K) the holes introduced in the system couple rigidly to the spins forming singlet with the P_i states. In the worst case this would limit the correlation length of the spin to the mean hole-hole distance $1/\delta$. In our case this happens at a doping ratio of $\delta \approx 0.15$ as can be read off from figure 3.6.

A word of caution should be mentioned with respect to comparison with experimental results. A still unresolved controversy is present between NMR (Refs. [35, 36, 37]) and neutron scattering [57, 124] experiments, where the latter see essentially no doping dependence of the spin gap. Without being able to resolve this issue, we would like, however, to stress, that beyond the uncertainties in experiments, the doping behavior obtained for the spin-gap agrees with the numerical results in TDMRG and is opposite to the one obtained in mean-field treatments, making clear the relevance of fluctuations.

Chapter 4

Green's function for the doped two-leg ladder

In the previous chapter we saw that in a doped antiferromagnetic two-leg ladder, the spin liquid state is not destroyed by a minimal concentration of carriers, but it survives up to a critical doping with parameters renormalized by the hole concentration. Having integrated out the holes we have no access anymore to information on the charge carriers. Anyway, introducing currents coupled to the fermions, so as to promote the partition function to a generating functional, we can obtain the one particle fermion propagator by differentiation with respect to the currents. The main question one would try to answer in this context is which kind of excitations are supported by the system and/or weather the Fermi gas character of the non interacting system remains for small doping for physical (not small) values of the interaction. The doping region we are going to study is always that close to the Mott transition, i.e. the limiting case where the doping δ approaches zero. In particular one asks oneself if the quasi-particle weight Z is non zero, in which case the free fermion picture is still essentially correct, and the system is at most renormalized to a Fermi liquid, or $Z = 0$ and the system support excitations which are of completely different nature. Although, from the ex-

perimental side, such a question cannot still unambiguously answered, it is of great theoretical interest to asses which kind of excitations are supported by the fermions. Typically, interacting fermions in one dimension do not support the Fermi liquid state. The system reorganizes itself in a new state, radically different from the free Fermi gas, called Luttinger liquid (see for instance the original paper [12] and the review [13] and references therein). In such a liquid elementary excitations have a bosonic character and the quasiparticle weight is zero [141, 142].

In the case of fermions interacting with a spin liquid, the only analytical result available up to now is the one of Schulz [143]. Generalizing the results of a particular perturbation expansion, to other regions of the parameter space, he shows that the Luttinger liquid parameter K_ρ takes the universal value $K_\rho = 1$ as the doping concentration goes to zero. For this particular value $K_\rho = 1$, the Luttinger liquid is compatible with a Fermi gas. Hence –according to Schulz– the answer to the previous question is that, contrary to the typical situation, very diluted fermions interacting with a spin liquid, are still well described by an essentially free picture. This is consistent with Quantum Monte Carlo simulations on the $t - J$ model on the two-leg ladder in the very diluite regime [137]. Applying finite size scaling to their data, the authors of [137] are able to show that the quasiparticle weight Z remains finite in the thermodynamic limit. Finiteness of the quasiparticle weight clearly support the picture of a Fermi liquid for the holes, in the very low doping regime.

In this chapter thanks to a generalization of the method exposed in the previous chapter, we will calculate explicitly the fermionic Green's function. It will be shown that, indeed, as the doping δ goes to zero, free fermionic excitations exist in a neighborhood of the Fermi energy, hence providing further proof to Schulz's result.

Before passing to our actual calculation we will first review Schulz's argument.

4.1 Schulz's approach

Based on a previous work from Troyer et. al. [126], Schulz (Ref. [143]) realized that in a doped antiferromagnetic two-leg ladder, when the doping concentration approaches zero, the Luttinger liquid parameter takes the universal value $K_\rho = 1$. This is compatible with fermionic excitations described by the free Fermi gas. His argument is simple enough that we will briefly sketch it here.

The starting point is the two-leg ladder $t - J - J_\perp$ model:

$$\begin{aligned} H_{t-J-J_\perp} &= -t\sum_{j,\sigma,a}\mathcal{P}\left(c^\dagger_{j,a,\sigma}c_{j+1,a,\sigma} + \text{h.c.}\right)\mathcal{P} - t_\perp\sum_{j,\sigma}\mathcal{P}\left(c^\dagger_{j,1,\sigma}c_{j,2,\sigma} + \text{h.c.}\right)\mathcal{P} \\ &\quad + J\sum_{j,a}\left(\mathbf{S}_{j,a}\cdot\mathbf{S}_{j+1,a} - \frac{1}{4}n_{j,a}n_{j+1,a}\right) \\ &\quad + J_\perp\sum_{j}\left(\mathbf{S}_{j,1}\cdot\mathbf{S}_{j,2} - \frac{1}{4}n_{j,1}n_{j,2}\right), \end{aligned} \tag{4.1}$$

where j runs over L rungs, $\sigma\,(=\uparrow,\downarrow)$ ans $a\,(=1,2)$ are spin and leg indexes. The constants t, $(t_\perp)$ and J, $(J_\perp)$ refer respectively to the hopping energy and exchange integral along the ladder (rungs). The projector operator $\mathcal{P} = \prod_{j,a}(1 - n_{j,a,\uparrow}n_{j,a,\uparrow})$ prohibits double occupancy of a site. As we already observed in the previous chapter, in the limit $J_\perp \gg (t, J)$ the ground state without holes (i.e. at half filling) consists of spin singlets at each rung. When we add holes to the system, they try to stay on the same rung in order to break the minimum number of $J_\perp$ bonds. Indeed holes are seen to form a bound pair even in the isotropic case $J = J_\perp$, although the pair is more spread in this case [126]. Hence in the large $J_\perp$ limit, an appropriate picture for the system is that of tightly bound hole pairs (with state $|00\rangle_j$ at rung j) moving in a background of singlet rungs (i.e. the state: $\left(|\uparrow\downarrow\rangle_j - |\downarrow\uparrow\rangle_j\right)/\sqrt{2}$). The Hilbert space here constructed is that of a spin 1/2 chain of length L, hence it is not surprising that, in second order perturbation theory with this

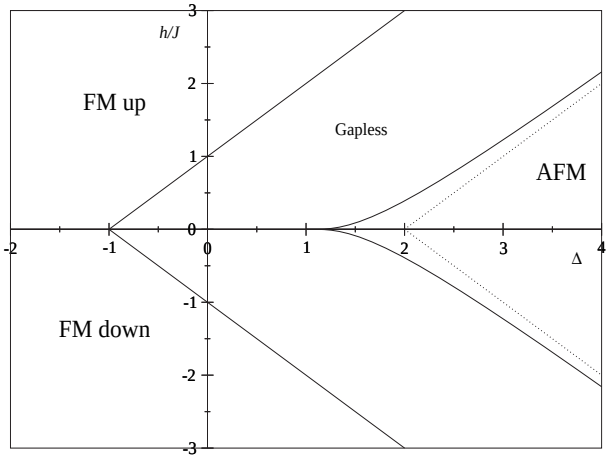

Figure 4.1: Ground-state phase diagram of the XXZ model in magnetic field.

model space, the effective Hamiltonian is that of the XXZ model:

$$H_{eff} = J^* \sum_j \left(S_j^x S_{j+1}^x + S_j^y S_{j+1}^y + \Delta S_j^z S_{j+1}^z \right) \tag{4.2}$$

where the constant are

$$J^* = \frac{4t^2}{J_\perp - 4t_\perp^2/J_\perp} \tag{4.3}$$

$$V^* = -\frac{J}{2} - \frac{3J^2}{8J_\perp} + \frac{4t^2}{J_\perp - 4t_\perp^2/J_\perp} \tag{4.4}$$

$$\Delta = \frac{V^*}{J^*} \tag{4.5}$$

($J^* = 2t^*$ of reference [126]) and the relation between the doping fraction δ=(# holes)/(# sites) and the magnetization per site $m = \left(\sum_i S_i^z\right)/L$ is

$$m = \delta - \frac{1}{2}, \tag{4.6}$$

(clearly another convention gives $m = 1/2 - \delta$ which is equivalent).

The phase diagram for the XXZ chain in magnetic field is depicted in figure

4.1. When $\delta \to 0^+$, $m \to -\frac{1}{2}^+$, hence we are in the portion of the phase diagram approaching the "FM down" region from the gapless phase (the line $h = J(1-\Delta)$ is approached from above in figure 4.1). In this region the excitations are almost non-interacting magnons $\psi_k \sim S_k^+ |FM\downarrow\rangle$. As they are exact eigenstate of the model, they show up as a delta function contribution in the dynamical structure factor, i.e. magnons are undamped. It is then not surprising that the Luttinger parameter K_ρ obtained after bosonizing the theory[1], assumes the value $K_\rho = 1$ [81]. For this value, in fact, the Luttinger liquid is compatible with a description based on free fermions.

The final point of Schulz's argument is the following. He argues that the model (4.1) is in the same phase in a large region of interaction strength, both for weak and strong correlation. At exactly half filling it is a well established result that the spin liquid state is present for any interaction strength ranging from strong coupling down to infinitesimal $J_\perp$. On top of that, away from half filling, some calculation on the model (4.1) in both weak and strong coupling regime, give the same results [144, 145, 146]. In particular they predict quasi long range superconducting d-wave correlation:

$$\left\langle \Delta_r^\dagger \Delta_0 \right\rangle \approx \frac{1}{r^{\eta_{SCd}}}, \tag{4.7}$$

where Δ_r is a "d-wave"[2] order parameter:

$$\Delta_r = \frac{1}{\sqrt{2}} \left(c_{r,1,\uparrow} c_{r,2,\downarrow} - c_{r,1,\downarrow} c_{r,2,\uparrow} \right).$$

A power law decay is also predicted for the $4k_F$ component of the particle density:

$$\langle n_r n_0 \rangle \approx \frac{\cos(4k_F r)}{r^{\eta_{4k_F}}}. \tag{4.8}$$

[1] One should first use a Jordan-Wigner transformation to map the model into one of interacting spinless fermions.

[2] A ladder is obviously not rotational invariant. This makes impossible to define spherical harmonics. The name "d-wave" order parameter, refers to the fact that in Fourier space, components with transfer wave-vector, 0 and π have opposite signs.

Moreover a scaling relation between the exponents holds

$$\eta_{SCd}\,\eta_{4k_F} = 1. \tag{4.9}$$

Since the same qualitative results are obtained through calculation valid both in the strong and weak coupling regime, it is argued that the system is in the same phase for a wide range of the parameters.

Hence the result $K_\rho \to 1$ at very low doping, which was obtained through an approximation in the regime $J_\perp \gg (t, J)$, should be a general feature shared by any value of the coupling, both strong and weak[3].

4.2 Green's function for the two-leg ladder

If we add currents coupled to Fermions to the action in eq. 3.3 on page 69, we can obtain the (imaginary time) fermionic Green's function by differentiating with the respect to the current. With the notation of chapter three ($f_{k,\sigma}$ are the Wannier states for the Oxygen site), the generating functional is

$$Z\left[J^*, J\right] = \int D\left[f\ f^*\right] D\left[\hat{\Omega}\right] e^{-f^* G^{-1} f - S_h + J^* f + f^* J} \tag{4.10}$$

The imaginary time Green's function is obtained then via differentiation:

$$\begin{aligned} \mathcal{G}\left(k, q, \tau\right) &= \left\langle T_\tau f_k\left(\tau\right) f_q^\dagger\left(0\right)\right\rangle \\ &= \frac{1}{Z\left[0\right]} \left.\frac{\delta^2 Z\left[J^*, J\right]}{\delta J_q\left(0\right) \delta J_k\left(\tau\right)}\right|_{J=J^*=0} \end{aligned} \tag{4.11}$$

Integrating out the fermions, the generating functional becomes

[3] Of course the exchange integral J in the chain direction must be of antiferromagnetic nature ($J > 0$) in order to assure a spin liquid state at half filling.

$$Z\left[J^*,J\right]=\int D\left[\mathbf{N}\right]D\left[\mathbf{l}\right]\delta\left(\mathbf{N}^2-1\right)\delta\left(\mathbf{N}\cdot\mathbf{l}\right)e^{-S_{eff}+J^*M^{-1}\hat{G}M^{-1}J} \tag{4.12}$$

where S_{eff} has been already evaluated in the previous chapter. Here we completely discard the fluctuating ferromagnetic field $\mathbf{M}$ as we already saw it decouples completely from the problem. The factors M^{-1} in equation (4.12) are present because the original propagator was $G=M^{-1}\hat{G}M^{-1}$. Now on, for simplicity, we absorb the M^{-1} factors in the currents, i.e. we redefine $J^*M^{-1}\rightarrow J^*$and $M^{-1}J\rightarrow J$. The effective action is

$$\begin{aligned}
S_{eff} &= S_h-\mathrm{tr}\ln\left(G^{-1}\right)\\
&= -\int dxd\tau\left\{\left(\frac{\bar{\chi}_{xx}}{2}-S^2J_{||}\right)a\left|\partial_x\mathbf{N}\right|^2+\frac{\bar{\chi}_{\tau\tau}}{2a}\left|\partial_\tau\mathbf{N}\right|^2\right\}\\
&\quad +a^2\sum_q\left\{\left[\chi_{\mathrm{spin}}^{-1}\left(q\right)+\frac{g^2}{S^2}\tilde{\chi}\right]\mathbf{l}_q\cdot\mathbf{l}_{-q}\right.\\
&\quad \left.+2ia\left(1+\frac{g^3}{S}\hat{\chi}_\tau\right)\left(\mathbf{N}\times\partial_\tau\mathbf{N}\right)_q\cdot\mathbf{l}_{-q}\right\}
\end{aligned} \tag{4.13}$$

We wrote the $\mathbf{l}$ part in Fourier space ($q=(q_x,q_y,i\nu_n)$) as here this contribution is diagonal. The inverse spin (bare) susceptibility for a two-leg ladder is

$$\chi_{\mathrm{spin}}^{-1}\left(q_x,q_y\right)=2J_{||}\left(\cos\left(q_xa\right)+1\right)+J_\perp\left(\cos\left(q_ya\right)+1\right). \tag{4.14}$$

The next steps are clear. We need to find the inverse of $\hat{G}^{-1}$ and then we will integrate out the ferromagnetic fluctuation in the ladder direction $\mathbf{l}$. Only then will we differentiate and obtain the Green's function. According to the "dimensional engineering" argument, we need the inverse of $\hat{G}^{-1}$ up to second order in the lattice spacing. In appendix B it is shown that the desired result is:

$$\begin{aligned}\hat{G} &= F_0 + a\left(-F_0 R_1 D^{-1} + F_0 \Sigma_1 F_0\right) \\ &\quad + a^2\left(-F_0 R_2 D^{-1} + F_0 R_1 D^{-1} R_1 D^{-1} + F_0 \Sigma_2 F_0\right. \\ &\quad \left. + F_0 \Sigma_1 F_0 \Sigma_1 F_0\right) \\ &= G_N + G_l + G_{l^2} \end{aligned} \tag{4.15}$$

where we regrouped terms depending on $\mathbf{N}$ only, on $\mathbf{l}$ or $\mathbf{l}^2$:

$$G_N = F_0 - a\left(F_0 R_1 D^{-1}\right) + a^2\left(F_0 R_1 D^{-1} R_1 D^{-1} - F_0 R_2 D^{-1}\right) \tag{4.16}$$

$$G_l = a F_0 \Sigma_1 F_0 \tag{4.17}$$

$$G_{l^2} = a^2 F_0 \Sigma_2 F_0 + a^2 F_0 \Sigma_1 F_0 \Sigma_1 F_0. \tag{4.18}$$

and the various matrices are

$$(D)_{k,q} = \left(g^{-1}(k)\,\bar{g}^{-1}(k) - g^2\right)\delta_{k,q}\delta_{\alpha,\beta} \tag{4.19}$$

$$(F_0)_{k,q} = G_0(k)\,\delta_{k,q}\delta_{\alpha,\beta} - gD^{-1}(q)\,\mathbf{N}_{k-q+Q}\cdot\boldsymbol{\sigma}_{\alpha,\beta} \tag{4.20}$$

$$(\Sigma_1)_{k,q} = -\frac{g}{S}\mathbf{l}_{k-q}\cdot\boldsymbol{\sigma}_{\alpha\beta} \tag{4.21}$$

$$(\Sigma_2)_{k,q} = \frac{g}{2S^2}\left(\mathbf{N}\,|\mathbf{l}|^2\right)_{k-q+Q}\cdot\boldsymbol{\sigma}_{\alpha\beta} \tag{4.22}$$

$$(R_1)_{k,q} = ig\partial_\mu \bar{g}_0^{-1}(q)\left(\partial_\mu \mathbf{N}\right)_{k-q+Q}\cdot\boldsymbol{\sigma}_{\alpha\beta} \tag{4.23}$$

$$(R_2)_{k,q} = g\frac{1}{2}\partial^2_{\mu\nu}\bar{g}_0^{-1}(q)\left(\partial^2_{\mu,\nu}\mathbf{N}\right)_{k-q+Q}\cdot\boldsymbol{\sigma}_{\alpha\beta} \tag{4.24}$$

in the last two lines summation over indexes μ, ν is assumed. The propagator that we indicated with G_0 is

$$G_0(k) = \bar{g}_0^{-1}(k)\,D^{-1}(k). \tag{4.25}$$

4.3 Integration of the ferromagnetic fluctuation

We first regroup the **l**-dependent part of the action in

$$S_l = +\sum_{kq} \mathbf{l}^a_k \left(A\right)^{ab}_{k,q} \mathbf{l}^b_{-q} - \sum_q \mathbf{B}^a_{-q} \mathbf{l}^a_q \tag{4.26}$$

we also define

$$\begin{aligned} A &= A_0 + A_J & (4.27)\\ \mathbf{B} &= \mathbf{B}_0 + \mathbf{B}_J & (4.28) \end{aligned}$$

where the $A_0, \mathbf{B}_0$ do not contain the currents, whereas $A_J, \mathbf{B}_J$ are quadratic in the currents. Their explicit expression are

$$\begin{aligned} \left(\mathbf{B}_J\right)_\eta &= -\frac{ga}{S} \sum J^*_k \left(F_0\right)_{k,\xi-\eta} \boldsymbol{\sigma} \left(F_0\right)_{\xi,q} J_q & (4.29)\\ \left(A_J\right)^{a,b}_{k,q} &= \frac{g^2a^2}{S^2} \sum J^*_{\xi_1} \left(F_0\right)_{\xi_1,\xi_2} \sigma^a \left(F_0\right)_{\xi_2,\xi_4+k} \sigma^b \left(F_0\right)_{\xi_4,\xi_6-q} J_{\xi_6} + \\ &\quad \frac{ga^2}{2S^2} \sum \delta^{a,b} J^*_{\xi_1} \left(F_0\right)_{\xi_1,\xi_2} \mathbf{N}_{\xi_2-\xi_3+q-k+Q} \cdot \boldsymbol{\sigma} \left(F_0\right)_{\xi_3,\xi_4} J_{\xi_4} & (4.30)\\ \left(\mathbf{B}_0\right)_\eta &= 2ia \left(1 + \frac{g^3}{S} \hat{\chi}_\tau\right) \left(\mathbf{N} \times \partial_\tau \mathbf{N}\right)_\eta & (4.31)\\ \left(A_0\right)^{a,b}_{k,q} &= a^2 \left[\chi^{-1}_{\text{spin}}\left(k\right) + \frac{g^2}{S^2} \tilde{\chi}\right] \delta^{a,b} \delta_{k,q} & (4.32) \end{aligned}$$

Where it should be understood that in the first three lines also spin indexes should be summed although they are not explicitly written for notational convenience. To integrate out the field **l** we express again the constraint through a functional delta function. The steps are

$$\begin{aligned}\int D\mathbf{l}\delta\left(\mathbf{N}\cdot\mathbf{l}\right)e^{-a^2\mathbf{l}A\mathbf{l}+a\mathbf{l}\mathbf{B}} &= \int D\mathbf{l}Dk e^{-a^2\mathbf{l}A\mathbf{l}+a\mathbf{l}(\mathbf{B}+i\mathbf{N}k/a)} \\ &= e^{-\frac{1}{2}\mathrm{tr}\ln\left(a^2A\right)+\frac{1}{4}\mathbf{B}A^{-1}\mathbf{B}}\int Dk\, e^{-\frac{1}{4a^2}k\mathbf{N}A^{-1}\mathbf{N}k+\frac{i}{2a}\mathbf{B}A^{-1}\mathbf{N}k} \\ &= \exp\left[-\frac{1}{2}\mathrm{tr}\ln\left(a^2A\right)+\frac{1}{4}\mathbf{B}A^{-1}\mathbf{B}\right. \\ &\quad -\frac{1}{2}\mathrm{tr}\ln\left(\frac{\mathbf{N}\mathbf{A}^{-1}A^{-1}\mathbf{N}}{a^2}\right) \\ &\quad \left.-\frac{1}{4}\mathbf{N}A^{-1}\mathbf{B}\left(\mathbf{N}A^{-1}\mathbf{N}\right)^{-1}\mathbf{B}A^{-1}\mathbf{N}\right] \end{aligned} \tag{4.33}$$

At this point the total action is

$$S = S_{NL\sigma M}\left[\mathbf{N}\right] + S_I\left[\mathbf{N};J^*,J\right] \tag{4.34}$$

where the non linear sigma model action is that defined in Eq. 3.49 on page 79. The remaining term, at least bilinear in the currents is

$$\begin{aligned} S_I\left[\mathbf{N};J^*,J\right] &= -J^*G_NJ+\frac{1}{2}\mathrm{tr}\ln\left(a^2A\right)+\frac{1}{2}\mathrm{tr}\ln\left(\frac{\mathbf{N}A^{-1}\mathbf{N}}{a^2}\right)-\frac{1}{4}\mathbf{B}A^{-1}\mathbf{B} \\ &\quad +\frac{1}{4}\mathbf{B}_0A_0^{-1}\mathbf{B}_0+\frac{1}{4}\mathbf{N}A^{-1}\mathbf{B}\left(\mathbf{N}A^{-1}\mathbf{N}\right)^{-1}\mathbf{B}A^{-1}\mathbf{N} \end{aligned} \tag{4.35}$$

Since we are only interested in two point function, we can expand the action up to bilinear terms in the currents. After the expansion the two tr ln terms cancel one another because of the constraint $|\mathbf{N}|^2 = 1$. The last term in equation (4.35) give exactly zero at this order, the final result is

$$S_I\left[\mathbf{N};J^*,J\right] = -J^*G_NJ-\frac{1}{2}\mathbf{B}_JA_0^{-1}\mathbf{B}_0+\frac{1}{4}\mathbf{B}_0A_0^{-2}A_J\mathbf{B}_0 \tag{4.36}$$

This action now depends only on the dynamical field $\mathbf{N}$ and is bilinear in the currents. Hence it can be written as

$$S_I = -J^* \tilde{G}_N J \tag{4.37}$$

Where $\tilde{G}_N$ contains also zero, first and second order contribution in the lattice constant:

$$\tilde{G}_N = \tilde{G}_N^0 + a\tilde{G}_N^1 + a^2\tilde{G}_N^2 \tag{4.38}$$

After differentiating with respect to the currents, we see that the Green's function is obtained by averaging the above quantity with the non linear sigma model action:

$$\mathcal{G}(k,q) = \left\langle \epsilon_k^{-1/2} \left(\tilde{G}_N\right)_{k,q} \epsilon_q^{-1/2} \right\rangle_{NL\sigma M}, \tag{4.39}$$

the factors $\epsilon_k^{-1/2}$ are due to the rescaling $M^{-1}J \to J$. Hence we see that we managed to have an expansion for the hole's Green's function in term of the small parameter a.

4.4 Zero order propagator

The zero order part of the propagator can be read off from equation (4.16). We see that

$$\tilde{G}_N^0 = F_0, \tag{4.40}$$

and the explicit form is given in equation (4.20). Averaging the above quantity with respect to the non linear sigma model action is straightforward, as in (1+1) dimension there cannot be symmetry breaking. Hence we obtain a zero order propagator

$$\mathcal{G}_0(k) = \frac{G_0(k)}{\epsilon(k)} = \frac{\bar{g}_0^{-1}(k)\, D^{-1}(k)}{\epsilon(k)} \tag{4.41}$$

which looks

$$\mathcal{G}_0(k) = \frac{Z_1(k)}{i\omega + e_1(k) - \mu} + \frac{Z_2(k)}{i\omega + e_2(k) - \mu}. \tag{4.42}$$

From equation (4.42) is clear that the poles of $\mathcal{G}_0$ are the zeros of D. Hence the two bands e_1, e_2 appearing in the above equation are exactly the "mean-field" bands that we encountered in the previous chapter. The lowest band, e_1, is separated from e_2 by a gap of order $4SJ_K$. Thanks to the prefactors in Eq. (4.25), the weights in the zero order propagator (4.42) satisfy the sum rule

$$Z_1(k) + Z_2(k) = \int d\omega A(k,\omega) = 1 \tag{4.43}$$

where, with our convention for the Fourier transform, the spectral density is

$$A(k,\omega) = \frac{1}{\pi}\mathrm{Im}\left(\mathcal{G}\left(i\omega = -\omega - i\delta^+, k\right)\right) \tag{4.44}$$

4.5 First order self energy

A Taylor expansion for the Green's function always produce incoherent background unless one sums an infinite number of terms. Instead we calculate the vertex function Γ, the Legendre transform of the free energy. Double differentiation with respect to the conjugate fields gives the inverse propagator:

$$\left.\frac{\delta^2\Gamma}{\delta\phi\delta\phi^*}\right|_{\phi=\phi^*=0} = \mathcal{G}^{-1} \tag{4.45}$$

The self energy is then obtained via Dyson's equation

$$\Sigma = \mathcal{G}_0^{-1} - \mathcal{G}^{-1} \tag{4.46}$$

At first order in the lattice spacing we obtain the following contribution

$$\Sigma(k,q) = a\mathcal{G}_0^{-1}(k) \left\langle \epsilon_k^{-1/2} \left(\tilde{G}_N^1\right)_{k,q} \epsilon_q^{-1/2} \right\rangle_{NL\sigma M} \mathcal{G}_0^{-1}(q) \tag{4.47}$$

of course, translation invariance will imply $k = q$. To evaluate the above self energy we need basically to take the first order part of the action in Eq. (4.36), take the derivative with respect to the currents and average it with the non linear sigma model. Indeed taking the derivative at zero currents and averaging with the NLσM, are commuting operation.

The first order term $\tilde{G}_N^1$ contains terms with up to four fields $\mathbf{N}$. Evaluating average of these term, i.e. four-point function for the non linear sigma model, can be a quite complicated task on its own. We will evaluate such average using an approximate version of the non linear sigma model which consists of free massive bosons. A result of this approximation is, among others, that the spin excitations at small momenta (around the modulation vector $Q = \pi/a$) have a relativistic dispersion $\omega = \sqrt{\Delta^2 + v^2k^2}$. This is indeed obeyed with very high accuracy by the original spin problem, as numerical simulations confirm [147]. The massive boson free theory is the leading (saddle point) term of a large $\mathcal{N}$ expansion where $\mathcal{N}$ is the number of component of the symmetry group of the theory $O(3)$ generalized to $O(\mathcal{N})$. We do not discuss here this large-$\mathcal{N}$ expansion rather refer the reader to the literature – see e. g. chapter 8 of Polyakov's book [148]. In this approximation we can use a Wick theorem and evaluation of any N-point function is straightforward.

The free massive boson approximation to the non linear sigma model is

$$S_{FB} = \frac{1}{2f} \int dx d\tau \left[v \left|\partial_x \mathbf{N}\right|^2 + \frac{1}{v} \left|\partial_\tau \mathbf{N}\right|^2 + vm^2 \left|\mathbf{N}\right|^2 \right] \tag{4.48}$$

where the field $\mathbf{N}$ is not anymore subject to the constraint $|\mathbf{N}|^2 = 1$. The mass term has been generated dynamically, its value is fixed by the saddle point equations (which we do not discuss here), but are equivalent to the requirement that the constraint is satisfied in average: $\langle \mathbf{N}^2 \rangle_{S_{FB}} = 1$. This leads to

$$\int \frac{d\omega}{2\pi} \int \frac{dq}{2\pi} \frac{vf\mathcal{N}}{\omega^2 + v^2q^2 + v^2m^2} = 1, \tag{4.49}$$

and gives us a relation for the mass term:

$$m = \frac{\Lambda}{\sinh\left(\frac{2\pi}{f\mathcal{N}}\right)} \tag{4.50}$$

where Λ is a momentum cut-off of the order of the inverse lattice spacing. We see that this formula agrees in leading order with eq. (3.52) on page 80 obtained with more refined methods, the only difference being that $\mathcal{N}$ is replaced by $\mathcal{N} - 2$ in formula (3.52). For a discussion on this point, again see Polyakov's book [148] page 127.

Finally the evaluation of all the contribution in equation (4.47) is simple algebra, but being a bit lengthy is relegated to Appendix B. The result is

$$\begin{aligned} \Sigma(q) &= \mathcal{G}_0^{-1}(q)\,\bar{g}_0(q) \Bigg(-ig^2 \partial_\mu \bar{g}_0^{-1}(q)\,\Gamma_\mu(q) \\ &\quad + \frac{6\left(1 + \frac{g^3}{S}\hat{\chi}_\tau\right) g^3}{\left(4J_{\|} + 2J_\perp + \frac{g^2}{S^2}\tilde{\chi}\right)} \Gamma_\tau(q) \Bigg), \end{aligned} \tag{4.51}$$

and summation over μ is understood. The function Γ_μ is defined by

$$\Gamma_\mu(q) = \frac{1}{L\beta} \sum_\eta D^{-1}(\eta + q) \left\langle \mathbf{N}_{-\eta} \cdot (\partial_\mu \mathbf{N})_\eta \right\rangle_{S_{MB}}, \tag{4.52}$$

which resemble the rising sun diagram for the self energy, note however the presence of the derivative.

A last step should be mentioned before we pass to the results. To evaluate the self energy (4.51) at zero temperature, near the Fermi energy, we will finally pass to the continuum limit also for the fermionic variables. The important k points are those close to the minimum of the lowest band, hence we will

expand around this point. As we want to study the limiting case in which the doping concentration approaches zero, the usual procedure of expanding linearly around the Fermi momenta does not work, since the Fermi velocity goes to zero as $\delta \to 0$. The zero order Green's function becomes in this limit

$$\mathcal{G}_0\left(k, i\omega_n\right) = \frac{1/2}{\left(i\omega + \frac{1}{2m}k^2 - \mu\right)}, \tag{4.53}$$

here we absorbed constant terms in the chemical potential, and discarded the highest energy band as it is separated by a gap of order J_K, which is the biggest energy scale of the problem. The band curvature is given by

$$\frac{1}{2m} = \frac{3\left(S^2 J_K^2 - t^2\right) a^2}{8 S J_K} \tag{4.54}$$

4.6 Zero doping limit

In the limit of zero doping at the Fermi energy Γ_x is identically zero as can be expressed as an integral of an odd function. The main contribution comes then from Γ_τ . When evaluating the frequency sum in Eq. (4.52), we have three poles; one comes from the zero order band, the other two are at $\pm E_\eta$, where $E_\eta = \sqrt{\Delta^2 + v^2\eta^2}$ is the boson's dispersion. In fact the bosonic average is

$$\left\langle \mathbf{N}_{-\eta} \cdot \left(\partial_\tau \mathbf{N}\right)_\eta \right\rangle_{S_{MB}} = \frac{f v \left(-i\eta_0\right)}{\left(E_\eta + i\eta_0\right)\left(E_\eta - i\eta_0\right)}. \tag{4.55}$$

The result of the frequency sum, at zero temperature is a term proportional to doping, which is zero in the limit we are considering, and another term which gives

$$\Gamma_\tau\left(i\omega\right) \sim -\frac{f v}{4g}\int \frac{dk}{2\pi} \frac{1}{i\omega + \sqrt{\Delta^2 + v^2 k^2} + \frac{1}{2m}k^2} \tag{4.56}$$

if $|\omega| \ll \Delta$ we can approximate the relativistic dispersion with

$$\sqrt{\Delta^2 + v^2 k^2} \approx \Delta + \frac{v^2}{2\Delta} k^2 \tag{4.57}$$

the integral is then easily evaluated with contour integration. The result is

$$\Gamma_\tau (i\omega) \sim -\frac{fv}{8g} \frac{\sqrt{2m^*}}{\sqrt{i\omega + \Delta}}, \tag{4.58}$$

and we are measuring the energy from the Fermi level. The effective mass is

$$\frac{1}{2m^*} = \frac{1}{2m} + \frac{v^2}{2\Delta}. \tag{4.59}$$

Putting together all the contributions, the result for the imaginary time self energy is then

$$\Sigma (i\omega) \sim -\frac{i\omega}{\sqrt{i\omega + \Delta}}, \tag{4.60}$$

where in the square root, we must take the root with positive real part. As we are in the regime $|\omega| \ll \Delta$, we can expand the square root and obtain

$$\Sigma (i\omega) \sim -i\omega. \tag{4.61}$$

Hence we see that at the Fermi energy, and for zero doping, the self energy only contributes to renormalize the quasiparticle weight:

$$Z \to \frac{Z}{1 + C} \tag{4.62}$$

where, in the limit of zero doping, the constant C is

$$C = \frac{fv}{4} \frac{g}{t} \left(1 + \frac{6g}{4J_{||} + 2J_\perp} \right) \sqrt{\frac{2m}{\Delta}}. \tag{4.63}$$

As the constant is evidently positive, the quasi-particle weight is renormalized toward smaller value.

This result is consistent with Schulz's prediction: in the limit of zero doping concentration, Fermi quasiparticle are well defined. Indeed, at least in a small

neighborhood around the Fermi surface, the self-energy shows no damping, i.e. the imaginary part of the retarded self energy is identically zero. This indicates that the holes, as the doping approaches zero, are indeed described by a free gas, as the result $K_\rho = 1$ suggests. Strictly speaking, a one component Luttinger liquid with $K_\rho = 1$ –as the one which emerged in the discussion in section 4.1– is indeed a Fermi gas.

Conclusions

The central interest of the research presented in this thesis lies in Copper-Oxide materials arranged in form of chains and ladders. In these materials mobile holes can be injected which then interact with a background of spins localized at the Copper sites. The microscopic theory for the undoped compounds is the antiferromagnetic Heisenberg model on the appropriate lattice. The low energy sector of these models is described by the non linear sigma model (NLσM) quantum field theory. The NLσM has a representation which admits a gauge field. It is natural to suppose that, at low energy, the interaction between the antiferromagnetic spin background and the mobile holes can be represented by a minimal coupling of this gauge field. In this work we showed that indeed, starting from a microscopic model for the Copper-Oxide chains and ladders, a very similar field theory can be obtained. The difference lies in the fact the besides the gauge coupling, an additional interaction coming from the off-diagonal elements of SU(2) matrices, is present.

Specializing to the most interesting case of a two leg ladder we were able to obtain more results. In the two leg ladder without additional mobiles charge carriers, the spins organize themselves in a spin liquid state. This is a rotational invariant state with gapped magnonic excitations. We showed that, for small doping concentration, the field theory describing the low energy modes is still a NLσM. As showed by numerical simulations and a number of experiments, the spin liquid state is not destroyed by doping but survives up to a finite concentration. The parameters of the spin liquid states become, in fact, only renormalized by the presence of the holes in a way which we were able to calculate explicitly. This method does not give information on

the dynamic of the holes as these are integrated out from the problem. A generalization of this method though, allowed to access the one particle hole propagator formally via differentiation with respect to Grassmann currents. In the continuum limit i. e. for low energy, long wave-length we obtained the vertex function as a power series in the lattice constant. Stopping at first order we obtained an expression for the one particle propagator which is consistent with a free fermionic description for small momenta and frequencies.

Zusammenfassung

Ende der sechziger Jahre dachten die meisten Festkörpertheoretiker, daß mit den Erfolgen der Landau Fermiflüssigkeitstheorie (1956) [1, 2, 3] und der BCS Theorie der Supraleitung (1957) [4, 5] ihre Forschung auf einem soliden Fundament gebaut sei. Erst zwanzig Jahre später wurde mit der Entdeckung der Hochtemperatursupraleitung (1986) [6], den Schwerfermion-Systemen (um 1980) [7] und dem Quantenhallefekt (Anfang 80er Jahre) [8, 9] offensichtlich, dass grundlegend neue Theorien benötigt würden. Schnell wurde klar, dass die neuen Systeme eine gemeinsame Eigenschaft besitzen, nämlich dass durch verminderte Dimensionalität oder durch starke elektronische Wechselwirkung die Bewegungsfreiheit der Elektronen stark beeinträchtigt wird. Infolge einer reduzierten Beweglichkeit ergeben sich dann komplizierte Korrelationen in der Statik und Dynamik der Elektronen. Daher auch der Name 'Stark korrelierte Elektronensysteme' der synomym für all die oben genannten neuen Syteme steht.

Typisch für die wechselseitige Beziehung von Dimensionalität und elektronischen Korrelationen ist das Versagen der Landau Fermiflüssigkeitstheorie (FFT) bei abnehmender Dimensionalität. In der Fermiflüssigkeitstheorie wird postuliert, dass das niederenergetische Spektrum des wechselwirkenden Systems eins zu eins mit dem eines freien Fermigases korrespondiert. Da sich die Quasiteilchen, die im wechselwirkenden System die niedrigsten kollektiven Anregungen beschreiben, genau wie freie Elektronen verhalten, ist die ganze FFT im wesentlichen eine freie Theorie. Ursprünglich wurde die FFT zur Beschreibung von ^{3}He entwickelt. Es folgten Erweiterungen, um Elektronen in Metallen und Atomkernen zu beschreiben. Solche Rechnungen wurden mit

großem Erfolg bei vielen Metallen mit dreidimensionaler Struktur angewandt, wobei natürlich eine tiefe Temperatur Voraussetztung ist. Bei den eher zweidimensionalen Kuprat-Supraleitern wurden die anormalen Eigenschaften des (nicht supraleitenden) Normalzustands (siehe [10]) von vielen Forschern in Zusammenhang mit Nicht-Fermiflüßigkeits-Verhalten gebracht, was zu einer Suche nach alternativen Theorien Anlaß gab. Andererseits ist der FF-Zustand auch in zwei Dimensionen noch robust und kann nur unter besonderen Bedingungen, so z.B. einer langreichweitigen Wechselwirkung, Singularitäten im freien Propagator oder sehr starker Kopplung zerstört werden [11]. Unter solchen Umständen spricht man dann von einer Nicht-Fermiflüssigkeit (NFF) oder einer "marginalen"-Fermiflüssigkeit (MFF).

Im Gegensatz zu den vielen Fragezeichen, die es heute noch bei zweidimensionalen Fermionen gibt, sind die eindimensionalen Systeme sehr gut verstanden. Insbesondere ist schon lange bekannt, dass das Fermiflüssigkeitsbild in einer Dimension zusammenbricht. Der Grund sind die Quantenfluktuationen, die in einer Dimension so stark sind, dass jede noch so kleine Wechselwirkung das Fermigas in einen vollständig anderen Zustand, nämlich in eine sogenannte Luttingerflüssigkeit (LF) treibt (siehe die Originalarbeit [12] und den Übersichtsartikel [13]).

Dieser neuartige Zustand ist durch das gänzliche Fehlen von fermionischen Quasiteilchen[4] charakterisiert. Anders ausgedrückt verschwindet die Renormierung der Quasiteilchen Z, vollständig und zugleich wird eine Trennung von Spin-und Ladungsfreiheitsgraden beobachtet. In der Luttingerflüssigkeit findet man dann ausschließlich bosonische Anregungen, entweder mit Ladungs- (Ladungsdichtewelle) oder Spin-Charakter (Spindichtewelle).

Aufgrund dieser Eigenschaften sind die eindimensionalen Systeme ideal geeignet, neue Theorien (wie z.B. verschiedene Formen einer NFF) für stark korrelierte Systeme zu erproben. Tatsächlich gibt es für die eindimensionalen Systeme viele leistungsstarke Rechenmethoden, die in mehr Dimensionen nicht zur Verfügung stehen. An wichtigster Stelle sei hier der Bethe Ansatz

[4] Tomonaga hatte als erster schon 1950 die bosonischen Anregungen in den eindimensionalen Systemen beschrieben [14].

erwähnt, der für spezielle Modelle und besonderen Kopplungsstärken exakte Ergebnisse liefert. Desweiteren waren es die Bosonisierungsmethoden, die dem Konzept der Luttingerflüssigkeit sicheren Boden verschafft haben. In einer Dimension sind auch numerische Simulationen sehr erfolgreich (verglichen mit Simulationen in mehreren Dimensionen) und große Systeme können bei tiefer Temperatur untersucht werden.

Das Interesse an niedrigdimensionalen Systemen beschränkt sich nicht nur auf die theoretische Physik. Chemiker haben sich schon lange mit organischen Systemen beschäftigt, in denen die Anisotropie[5] Werte von 10^3 erreicht, und man also von quasi ein- oder zweidimensionalen Strukturen sprechen kann (TTF-TCNQ ist einer der bekanntesten Vertreter dieser Klasse, siehe [15]). Als nächstes wurden dann auch Quanten-Spinketten erfolgreich synthetisiert und untersucht. Ausgelöst wurde das vermehrte Interesse an Spinsystemen einerseits durch die Entdeckung der Hochtemperatur-Supraleitung mit der wichtigen antiferromagnetischen Phase in der Nähe der Supraleitung und andererseits durch theoretischen Voraussagen von Haldane [16]. Haldanes Behauptung [16] (1983)besagt in ihrer ursprünglichen Form, dass antiferromagnetische Spinketten abhängig von ihrem Spin qualitativ unterschiedlich verhalten, je nachdem ob der Spin ganz- oder halbzahlig ist. Ketten mit halbzahligen Spinwerten gehören in die Universalitätsklasse der Spin-1/2 Ketten, haben verschwindent kleine Anregungsenergien und zeigen Spin-Spin Korrelationen die algebraisch mit wachsendem Abstand zerfallen. Andererseits haben Ketten mit ganzzahligem Spin Anregungen mit klarer Lücke zum Grundzustand und demnach exponentiell zerfallende Korrelationsfunktionen. Zehn Jahre später schlugen Rice *et al.* [17] ein ähnliches Verhalten für Spinleitern vor, die aus M wechselwirkenden Ketten bestehen (analog zur $M = 2$ Leiter auch M-leg Leiter genannt). Für die S, M-leg Leiter soll dann gelten, dass sie entweder in die Universalitätsklasse der Spin-1/2 oder der Spin-1 Ketten gehört, je nachdem ob das Produkt SM halb- oder ganzzahlig ist. Abgesehen von vielen numerischen Studien, die diese verallgemeinerte Haldane-Hypothese bestätigen [18, 19, 20, 21, 22], haben die theoretischen

[5]Die Anisotropie wird hier als das Verhältnis von den Leitfähigkeiten parallel und senkrecht zur Ausrichtung der Ketten definiert.

Vorhersagen auch eine enorme experimentelle Anstrengung ausgelöst, weitere Ketten- und Leitermaterialien zu synthetisieren, an denen sich die theoretischen Aussagen, insbesondere die zur Spin-Anregungslücke für Spin-1 Ketten und Spin-1/2 Leitern testen lassen [25, 26, 27, 28]. Damit wurden die theoretischen Voraussagen auch experimentell "bewiesen". In folge dieser Arbeiten sind die reinen Spinsysteme heute auf der theoretischen Seite zufriedenstellend verstanden.

Damit drängt sich als nächstes natürlich die Frage nach Dotierungseffekten in niedrigdimensionalen Spinsystemen auf. Mitte der neunziger Jahre wurden erstmals Ketten und Leitersysteme synthetisiert, die auf der selben Cu-O Basis aufgebaut sind, wie die Hoch-T_c Supraleiter [27]. In einigen dieser Verbindungen –insbesondere $La_{1-x}Sr_xCuO_{2.5}$ und $Sr_{14-x}Ca_xCu_{24}O_{41}$– kann man die Zahl der mobilen Löcher durch dotieren gut verändern. So kann man Verhältnisse analog zu den Hochtemperatur-Supraleitern auch in Systemen mit der noch weiter reduzierten Dimensionalität von Ketten und Leitern studieren. Die Hoffnung besteht, dass so mit der Untersuchung von Cu-O Leitern wesentliches Verständnis für die weitaus komplexeren zweidimensionalen Hoch-T_c Materialien gewonnen werden kann. Tatsächlich konnten einige Ähnlichkeiten der ein- und zweidimensionalen Systeme beobachtet werden. Die wohl bemerkenswerteste Leistung war der Nachweis von Supraleitung in einem (2-leg) Leitersystem unter hohem Druck [29]. Das Studium der eindimensionalen Materialien hat aber noch viel Interessantes und Unverstandenes zu Tage gefördert, das dem vielfältigem Verhalten der Übergangsmetalloxide hinzuzufügen ist.

Zur Modellierung stark korrelierter Systeme steht heute einen Vielzahl theoretischer Methoden zur Verfügung. Bei den störungtheoretischen Ansätzen in schwacher oder starker Kopplung wird grob gesagt angenommen, dass die Wechselwirkung klein respektive sehr groß gegenüber der kinetischen Energie ist. Leider sind in den meisten realen Systemen die Wechselwirkungs- und kinetische Energie von gleicher Größenordnung, und es gibt keinen kleinen Parameter, der eine störungstheoretische Entwicklung erlaubt. Mean-Field-Rechnungen sind allgemein nur in hoher Dimension und bei langreichweitiger

Wechselwirkung zuverlässig. Die Bosonisierung ist, wie wir schon bemerkt haben, besonders in einer Dimension ein mächtiges Werkzeug, und allgemeiner erlaubt sie die Behandlung schwach koppelnder Systeme in der Nähe einer verschwindenden Anregungslücke, eine Bedingung, die wie wir gleich sehen werden, in unserem Fall nicht zutrifft. Zuletzt sollen noch die numerischen Methoden erwähnt werden, exakte Diagonalisierung (ED), Dichtematrix-Renormierung (DMRG) und Quanten-Monte-Carlo (QMC), die alle in einer Dimension erfolgreich eingesetzt wurden, und viel zum Verständnis eindimensionaler Systeme beigetragen haben. Numerische Rechnungen leiden aber unter zweierlei Einschränkungen. Einerseits werden natürlich endlich große Systeme studiert, und die Extrapolation zum thermodynamischen Limes ist zumindest heikel, und andererseits ist es schwierig, ein einheitliches Bild zu gewinnen, wie es analytische Ergebnisse oft ermöglichen.

Die Untersuchung von effektiven Kontinuumsmodellen ist eine weitere Methode zur quantitativen Beschreibung mikroskopischer Modelle. Die Voraussetzung ist, daß man die relevanten niederenergetischen Anregungen identifizieren kann, daß bezüglich dieser Anregungen die Gitterkonstante verschwindend klein ist, und daß schlußendlich eine effektive Kontinuumstheorie –die Quantenfeldtheorie (QFT) – aus dem mikroskopischen Gittermodell abgeleitet werden kann. Dieser Zugang bietet zwei wesentliche Vorzüge, die miteinander einhergehen: einerseits ist das Kontinuumsmodell oft einfacher als der Hamiltonoperator des Ausgangsmodells. Das folgt hauptsächlich daraus, daß dank der Renormierungsgruppentheorie verstanden ist, welche Operatoren, nämlich nur die relevanten und marginalen, in die Kontinuumstheorie eingehen. Daraus folgt, daß nur eine kleine Zahl von Quantenfeldtheorien für ein gegebenes mikroskopisches Modell in Frage kommen, zumindest wenn Renormierbarkeit vorausgesetzt wird, und diese Zahl wird durch die gegebenen Symmetrien noch weiter eingeschränkt. Auf der anderen Seite erlaubt ein solcher Zugang eine Art von Universalität in ganz verschiedenen physikalischen Phenomänen zu entdecken; das liegt daran, daß die verschiedensten Modellsysteme durch die gleiche niederenergetische effektive Theorie beschrieben werden, und demnach bei niederen Energien die selbe Physik zeigen. Einige Quantenfeldtheorien sind in der heutigen Festkörperphysik zu besonderer Be-

deutung gekommen. Einige Beispiele sind im Folgenden angeführt: das freie bosonische Gauß'sche Modell in (1+1) Dimensionen, das über Bosonisierung mit dem eindimensionalen wechselwirkenden Fermisystem verbunden ist. Das "Sine-Gordon" Modell, das mit dem magnetischen XY-Modell verbunden ist oder in zwei Dimensionen ein klassisches Plasma beschreibt, und den Berezin-Kosterlitz-Thouless Phasenübergang zeigt. Die Quantenfeldtheorie, die wir hier einsetzen, ist das nichtlineare Sigma-Modell (NLσM). Das NLσM stammt aus der Teilchenphysik, wo es als Spielzeugmodell in der Quantenchromodynamik entwickelt wurde, heute ist es aber eines der wichtigsten Modelle in der Theorie der kondensierten Materie, da es einen vereinigenden Blick auf die Quantenantiferromagnete erlaubt [16, 30, 31, 32].

Zusammenfassend haben wir in dieser Einleitung versucht (a) ganz allgemein das Interesse für eindimensionale Systeme und (b) das für die eindimensionalen dotierten Antiferromagnete zu motivieren. Zudem haben wir unseren Zugang eingeführt, der sich rund um das nicht lineare Sigma-Modell, die effektive Feldtheorie für Antiferromagnete, dreht. In dieser Arbeit benützen wir die Ergebnisse dieser Theorie und erweitern sie für den komplexeren und interessanteren Fall der dotierten Systeme.

Im ersten Kapitel stellen wir die verschiedenen mikroskopischen Modelle vor, die zur Beschreibung dotierter Antiferromagnete in ein oder zwei Dimensionen benützt werden. Experimentelle Ergebnisse haben bestätigt, dass das Drei-Band Hubbard Modell die relevanten Freiheitsgrade von Materialien, die aus Kupfer-Sauerstoff Plaketten aufgebaut sind, korrekt beschreibt. Im realistischen Parameterbereich dieses Modells, der durch Quanten-Monte-Carlo Simulationen und Experimente bestimmt wurde, lässt sich das Drei-Band Modell auf das wesentlich einfachere Spin-Fermion Modell abbilden. Weitere Reduktion führt zum sogenannten $t - J$ Modell. Dieses beschreibt im Vergleich zum Spin-Fermion Modell noch weniger Freiheitsgrade, ist jedoch vom analytischen Gesichtspunkt immer noch zu schwierig, wobei die wesentliche Schwierigkeit auf den strikten Ausschluss von Doppelbesetzung zurückzuführen ist. Zuletzt noch eine Bemerkung zum ganz wichtigen undotierten Fall. Das nicht lineare Sigma-Modell in (D+1) Dimension wird

allgemein als die korrekte niederenergetische Wirkung des D dimensionalen antiferromagenetischen Heisenberg-Modells angesehen. Das unterschiedliche Verhalten von Spin S, M-leg Leitern mit halb- oder ganzzahligem SM Wert, wird dann auf einen zusätzlichen topologischen Ausdruck in der effektiven Wirkung zurückgeführt.

Im zweiten Kapitel leiten wir die Feldtheorie für den dotierten Fall her, sowohl für Ketten als auch für Leitern mit beliebiger Zahl von Beinen. Eine ähnliche Feldtheorie wurde für den Fall von (2+1) Dimensionen vorgeschlagen, jedoch nur phenomänologisch als sinnvolle Beschreibung der Hochtemperatur-Supraleiter motiviert. Wir zeigen, daß eine solche Lagrangedichte, oder besser gesagt, unsere Erweiterung, in natürlicher Weise im Kontinuumslimes eines mikroskopischen Modells für Kuprat-Ketten und Leitern, auftaucht.

Im Kapitel drei konzentrieren wir uns auf den Fall der normalen zweibeinigen ($M = 2$) Leiter. Beim Ausintegrieren der Ladungsfreiheitsgrade finden wir eine Wirkung, die die Dynamik der Spins bei endlicher Lochkonzentration beschreibt. Diese Wirkung kann explizit im Kontinuumslimes ausgewertet werden und ist ein nichtlineares Sigma-Modell mit Kopplungskonstanten, die von der Konzentration der dotierten Löcher abhängt. Wie eine Vielzahl von numerischen Simulationen [33, 34] und Experimenten [35, 36, 37, 38] gezeigt haben, wird der Spinflüssigkeitszustand der undotierten Leiter bei minimaler Konzentration der Löcher nicht zerstört. Unser Zugang ermöglicht die explizite Berechnung, wie sich die Parameter der Spinflüssigkeit bei Dotierung verändern. Und wir finden gute Übereinstimmung mit den Messungen an $Sr_{14-x}A_xCu_{24}O_{41}$.

Im vierten Kapitel entwickeln wir den Formalismus, der im vorigen Kapitel eingeführt wurde, mit dem Ziel weiter, den Einteilchen-Propagator der Löcher zu bestimmen. Hierzu wird die Zustandssumme zu einem erzeugenden Funktional für die Greensche Funktion erweitert, indem die Wirkung um einen zusätzlicher Term, der die Fermionen an Hilfsfelder koppelt, ergänzt wird. Die Greensche Funktion der Löcher folgt dann formal aus Ableitung nach den Hilfsfeldern. Die Vertexfunktion kann weiters in der Gitterkonstante als kleinem Parameter entwickelt werden. In erster Ordnung einer solchen

Entwicklung erhalten wir einen analytischen Ausdruck für den Propagator. Bei kleinen Impulsen und Energien stimmt unser Resultat mit dem Bild von freien Fermionen überein.

Zum Abschluss diskutieren wir unsere Ergebnisse in einer Zusammenfassung.

Appendix A

Effective action in the continuum limit

A.1 The trace reduction formula

Later, for the evaluation of a Fermionic determinant in the continuum limit, we will need the trace of an arbitrary even number of Pauli matrices. The result is known as trace reduction formula [131]. It can be proved as follows. First, using $\sigma^a\sigma^b = 2\delta^{ab} - \sigma^b\sigma^a$ repeatedly and the cyclic property of the trace, one shows

$$\mathrm{tr}\left(\sigma^{a_1}\sigma^{a_2}\ldots\sigma^{a_m}\right) = \sum_{j=2}^{m}\delta_{a_1a_j}\mathrm{tr}\left(\sigma^{a_2}\ldots\hat{j}\ldots\sigma^{a_m}\right) \tag{A.1}$$

where the $\hat{j}$ indicates that the term σ^{a_j} is missing. Then one iterates this formula until we get the trace of the identity. For example, for $m = 4$ we get:

$$\begin{aligned}\mathrm{tr}\left(\sigma^{a_1}\sigma^{a_2}\sigma^{a_3}\sigma^{a_4}\right) &= 2\delta_{a_1a_2}\delta_{a_3a_4} - 2\delta_{a_1a_3}\delta_{a_2a_4} + 2\delta_{a_1a_4}\delta_{a_2a_3} \\ &= 2\sum_{\pi}{}'\,\mathrm{sgn}\left(\pi\right)\delta_{a_1a_{j_2}}\delta_{a_{j_3}a_{j_4}}\end{aligned} \tag{A.2}$$

where we have the following "paths"

$\mathrm{sgn}\,(\pi)$	a_{j_1}	a_{j_2}	a_{j_3}	a_{j_4}
$+1$	a_1	a_2	a_3	a_4
-1	a_1	a_3	a_2	a_4
$+1$	a_1	a_4	a_2	a_3

For $m = 6$ with an obvious notation, one has

$$\begin{aligned}\frac{1}{2}\mathrm{tr}\,(123456) \;=\;& +(12)\,(34)\,(56) - (12)\,(35)\,(46) + (12)\,(36)\,(45) \\ & -(13)\,(24)\,(56) + (13)\,(25)\,(46) - (13)\,(26)\,(45) \\ & +(14)\,(23)\,(56) - (14)\,(25)\,(36) + (14)\,(26)\,(35) \\ & -(15)\,(23)\,(46) + (15)\,(24)\,(36) - (15)\,(26)\,(34) \\ & +(16)\,(23)\,(45) - (16)\,(24)\,(35) + (16)\,(25)\,(34) \qquad \text{(A.3)}\end{aligned}$$

In the general case we have

$$\mathrm{tr}\,(\sigma^{a_1}\sigma^{a_2}\ldots\sigma^{a_m}) = 2\sum_{\pi}{}' \,\mathrm{sgn}\,(\pi)\,\delta_{a_1 a_{j_2}}\delta_{a_{j_3}a_{j_4}}\ldots\delta_{a_{j_{m-1}}a_{j_m}} \qquad \text{(A.4)}$$

where π is the permutation

$$\begin{pmatrix} 23\ldots m \\ j_2 j_3 \ldots j_m \end{pmatrix} \qquad \text{(A.5)}$$

and $\sum'_\pi$ means we have to sum over all permutations with different pairs $j_3 j_4$ or $j_5 j_6$ and so on. The number of elements in the sum is

$$1 \times 3 \times 5 \cdots (m-1) = (m-1)!! \qquad \text{(A.6)}$$

the product of all odd numbers smaller than m.

A.2 Calculation of the antiferromagnetic contributions

In this section we calculate

$$\mathrm{tr}\ln\left(\mathbb{1}-\hat{G}_0\Sigma_{00}\right)=-\sum_{m=1}^{\infty}\frac{1}{m}\mathrm{tr}\left(\hat{G}_0\Sigma_{00}\right)^m \tag{A.7}$$

We start from Eq. 3.35 on page 75. We define the following function

$$\begin{aligned}\Pi\left(q_2,q_3,\dots q_m\right) &= \frac{1}{L\beta}\sum_{k_x,k_y,\omega_n} g_0(k)\bar{g}_0(k+q_2)g_0(k+q_3)\cdots \\ &\quad\times\cdots g_0(k+q_{m-1})\bar{g}_0(k+q_m)\,\delta_{q_y^2,0}\dots\delta_{q_y^m,0}.\end{aligned} \tag{A.8}$$

where we included the delta functions of the q_y's variable as they are effectively hidden in the Fourier transformed field:

$$\mathbf{N}_q=\delta_{q_y,0}\mathbf{N}_{q_x,\nu_n}. \tag{A.9}$$

Now we can rewrite equation (A.10) as

$$\begin{aligned}\mathrm{tr}\left(\hat{G}_0\Sigma_{00}\right)^m &= (g)^m\sum_{k,q_2\dots q_m}\Pi\left(q_2,q_3,\dots q_m\right) \\ &\quad\times\mathbf{N}^{a_1}_{-q_2}\mathbf{N}^{a_2}_{q_2-q_3}\cdots\mathbf{N}^{a_m}_{q_m}\mathrm{tr}\left(\sigma^{a_1}\sigma^{a_2}\cdots\sigma^{a_m}\right),\end{aligned} \tag{A.10}$$

with m an even integer. Fourier transforming back the $\mathbf{N}_q$ fields and doing a change of variable we obtain

$$\begin{aligned}\mathrm{tr}\left(\hat{G}_0\Sigma_{00}\right)^m = g^m\left(\frac{1}{L\beta}\right)^{m-1}\sum_{q_2\ldots q_m}\Pi\left(q_2,q_3,\ldots q_m\right)\\ \times\int dy_1\ldots dy_m e^{-iq_2y_2}e^{-iq_3y_3}\ldots e^{-iq_my_m}\\ \times\mathbf{N}^{a_1}\left(y_1\right)\mathbf{N}^{a_2}\left(y_1+y_2\right)\ldots\mathbf{N}^{a_m}\left(y_1+\ldots+y_m\right)\end{aligned}\tag{A.11}$$

where we indicated

$$\int dy_j=\sum_{i_j}\int_0^\beta d\tau_j\to\frac{1}{a}\int dx_j\int_0^\beta d\tau_j\tag{A.12}$$

similarly the variables q_j contain only the x and temporal component.

Since the field $\mathbf{N}_q$ is peaked in zero, the summation over the variables $(q_2,\ldots q_m)$ in Eqs. (A.10) or (A.11) is effectively restricted in a neighborhood of the point $\vec{q_0}=(0,\ldots 0)$. The gradient expansion is then obtained expanding the function Π in powers of q_i around zero. Fourier transforming back, l powers of q_i will lead to l derivatives of $\mathbf{N}$ (spatial or temporal). Hence we consider

$$\begin{aligned}\Pi\left(q_2,q_3,\ldots q_m\right) &= \underbrace{\Pi\left(0,\ldots,0\right)}_{I}+\underbrace{\sum_{i=2}^m\Pi_i^\mu q_i^\mu}_{II}\\ &+\underbrace{\frac{1}{2}\sum_{i=2}^m\Pi_{ii}^{\mu\nu}q_i^\mu q_i^\nu}_{III}+\underbrace{\sum_{i<j=2}^m\Pi_{ij}^{\mu\nu}q_i^\mu q_j^\nu}_{IV}+\ldots\end{aligned}\tag{A.13}$$

We examine the contribution of these terms separately.

A.2.1 Contribution I

The first term in equation (A.13) yields a completely local term. After performing the sum over the q's, only one integration $\int dy$ survives and we are

left with

$$\int dy \mathbf{N}^{a_1}(y)\,\mathbf{N}^{a_2}(y)\ldots\mathbf{N}^{a_m}(y) \tag{A.14}$$

after contraction with the Pauli trace we get an integral proportional to 1 since $|\mathbf{N}(x,\tau)|^2 = 1$. So this term gives a constant and we can drop it.

A.2.2 Contribution II

After summing over the q_j's and using all the delta functions we get terms of the form

$$\int dy \mathbf{N}^{a_1}(y)\,\mathbf{N}^{a_2}(y)\ldots\partial_\mu\mathbf{N}^{a_l}(y)\ldots\mathbf{N}^{a_m}(y) \tag{A.15}$$

after contraction with the trace over Pauli matrices each of these term give zero as $\mathbf{N}\cdot\partial_\mu\mathbf{N} = 0$.

A.2.3 Contribution III

The contribution of this term is

$$\begin{aligned}(\mathrm{III}) \;=\; & \frac{1}{2}g^m\sum_{i=2}^{m}\frac{\partial^2\Pi}{\partial q_i^\mu\partial q_i^\nu}(\vec{q}_0)\sum_{q_2\ldots q_m} q_i^\mu q_i^\nu\int dy_1\ldots dy_m \\ & \times e^{-iq_2y_2}e^{-iq_3y_3}\ldots e^{-iq_my_m} \\ & \times\mathbf{N}^{a_1}(y_1)\,\mathbf{N}^{a_2}(y_1+y_2)\ldots\mathbf{N}^{a_m}(y_1+\ldots+y_m) \\ & \times\mathrm{tr}\left(\sigma^{a_1}\sigma^{a_2}\cdots\sigma^{a_m}\right)\end{aligned} \tag{A.16}$$

now

$$\begin{aligned}\sum_{q_2\ldots q_m} q_i^\mu q_i^\nu e^{-iq_2y_2}e^{-iq_3y_3}\ldots e^{-iq_my_m} = \\ -\,\delta(y_2)\ldots\partial_\mu\partial_\nu\left[\delta(y_i)\right]\ldots\delta(y_m)\end{aligned} \tag{A.17}$$

now we have to shift the derivatives from the delta function to the fields

$$\frac{\partial^2}{\partial y_i^\mu \partial y_i^\nu}\prod_{j=i}^{m}\mathbf{N}^{a_j} = \sum_{j=i}^{m}\mathbf{N}^{a_i}\ldots\partial_\mu\partial_\nu\mathbf{N}^{a_j}\ldots\mathbf{N}^{a_m} + \sum_{\substack{l\neq j\\ l=i}}^{m}\sum_{j=i}^{m}\mathbf{N}^{a_i}\ldots\partial_\mu\mathbf{N}^{a_j}\ldots\partial_\nu\mathbf{N}^{a_l}\ldots\mathbf{N}^{a_m} \quad \text{(A.18)}$$

after all the delta's are used we remain with

$$\mathrm{tr}\left(\sigma^{a_1}\sigma^{a_2}\cdots\sigma^{a_m}\right)\left\{\underbrace{\sum_{j=i}^{m}\int dy\mathbf{N}^{a_1}(y)\ldots\partial_\mu\partial_\nu\mathbf{N}^{a_j}(y)\ldots\mathbf{N}^{a_m}}_{a_i} + \underbrace{\sum_{\substack{l\neq j\\ l=i}}^{m}\sum_{j=i}^{m}\int dy\mathbf{N}^{a_1}(y)\ldots\partial_\mu\mathbf{N}^{a_j}(y)\ldots\partial_\nu\mathbf{N}^{a_l}(y)\ldots\mathbf{N}^{a_m}(y)}_{b_i}\right\} \quad \text{(A.19)}$$

So that

$$(\mathrm{III}) = -\frac{1}{2}g^m\sum_{i=2}^{m}\frac{\partial^2\Pi}{\partial q_i^\mu\partial q_i^\nu}(\vec{q}_0)(a_i+b_i) \quad \text{(A.20)}$$

Note also that

$$\frac{\partial^2\Pi}{\partial q_i^\mu\partial q_i^\nu}(\vec{q}_0) = \begin{cases} \frac{1}{N\beta}\sum_k g_0(k)^{m/2}\bar{g}_0(k)^{m/2-1}\partial^2_{\mu\nu}\bar{g}_0(k)\equiv P_e & i \text{ even} \\ \frac{1}{N\beta}\sum_k g_0(k)^{m/2-1}\bar{g}_0(k)^{m/2}\partial^2_{\mu\nu}g_0(k)\equiv P_o & i \text{ odd} \end{cases} \quad \text{(A.21)}$$

The first piece contracted with the Pauli trace gives

$$\begin{aligned} a_i &= 2\sum_{j=i}^{m}\int dy\,\mathbf{N}\cdot\partial^2_{\mu\nu}\mathbf{N}\sum_{\pi}{}'\mathrm{sgn}\,(\pi) \\ &= -2\sum_{j=i}^{m}\int dy\,\partial_\mu\mathbf{N}\cdot\partial_\nu\mathbf{N} \end{aligned} \tag{A.22}$$

The second one gives

$$\begin{aligned} b_i &= 2\sum_{l\neq j=i}^{m}\int dy\,\partial_\mu\mathbf{N}\cdot\partial_\nu\mathbf{N}\sum_{\pi}{}''\mathrm{sgn}\,(\pi) \\ &= -2\sum_{\substack{l\neq j\\ l=i}}^{m}\sum_{j=i}^{m}(-1)^{j+l}\int dy\,\partial_\mu\mathbf{N}\cdot\partial_\nu\mathbf{N} \end{aligned} \tag{A.23}$$

and the $\sum''_\pi$ means sums over allowed permutations with j contracted with l. Now

$$\begin{aligned} a_i + b_i &= -2\int dy\,\partial_\mu\mathbf{N}\cdot\partial_\nu\mathbf{N}\sum_{l,j=i}^{m}(-1)^{j+l} \\ &= -2\int dy\,\partial_\mu\mathbf{N}\cdot\partial_\nu\mathbf{N}\,\delta_{m-i+1,\mathrm{odd}} \end{aligned} \tag{A.24}$$

Finally

$$\begin{aligned}
(\mathrm{III}) &= -\frac{1}{2}g^m\left[P_e\sum_{i=2,\mathrm{even}}^{m}(a_i+b_i)+P_o\sum_{i=3,\ \mathrm{odd}}^{m}(a_i+b_i)\right]\\
&= g^m\left\{\int dy\,\partial_\mu\mathbf{N}\cdot\partial_\nu\mathbf{N}\left[P_e\sum_{i=2,\mathrm{even}}^{m}\delta_{m-i+1,\mathrm{odd}}+P_o\sum_{i=3,\mathrm{odd}}^{m}\delta_{m-i+1,\mathrm{odd}}\right]\right\}\\
&= g^m\int dy\,\partial_\mu\mathbf{N}\cdot\partial_\nu\mathbf{N}\,P_e\sum_{i=1,\mathrm{odd}}^{m-1}\delta_{i,\mathrm{odd}}\\
&= \frac{m}{2}g^m\left[\frac{1}{N\beta}\sum_k g_0\left(k\right)^{m/2}\bar{g}_0\left(k\right)^{m/2-1}\partial^2_{\mu\nu}\bar{g}_0\left(k\right)\right]\\
&\quad\times\int dy\,\partial_\mu\mathbf{N}\cdot\partial_\nu\mathbf{N}
\end{aligned}\tag{A.25}$$

A.2.4 Contribution IV

Here we calculate

$$\begin{aligned}
(\mathrm{IV}) &= g^m\sum_{i<j=2}^{m}\frac{\partial^2\Pi}{\partial q_i^\mu\partial q_j^\nu}\left(\vec{q}_0\right)\sum_{q_2\ldots q_m}q_iq_j\int dy_1\ldots dy_m\\
&\quad\times e^{-iq_2y_2}e^{-iq_3y_3}\ldots e^{-iq_my_m}\\
&\quad\times\mathbf{N}^{a_1}\left(y_1\right)\mathbf{N}^{a_2}\left(y_1+y_2\right)\ldots\mathbf{N}^{a_m}\left(y_1+\ldots+y_m\right)\\
&\quad\times\mathrm{tr}\left(\sigma^{a_1}\sigma^{a_2}\cdots\sigma^{a_m}\right)
\end{aligned}\tag{A.26}$$

First we notice

$$\frac{\partial^2\Pi}{\partial q_i^\mu\partial q_j^\nu}\left(0\right)=\begin{cases}
\frac{1}{NB}\sum_k g_0\left(k\right)^{m/2}\bar{g}_0\left(k\right)^{m/2-2}\left[\partial_\mu\bar{g}_0\left(k\right)\partial_\nu\bar{g}_0\left(k\right)\right] & \equiv\ P_{ee}\quad i\text{ even},\ j\text{ even}\\
\frac{1}{NB}\sum_k g_0\left(k\right)^{m/2-2}\bar{g}_0\left(k\right)^{m/2}\left[\partial_\mu g_0\left(k\right)\partial_\nu g_0\left(k\right)\right] & \equiv\ P_{oo}\quad i\text{ odd}\ ,\ j\text{ odd}\\
\frac{1}{NB}\sum_k g_0\left(k\right)^{m/2-1}\bar{g}_0\left(k\right)^{m/2-1}\left[\partial_\mu g_0\left(k\right)\partial_\nu\bar{g}_0\left(k\right)\right] & \equiv\ P_{eo}\quad i\text{ even},\ j\text{ odd}\\
\frac{1}{NB}\sum_k g_0\left(k\right)^{m/2-1}\bar{g}_0\left(k\right)^{m/2-1}\left[\partial_\mu\bar{g}_0\left(k\right)\partial_\nu g_0\left(k\right)\right] & \equiv\ P_{eo}\quad i\text{ odd}\ ,\ j\text{ even}
\end{cases}\tag{A.27}$$

Now we have

$$\sum_{q_2 \dots q_m} q_i^\mu q_j^\nu e^{-iq_2 y_2} e^{-iq_3 y_3} \dots e^{-iq_m y_m} = \\ - \delta(y_2) \dots \partial_\mu \delta(y_i) \dots \partial_\nu \delta(y_j) \dots \delta(y_m) \quad \text{(A.28)}$$

again we have to shift the derivatives to the fields. Let's say $i < j$

$$\begin{aligned} \frac{\partial}{\partial y_j^\nu} \frac{\partial}{\partial y_i^\mu} \prod_{l=i}^{m} \mathbf{N}^{a_l} &= \frac{\partial}{\partial y_j^\nu} \sum_{r=i}^{m} \mathbf{N}^{a_i} \dots \partial_{y_i^\mu} \mathbf{N}^{a_r} \dots \mathbf{N}^{a_m} \\ &= \sum_{s=j}^{m} \sum_{r=i}^{m} \mathbf{N}^{a_i} \dots \partial_{y_i^\mu} \mathbf{N}^{a_r} \dots \partial_{y_j^\nu} \mathbf{N}^{a_s} \dots \mathbf{N}^{a_m} \end{aligned} \quad \text{(A.29)}$$

after all the deltas have been used we get

$$\int dy \left[\sum_{s=j}^{m} \sum_{r=i}^{m} \mathbf{N}^{a_i} \dots \partial_\mu \mathbf{N}^{a_r} \dots \partial_\nu \mathbf{N}^{a_s} \dots \mathbf{N}^{a_m} \right] \mathrm{tr}\left(\sigma^{a_1} \sigma^{a_2} \cdots \sigma^{a_m}\right) \quad \text{(A.30)}$$

we can split the sum as follows

$$\underbrace{\sum_{r=j}^{m} \dots \partial_{\mu\nu}^2 \mathbf{N}^{a_r} \dots}_{-a_{ij}} + \underbrace{\sum_{r=i}^{m} \sum_{s \neq r=j}^{m} \dots \partial_\mu \mathbf{N}^{a_r} \dots \partial_\nu \mathbf{N}^{a_s} \dots}_{-b_{ij}} \quad \text{(A.31)}$$

so that

$$\text{(IV)} = g^m \sum_{i<j=2}^{m} \frac{\partial^2 \Pi}{\partial q_i^\mu \partial q_j^\nu}(0) \left(a_{ij} + b_{ij}\right) \quad \text{(A.32)}$$

the first one contracted with Pauli matrices, gives 1 times the integral. The second gives instead $(-1)^{r+s+1}$ times the integral. So the first gives

$$\begin{aligned} a_{ij} &= -2\sum_{r=j}^{m}\int dy\,\mathbf{N}\cdot\partial^2_{\mu\nu}\mathbf{N} \\ &= 2\sum_{r=j}^{m}\int dy\,\partial_\mu\mathbf{N}\cdot\partial_\nu\mathbf{N} \end{aligned} \tag{A.33}$$

while the second gives

$$\begin{aligned} b_{ij} &= -2\sum_{r=i}^{m}\sum_{s\neq r=j}^{m}(-1)^{r+s+1}\int dy\,\partial_\mu\mathbf{N}\cdot\partial_\nu\mathbf{N} \\ &= 2\sum_{r=i}^{m}\sum_{s\neq r=j}^{m}(-1)^{r+s}\int dy\,\partial_\mu\mathbf{N}\cdot\partial_\nu\mathbf{N} \end{aligned} \tag{A.34}$$

so that

$$a_{ij}+b_{ij} = 2\sum_{r=i}^{m}\sum_{s=j}^{m}(-1)^{r+s}\int dy\,\partial_\mu\mathbf{N}\cdot\partial_\nu\mathbf{N} \tag{A.35}$$

so

$$(IV) = 2g^m\int dy\,\partial_\mu\mathbf{N}\cdot\partial_\nu\mathbf{N}\sum_{i<j=2}^{m}\frac{\partial^2\Pi}{\partial q_i^\mu\partial q_j^\nu}(0)\sum_{r=i}^{m}\sum_{s=j}^{m}(-1)^{r+s} \tag{A.36}$$

Now $\sum_{r=i}^{m}\sum_{s=j}^{m}(-1)^{r+s} = \delta_{m-i+1,\mathbf{odd}}\delta_{m-j+1,\mathbf{odd}}$ so when we insert P_{ee}, $P_{oo}\ldots$ only the sum with P_{ee} survives and gives:

$$
\begin{aligned}
(IV) &= 2g^m \int dy\, \partial_\mu \mathbf{N} \cdot \partial_\nu \mathbf{N}\, P_{ee} \sum_{\substack{i<j=2 \\ i,j \text{ even}}}^{m} \delta_{m-i+1,\text{odd}} \delta_{m-j+1,\text{odd}} \\
&= 2g^m \int dy\, \partial_\mu \mathbf{N} \cdot \partial_\nu \mathbf{N}\, P_{ee} \frac{m}{4} \left(\frac{m}{2} - 1 \right) \\
&= \frac{m}{2} \left(\frac{m}{2} - 1 \right) g^m \left(\frac{1}{NB} \sum_k g_0 (k)^{m/2} \bar{g}_0 (k)^{m/2-2} \left[\partial_\mu \bar{g}_0 (k)\, \partial_\nu \bar{g}_0 (k) \right] \right) \\
&\quad \times \int dy\, \partial_\mu \mathbf{N} \cdot \partial_\nu \mathbf{N}
\end{aligned} \tag{A.37}
$$

A.2.5 All the AFM contributions

We sum up here all the contribution

$$
\begin{aligned}
\operatorname{tr} \ln \left(\mathbb{1} - \hat{G}_0 \Sigma_{00} \right) &= -\sum_{m=1}^{\infty} \frac{1}{m} \operatorname{tr} \left(\hat{G}_0 \Sigma_{00} \right)^m \\
&= -\sum_{m=1}^{\infty} \frac{((\text{III}) + (\text{IV}))}{m} \\
&= -\frac{1}{2} \sum_{\substack{m=1 \\ m \text{ even}}}^{\infty} g^m \left[\frac{1}{N\beta} \sum_k g_0 (k)^{m/2} \bar{g}_0 (k)^{m/2-1} \partial^2_{\mu\nu} \bar{g}_0 (k) + \right. \\
&\quad \left. + \left(\frac{m}{2} - 1 \right) \left(\frac{1}{NB} \sum_k g_0 (k)^{m/2} \bar{g}_0 (k)^{m/2-2} \left[\partial_\mu \bar{g}_0 (k)\, \partial_\nu \bar{g}_0 (k) \right] \right) \right] \\
&\quad \times \int dy\, \partial_\mu \mathbf{N} \cdot \partial_\nu \mathbf{N} \\
&= -\frac{1}{2} \sum_{p=1}^{\infty} g^{2p} \left[\frac{1}{N\beta} \sum_k g_0 (k)^{m/2} \bar{g}_0 (k)^{m/2-1} \partial^2_{\mu\nu} \bar{g}_0 (k) + \right. \\
&\quad \left. + (p-1) \left(\frac{1}{NB} \sum_k g_0 (k)^{m/2} \bar{g}_0 (k)^{m/2-2} \left[\partial_\mu \bar{g}_0 (k)\, \partial_\nu \bar{g}_0 (k) \right] \right) \right] \\
&\quad \times \int dy\, \partial_\mu \mathbf{N} \cdot \partial_\nu \mathbf{N}
\end{aligned} \tag{A.38}
$$

Quite surprisingly this sum can be evaluated exactly. The result is

$$\mathrm{tr}\ln\left(\mathbb{1}-\hat{G}_0\Sigma_{00}\right)=\left.\frac{\partial^2}{\partial q^\mu\partial q^\nu}\Phi\left(q\right)\right|_0 \tag{A.39}$$

where the function Φ is

$$\Phi\left(q_x,\nu_m\right)=\frac{1}{N\beta}\sum_{k_y,k_x,\omega_n}\ln\left(1-g^2g_0\left(k_x,k_y,\omega_n\right)\bar{g}_0\left(k_x+q_x,k_y,\omega_n+\nu_m\right)\right). \tag{A.40}$$

This expression is very reminiscent of the free energy of fermions in an exactly staggered field:

$$f_{\text{Neèl}}=f_0-\frac{1}{N\beta}\sum_k\ln\left(1-g^2g_0\left(k\right)\bar{g}_0\left(k\right)\right) \tag{A.41}$$

where f_0 is the free energy without the staggered field.

A.3 Calculation of ferromagnetic and mixed contribution

Here we want to calculate the contribution coming from

$$\mathrm{tr}\ln\left(\mathbb{1}-F\left(\Sigma_{01}+\Sigma_{02}+\Sigma_1+\Sigma_2\right)\right) \tag{A.42}$$

which contains both ferromagnetic contribution $\sim \mathbf{l},\mathbf{M}$ and mixed one $\sim \mathbf{lN},\mathbf{MN}$. Now we insert Eq. (3.39) in (A.42) and expand up to second order in a. We obtain

$$\begin{aligned}\mathrm{tr}\ln\left(\mathbb{1}-F\left(\Sigma_{01}+\Sigma_{02}+\Sigma_1+\Sigma_2\right)\right) &= -a\mathrm{tr}\left(F_0\hat{\Sigma}_{01}\right)+a^2\mathrm{tr}\left(F_0R_1D^{-1}\hat{\Sigma}_{01}\right)\\ &\quad -\frac{a^2}{2}\mathrm{tr}\left(F_0\hat{\Sigma}_{02}\right)-\frac{a^2}{2}\mathrm{tr}\left(F_0\hat{\Sigma}_{01}\right)^2\\ &\quad -a^2\mathrm{tr}\left(F_0\hat{\Sigma}_{01}F_0\hat{\Sigma}_1\right)\\ &\quad -a\mathrm{tr}\left(F_0\hat{\Sigma}_1\right)+a^2\mathrm{tr}\left(F_0RD^{-1}\hat{\Sigma}_1\right)\\ &\quad -a^2\mathrm{tr}\left(F_0\hat{\Sigma}_2\right)-\frac{a^2}{2}\mathrm{tr}\left(F_0\hat{\Sigma}_1\right)^2 \quad \text{(A.43)}\end{aligned}$$

where we defined also

$$\begin{aligned}F_0 &= \bar{F}D^{-1}\\ &= \underbrace{\bar{g}_0^{-1}\left(k\right)D^{-1}\left(k\right)}_{\equiv G_0(k)}\delta_{k,q}\delta_{\alpha,\beta}-gD^{-1}\left(q\right)\mathbf{N}_{k-q+Q}\cdot\boldsymbol{\sigma}_{\alpha,\beta}. \quad \text{(A.44)}\end{aligned}$$

The poles of $G_0\left(k\right)$ correspond to the zeros of $D\left(k\right)$ and define the mean field bands which we encountered in chapter 3. These bands originates from free fermion with propagator g_0, interacting with a perfectly antiferromagnetic (Nèel) spin background. In chapter four we will see that, besides a multiplicative constant, $G_0\left(k\right)$ is indeed the zeroth order term of the exact Fermion propagator in a certain expansion.

Carrying out the traces in Eq. (A.43) gives the following expressions:

$$\begin{aligned}
\mathrm{tr}\left(F_0\hat{\Sigma}_{01}\right) &= 0 && \text{(A.45)}\\
\mathrm{tr}\left(F_0R_1D^{-1}\hat{\Sigma}_{01}\right) &= 0 && \text{(A.46)}\\
\mathrm{tr}\left(F_0\hat{\Sigma}_{02}\right) &= 2g^2c_1\int dx\,d\tau\,|\mathbf{M}|^2 && \text{(A.47)}\\
\mathrm{tr}\left(F_0D^{-1}\hat{\Sigma}_{01}\right)^2 &= 2g^2c_2\int dx\,d\tau\,|\mathbf{M}|^2 && \text{(A.48)}\\
\mathrm{tr}\left(F_0\hat{\Sigma}_{01}F_0\hat{\Sigma}_1\right) &= 0 && \text{(A.49)}
\end{aligned}$$

and

$$\begin{aligned}
\mathrm{tr}\left(F_0\hat{\Sigma}_1\right) &= 0\\
\mathrm{tr}\left(F_0RD^{-1}\hat{\Sigma}_1\right) &= i\frac{g^3}{S}\sum_{\mu=x,\tau}\hat{\chi}_\mu\int dx\,d\tau\,(\mathbf{N}\times\partial_\mu\mathbf{N})\cdot(\mathbf{l}_1+\mathbf{l}_2)\\
&= i\frac{2g^3}{S}\sum_{\mu=x,\tau}\hat{\chi}_\mu(N\beta)\sum_q(\mathbf{N}\times\partial_\mu\mathbf{N})_q\cdot\mathbf{l}_{-q}\\
\mathrm{tr}\left(F_0\hat{\Sigma}_2\right) &= -\frac{g^2}{2S^2}\chi_0\int dx\,d\tau\left(|\mathbf{l}_1|^2+|\mathbf{l}_2|^2\right)\\
&= -\frac{g^2}{S^2}\chi_0(N\beta)\sum_q\mathbf{l}_q\cdot\mathbf{l}_{-q}\\
\mathrm{tr}\left(F_0\hat{\Sigma}_1\right)^2 &= \frac{2g^2}{S^2}(N\beta)\sum_q\left[\chi_1(q)-g^2\chi_2(q)\right]\mathbf{l}_q\cdot\mathbf{l}_{-q} \qquad \text{(A.50)}
\end{aligned}$$

We introduced again the three dimensional Fourier transform, for the ferromagnetic field $\mathbf{l}$ as in this case are the susceptibilities automatically diagonal. Remind also we used an unconventional normalization for Fourier transform of Bosonic field.

The various quantities entering in these expressions are

$$\begin{aligned}
\chi_\mu &= (-i)\frac{1}{N\beta}\sum_k D^{-1}(k)\,\partial_\mu g_0^{-1}(k)\,D^{-1}(k) \qquad \text{(A.51)}\\
\chi_0 &= \frac{1}{N\beta}\sum_k D^{-1}(k)\\
\chi_1(q) &= \frac{1}{N\beta}\sum_k D^{-1}(k)\,\bar{g}_0^{-1}(k)\,D^{-1}(k-q)\,\bar{g}_0^{-1}(k-q)\\
\chi_2(q) &= \frac{1}{N\beta}\sum_k D^{-1}(k)\,D^{-1}(k-q)
\end{aligned}$$

In equation (A.51) one shows that only the temporal part is non zero, χ_x is the integral of an odd function and cancels identically.

The total contribution to the action coming from the field $\mathbf{M}$ is simply

$$S_{\mathbf{M}} = 2g^2\,(c_1 + c_2/2)\int dx d\tau\,|\mathbf{M}|^2 \qquad \text{(A.52)}$$

direct computation shows that the constant $(c_1 + c_2/2)$ is positive, hence this field can be integrated out without further consequences.

The continuum limit is achieved by expanding the $\chi_j(q)$ function in Eq. (A.50) in $(q_x, q_\tau) = (0,0)$. In principle we can integrate out the field $\mathbf{l}$ still in the discrete, in its Fourier representation. In this way one shows explicitly that Gaussian integration and continuum limit commute.

In the continuum limit the $\mathbf{l}^2$contribution to the action can be given a simple form:

$$S_{\mathbf{l}^2} = \frac{g^2}{2S^2}\tilde{\chi} N\beta \sum_q \mathbf{l}_q \cdot \mathbf{l}_{-q} \qquad \text{(A.53)}$$

with the last definition

$$\begin{aligned}\tilde{\chi} &= 2\left(\chi_1(0) - g^2\chi_2(0) - \chi_0\right) \\ &= \frac{1}{N\beta}\sum_k \left[D^{-1}(k)\left(\bar{g}_0^{-1}(k) - g_0(k)\right)\right]^2 \end{aligned} \tag{A.54}$$

A.4 Integration of the ferromagnetic fluctuation

The integration of the fluctuating field $\mathbf{l}$ is simpler in Fourier representation. Including contribution both from the spin and for the hole part the $\mathbf{l}$ dependent part of the action is

$$S_{\mathbf{l}} = \sum_q \left\{ \frac{1}{2}\left[\chi_{\text{spin}}^{-1}(q) + \frac{g^2}{2S^2}\tilde{\chi}\right]\mathbf{l}_q \cdot \mathbf{l}_{-q} \right. \\ \left. -i\left(1 + \frac{g^3}{S}\hat{\chi}_\tau\right)\left(\mathbf{N}\times\partial_\tau\mathbf{N}\right)_q \cdot \mathbf{l}_{-q}\right\} \tag{A.55}$$

where we used here a correct normalization for the Fourier transform. $\chi_{\text{spin}}^{-1}(q)$ is the bare antiferromagnetic susceptibility:

$$\chi_{\text{spin}}^{-1}(q) = 2J_{||}\left[\cos(q_x a) + 1\right] + J_\perp\left[\cos(q_y a) + 1\right] \tag{A.56}$$

The Gaussian integration leads to

$$\int D\left[\mathbf{l}^\perp\right] e^{-S_{\mathbf{l}}} = \exp\int dx d\tau \left\{ -\frac{\left(1 + \frac{g^3}{S}\hat{\chi}_\tau\right)^2}{\left[\chi_\perp^{-1}(0,0) + \frac{g^2}{2S^2}\tilde{\chi}\right]}\left|\partial_\tau\mathbf{N}\right|^2 \right\}, \tag{A.57}$$

apart from a multiplicative, irrelevant constant. We note that, because of the constraint $\mathbf{N}\cdot\mathbf{l}_\lambda = 0$, the integration is restricted to the component of $\mathbf{l}$ orthogonal to $\mathbf{N}$, $\mathbf{l}_\perp$. This does not introduce complication in the Gaussian integration as:

$$\mathbf{l}_q \cdot \mathbf{l}_{-q} = \mathbf{l}_{\perp,q} \cdot \mathbf{l}_{\perp,-q} + \mathbf{l}_{||,q} \cdot \mathbf{l}_{||,-q} \tag{A.58}$$

whereas

$$\left(\mathbf{N} \times \partial_\tau \mathbf{N}\right)_q \cdot \mathbf{l}_{||,-q} = 0. \tag{A.59}$$

So the restriction in the integration changes simply the normalization factor in front of the integral. Summing the contribution coming from the antiferromagnetic part, one obtains finally equation (3.49).

Appendix B

Self energy for the doped two-leg ladder

B.1 Matrix inversion up to second order

Here we calculate the inverse of $\hat{G}^{-1}$. Throughout we use the convention of chapter three and four. Recalling equation 3.24 on page 73 we have the following expression for the (rescaled) propagator:

$$\hat{G}^{-1} = F^{-1} - \Sigma_{01} - \Sigma_{02} - \Sigma_1 - \Sigma_2 \tag{B.1}$$

where the various self energy are at least of order a weather F^{-1} is a zero order quantity. The only problem is given by the inversion of F^{-1}. This is a result that we also needed in chapter three, although only up to first order there. If we define the following quantity

$$\bar{F} = \bar{g}^{-1}(k)\,\delta_{kq}\delta_{\alpha\beta} - g\mathbf{N}_{k-q+Q}\cdot\boldsymbol{\sigma}_{\alpha\beta} \tag{B.2}$$

then one can easily check that

$$
\begin{aligned}
F^{-1}\bar{F} &= \sum_{\xi,\sigma}\left(g^{-1}(k)\,\delta_{k\xi}\delta_{\alpha\sigma}+g\mathbf{N}_{k-\xi+Q}\cdot\boldsymbol{\sigma}_{\alpha\sigma}\right)\left(\bar{g}^{-1}(\xi)\,\delta_{\xi q}\delta_{\sigma\beta}-g\mathbf{N}_{\xi-q+Q}\cdot\boldsymbol{\sigma}_{\sigma\beta}\right)\\
&= \left(g^{-1}(k)\,\bar{g}^{-1}(k)-g^{2}\right)\delta_{kq}\delta_{\alpha\beta}-g\left(g^{-1}(k)-g^{-1}(q+Q)\right)\mathbf{N}_{k-q+Q}\cdot\boldsymbol{\sigma}_{\alpha\beta}\\
&\approx D(k)\,\delta_{kq}\delta_{\alpha\beta}-ga\left[\sum_{r=x,\tau}(k-q+Q)_r\,\partial_{k_r}\,g^{-1}|_{q+Q}\right]\mathbf{N}_{k-q+Q}\cdot\boldsymbol{\sigma}_{\alpha\beta}\\
&\quad -ga^{2}\left[\frac{1}{2}\sum_{rs=x,\tau}(k-q+Q)_r\,(k-q+Q)_s\,\partial^{2}_{k_r,k_s}\,g^{-1}|_{q+Q}\right]\mathbf{N}_{k-q+Q}\cdot\boldsymbol{\sigma}_{\alpha\beta}\\
&= D+\underbrace{aR_1+a^{2}R_2}_{R}+O\left(a^{3}\right) \qquad \text{(B.3)}
\end{aligned}
$$

and in the last line we defined the quantities $R_1$and R_2 which appeared at page 94. In the third line of equation (B.3) we exploited once again the fact that the field $\mathbf{N}_k$, being slowly varying in real space, has small momentum transfer in Fourier space, so that it effectively constraints the points k and $q+Q$ to be close one another. This imply the inverse of F^{-1} up to second order in the lattice constant is

$$
F=\bar{F}D^{-1}-\bar{F}D^{-1}RD^{-1}+\bar{F}D^{-1}RD^{-1}RD^{-1}+O\left(a^{3}\right). \qquad \text{(B.4)}
$$

This encloses also the first order formula (3.39) which we used in section 3.4. Defining again, for convenience

$$
F_0=\bar{F}D^{-1}, \qquad \text{(B.5)}
$$

we finally obtain the inverse, complete propagator, up to second order:

$$
\begin{aligned}
\hat{G} &= F_0+a\left(-F_0R_1D^{-1}+F_0\Sigma_1F_0\right)\\
&\quad +a^{2}\left(-F_0R_2D^{-1}+F_0R_1D^{-1}R_1D^{-1}+F_0\Sigma_2F_0\right.\\
&\quad \left.+F_0\Sigma_1F_0\Sigma_1F_0\right), \qquad \text{(B.6)}
\end{aligned}
$$

which is equation 4.15 on page 94.

B.2 Self energy contribution up to first order

In this section we evaluate the contribution to the fermionic self energy up to first order. This amount to show the necessaru steps between equation (4.47) on page 99 and Eq. (4.51) on page 100. Here we will use the free massive boson approximation to the non linear sigma model action. Hnece we need to evaluate the following average

$$\left\langle \tilde{G}_N \right\rangle_{S_{MB}} \tag{B.7}$$

where the propagator has the following contributions

$$\tilde{G}_N = \underbrace{G_N}_{\text{I}} + \frac{1}{2}\underbrace{\left(\mathcal{D}\mathbf{B}_J\right) A_0^{-1}\mathbf{B}_0}_{\text{II}} + \frac{1}{4}\underbrace{\mathbf{B}_0 A_0^{-1}\left(\mathcal{D}A_J\right) A_0^{-1}\mathbf{B}_0}_{\text{III}}. \tag{B.8}$$

Here we $\mathcal{D}$ stands for the following differential operator:

$$\mathcal{D} \equiv \left.\frac{\partial^2}{\partial J_q \partial J_k^*}\right|_{J^*=J=0} \tag{B.9}$$

After averaging, we get contribution from terms I), II), III) as depicted in the above equation.

B.2.1 Contribution I

The contribution coming from (I) up to first order are:

$$\left(F_0\right)_{k,q} - a\left(F_0 R_1 D^{-1}\right)_{k,q}. \tag{B.10}$$

Performing the matrix multiplications and the average (now on is always implicitly assumed that angle brackets means average with respect to the massive boson theory) we obtain

$$\text{I)} = G_0(q)\,\delta_{k,q} - ig^2 D^{-1}(q)\,\partial_\mu \bar{g}^{-1}(q)\,\delta_{k,q} \sum_\xi D^{-1}(\xi) \left\langle \mathbf{N}_{q-\xi} \cdot (\partial_\mu \mathbf{N})_{\xi-q} \right\rangle . \tag{B.11}$$

B.2.2 Contribution II

First we calculate the product $\mathbf{B}_0 A_0^{-1} \mathbf{B}_J$ (remind the matrix A_0 is diagonal):

$$\begin{aligned}
\mathbf{B}_0 A_0^{-1} \mathbf{B}_J &= 2i\lambda \sum_\eta (\mathbf{N} \times \partial_\tau \mathbf{N})_{-\eta} \cdot \mathbf{B}_J(\eta) \\
&= -2i\frac{g\lambda}{S} \sum_{\eta\xi kq} (\mathbf{N} \times \partial_\tau \mathbf{N})_{-\eta} J_k^* (F_0)_{k,\xi-\eta} \boldsymbol{\sigma} (F_0)_{\xi,q} J_q \\
\text{(i)} &= -2i\frac{g\lambda}{S} \sum_{q\eta} J_{q-\eta}^* (\mathbf{N} \times \partial_\tau \mathbf{N})_{-\eta} \cdot \boldsymbol{\sigma} G_0(q-\eta) G_0(q) J_q \\
\text{(ii)} &\quad -2i\frac{g^3\lambda}{S} \sum_{\eta\xi kq} J_k^* D^{-1}(\xi-\eta) D^{-1}(q) \mathbf{N}_{k-\xi+\eta+Q} \cdot \boldsymbol{\sigma} \\
&\qquad (\mathbf{N} \times \partial_\tau \mathbf{N})_{-\eta} \cdot \boldsymbol{\sigma} \mathbf{N}_{\xi-q+Q} \cdot \boldsymbol{\sigma} J_q \\
\text{(iii)} &\quad -2i\frac{g^2\lambda}{S} \sum_{\eta kq} J_k^* G_0(k) D^{-1}(q) (\mathbf{N} \times \partial_\tau \mathbf{N})_{-\eta} \cdot \boldsymbol{\sigma} \\
&\qquad \mathbf{N}_{k+\eta-q+Q} \cdot \boldsymbol{\sigma} J_q \\
\text{(iv)} &\quad -2i\frac{g^2\lambda}{S} \sum_{\eta kq} J_k^* D^{-1}(q-\eta) G_0(q) \mathbf{N}_{k-q+\eta+Q} \cdot \boldsymbol{\sigma} \\
&\qquad (\mathbf{N} \times \partial_\tau \mathbf{N})_{-\eta} \cdot \boldsymbol{\sigma} J_q .
\end{aligned} \tag{B.12}$$

The constant λ appearing in this equation is:

$$\lambda = \frac{\left(1 + \frac{g^3}{S}\hat{\chi}_\tau\right)}{4J_{||} + 2J_\perp + \frac{g^2}{S^2}\tilde{\chi}}. \tag{B.13}$$

After averaging, the term (i) gives zero because of the Levi-Civita symbol in the cross product. Terms (iii) and (iv) give zero, as, in a theory without

symmetry breaking, averages of an odd numbers of fields give zero, because of Wick theorem. Hence, after differentiating and averaging, only the second term remains and we obtain the following contribution

$$\begin{aligned} \text{II)} &= -2i\frac{g^3\lambda}{S}\sum_{\xi,\eta} D^{-1}(\xi-\eta)\,D^{-1}(q) \\ &\qquad \times\left\langle \mathbf{N}_{k-\xi+\eta}\cdot\boldsymbol{\sigma}\left(\mathbf{N}\times\partial_\tau\mathbf{N}\right)_{-\eta}\cdot\boldsymbol{\sigma}\mathbf{N}_{\xi-q}\cdot\boldsymbol{\sigma}\right\rangle \\ &= -2i\frac{g^3\lambda}{S}\sum_{\xi,\eta,s} D^{-1}(\xi-\eta)\,D^{-1}(q) \\ &\qquad \times\left\langle \mathbf{N}^a_{k-\xi+\eta}\mathbf{N}^\alpha_{s-\eta}\left(\partial_\tau\mathbf{N}\right)^\beta_{-s}\mathbf{N}^c_{\xi-q}\right\rangle \epsilon^{b\alpha\beta}\sigma^a\sigma^b\sigma^c. \end{aligned} \tag{B.14}$$

After using the Wick theorem, the following identities for Pauli matrices are useful:

$$\left(\sigma^a\sigma^b\sigma^d\right) = i\epsilon^{abc}\mathbb{1} + \sigma^a\delta_{bc} - \delta_{ca}\sigma^b + \delta_{ba}\sigma^c \tag{B.15}$$

which in turn implies

$$\epsilon^{abc}\sigma^a\sigma^b\sigma^c = (\boldsymbol{\sigma}\times\boldsymbol{\sigma})\cdot\boldsymbol{\sigma} = 2i\boldsymbol{\sigma}\cdot\boldsymbol{\sigma} = 6i\mathbb{1}. \tag{B.16}$$

One obtains then

$$\begin{aligned} \text{II)} &= +\frac{12\lambda g^3}{S}\delta_{k,q}D^{-1}(q)\sum_{\eta,s} D^{-1}(q-s)\left\langle \mathbf{N}_s\cdot\left(\partial_\tau\mathbf{N}\right)_{-s}\right\rangle\left\langle \mathbf{N}_{s-\eta}\cdot\mathbf{N}_{\eta-s}\right\rangle \\ &\quad -\frac{12\lambda g^3}{S}\delta_{k,q}D^{-1}(q)\sum_{\eta,s} D^{-1}(q-\eta)\left\langle \mathbf{N}_\eta\cdot\mathbf{N}_{-\eta}\right\rangle\left\langle \left(\partial_\tau\mathbf{N}\right)_{-s}\cdot\mathbf{N}_s\right\rangle. \end{aligned} \tag{B.17}$$

As the constraint is still satisfied on average we have :

$$\begin{aligned} \sum_s \left\langle (\partial_\tau \mathbf{N})_{-s} \mathbf{N}_s \right\rangle &= 0 \\ \sum_\eta \left\langle \mathbf{N}_{s-\eta} \mathbf{N}_{\eta-s} \right\rangle &= 1 \,. \end{aligned} \tag{B.18}$$

So finally the contribution up to first order is

$$\text{II)} = \frac{12\lambda g^3}{S} \delta_{k,q} \delta_{\alpha,\beta} D^{-1}(q) \sum_s D^{-1}(q-s) \left\langle \mathbf{N}_s (\partial_\tau \mathbf{N})_{-s} \right\rangle . \tag{B.19}$$

Reminding formula (4.41) on page 97, we obtain then a first order Green's function which has the form

$$\mathcal{G}_1(q) = \bar{g}_0(q) \mathcal{G}_0(q) \left[\frac{6\lambda g^3}{S} \Gamma_\tau(q) - i\partial_\mu \bar{g}_0^{-1}(q) \Gamma_\mu(q) \right], \tag{B.20}$$

where the quatinty Γ_μ has been defined at page (4.52).

Amputating the two external legs one obtains finally the self energy at first order, equation (4.51) on page 100.

Bibliography

[1] L. D. Landau, *The theory of a fermi liquid*, Sov. Phys. JETP **3**, 920 (1957).

[2] L. D. Landau, *Oscillations in a fermi liquid*, Sov. Phys. JETP **5**, 101 (1957).

[3] L. D. Landau, *On the theory of the fermi liquid*, Sov. Phys. JETP **8**, 70 (1959).

[4] L. Cooper, *Bound electron pairs in a degenerate fermi gas*, Phys. Rev. **104**, 1189 (1956).

[5] J. Bardeen, L. Cooper, and J. Schrieffer, *Theory of superconductivity*, Phys. Rev. **108**, 1175 (1957).

[6] J. G. Bednorz and K. A. Müller, Z. Phys. B **64**, 188 (1986).

[7] A. C. Hewson, *The Kondo Problem to Heavy Fermions* (Cambridge University Press, 1993).

[8] K. von Klitzing, G. Dorda, and M. Pepper, *New method for high-accuracy determination of the fine-structure constant based on quantized hall resistance*, Phys. Rev. Lett. **45**, 494 (1980).

[9] R. B. Laughlin, *Anomalous quantum hall effect: An incompressible quantum fluid with fractionally charged excitations*, Phys. Rev. Lett. **50**, 1395 (1983).

[10] E. Dagotto, *Correlated electrons in high-temperature superconductors*, Rev. Mod. Phys. **66**, 763 (1994).

[11] R. Shankar, *Renormalization-group approach to interacting fermions*, Rev. Mod. Phys. **66**, 129 (1994).

[12] J. M. Luttinger, J. Math. Phys. **4**, 1154 (1963).

[13] J. Voit, *One-dimensional fermi liquids*, Rep. Prog. Phys. **57**, 977 (1994).

[14] S. Tomonaga, Prog. Theor. Phys. (Kyoto) **5**, 544 (1950).

[15] H. G. Schuster, editor, *One-Dimensional Conductors*volume 34 of *Lecture Notes in Physics* (Springer-Verlag, Berlin, 1975).

[16] F. D. M. Haldane, Phys. Rev. Lett. **50**, 1153 (1983).

[17] T. M. Rice, S. Gopalan, and M. Sigrist, Europhys. Lett. **23**, 445 (1993).

[18] R. Botet and R. Jullien, *Ground-state properties of a spin-1 antiferromagnetic chain*, Pyhs. Rev. B **27**, 613 (1983).

[19] M. P. Nightingale and H. W. J. Blöte, Phys. Rev. B **33**, 659 (1986).

[20] O. Golinelli, T. Jolicoeur, and R. Lacaze, J. Phys. Condens. Matter **5**, 1399 (1993).

[21] S. R. White, R. M. Noack, and D. J. Scalapino, Phys. Rev. Lett. **73**, 886 (1994).

[22] M. Greven, R. J. Birgenau, and U. J. Wiese, Phys. Rev. Lett. **77**, 1865 (1996).

[23] W. J. L. Buyers *et al.*, Phys. Rev. Lett. **56**, 371 (1986).

[24] J. P. Renard *et al.*, Europhys. Lett. **3**, 945 (1987).

[25] D. C. Johnston, J. W. Johnson, D. P. Goshorn, and A. J. Jacobson, *Magnetic susceptibility of $(VO)_2P_2O_7$: A one-dimensional spin-1/2 heisenberg antiferromagnet with a ladder spin configuration and a singlet ground state*, Phys. Rev. B **35**, 219 (1987).

[26] R. S. Eccleston, T. Barnes, J. Brody, and J. W. Johnson, *Inelastic neutron scattering from the spin ladder compound $(VO)_2P_2O_7$*, Phys. Rev. Lett. **73**, 2626 (1994).

[27] M. Azuma, Z. Hiroi, M. Takano, K. Ishida, and Y. Kitaoka, Phys. Rev. Lett. **73**, 3463 (1994).

[28] R. Calemczuk *et al.*, *Thermodynamic properties of the spin-1/2 antiferromagnetic ladder $Cu_2(C_2H_{12}N_2)Cl_4$ under magnetic field*, Eur. Phys. J. B **7**, 171 (1999).

[29] U. M *et al.*, *Superconductivity in the ladder material $Sr_{0.4}Ca_{13.6}Cu_{24}O_{41.84}$*, J. Phys. Soc. Japan **65**, 2764 (1996).

[30] F. D. M. Haldane, Phys. Rev. Lett. **61**, 1029 (1988).

[31] I. Affleck, in *Fields, Strings and Critical Phenomena*, edited by E. Brézin and J. Zinn-Justin, Les Houches, Session XLIX, 1988, Elsevier Science Publishers, 1989.

[32] S. Dell'Aringa, E. Ercolessi, G. Morandi, P. Pieri, and M. Roncaglia, Phys. Rev. Lett. **78**, 2457 (1997).

[33] R. M. Noack, S. R. White, and D. J. Scalapino, *Correlations in a two-chain hubbard model*, Phys. Rev. Lett. **73**, 882 (1994).

[34] B. Ammon, M. Troyer, T. M. Rice, and N. Shibata, Phys. Rev. Lett. **82**, 3855 (1999).

[35] K. ichi Kumagai *et al.*, Phys. Rev. Lett. **78**, 1992 (1997).

[36] K. Magishi *et al.*, Phys. Rev. B **57**, 11533 (1998).

[37] P. Carretta, P. Ghigna, and A. Lasciafari, Phys. Rev. B **57**, 11545 (1998).

[38] A. Gozar *et al.*, Phys. Rev. Lett. **87**, 197202 (2001).

[39] S. Reich and Y. Tsabba, *Possible nucleation of a 2D superconducting phase on WO_3 single crystals surface doped with Na^+*, Eur. Phys. J. B **9**, 1.

[40] A. Shengelaya *et al.*, Eur. Phys. J. B **12**, 13 (1999).

[41] V. J. Emery, Phys. Rev. Lett. **58**, 2794 (1987).

[42] H. M. S., M. Schlüter, and N. E. Christensen, Phys. Rev. B **39**, 9028 (1989).

[43] G. Dopf *et al.*, Physica B **165-166**, 1015 (1990).

[44] G. Dopf, A. Muramatsu, and W. Hanke, *Three-band hubbard model: A monte carlo study*, Phys. Rev. B **41**, 9264 (1990).

[45] G. Dopf, A. Muramatsu, and W. Hanke, *Consistent description of high-tc superconductors with the three-band hubbard model*, Phys. Rev. Lett. **68**, 353 (1992).

[46] N. Nücker *et al.*, Z. Phys. B **67**, 9 (1987).

[47] A. Muramatsu, R. Zeyher, and D. Schmeltzer, Europhys. Lett. **7**, 473 (1988).

[48] J. Zaanen and A. M. Oleś, Phys. Rev. B **37**, 9423 (1988).

[49] F. C. Zhang and T. M. Rice, Phys. Rev. B **37**, 3759 (1988).

[50] P. W. Anderson, Science **235**, 1196 (1987).

[51] P. W. Anderson, in *Frontiers and Borderlines in Many-Particle Physics*, Varenna, Italy, 1987, Varenna Summer School.

[52] D. C. Mattis and C. Y. Pan, *Ground-state energy of heisenberg antiferromagnet for spins s=1 / 2 and s=1 in d=1 and 2 dimensions*, Phys. Rev. Lett. **61**, 463 (1988).

[53] A. W. Sandvik and R. R. P. Singh, *High-energy magnon dispersion and multi-magnon continuum in the two-dimensional heisenberg antiferromagnet*, Phys. Rev. Lett. **86**, 528 (2001).

[54] D. Vaknin *et al.*, Phys. Rev. Lett. **58**, 2802 (1987).

[55] G. Shirane *et al.*, Phys. Rev. Lett. **59**, 1613 (1987).

[56] E. Dagotto, J. Riera, and D. J. Scalapino, Phys. Rev. B **45**, 5744 (1992).

[57] R. S. Ecclestone *et al.*, Phys. Rev. Lett. **81**, 1702 (1998).

[58] S. Katano *et al.*, Phys. Rev. Lett. **82**, 636 (1999).

[59] H. Mayaffre *et al.*, Science **279**, 345 (1998).

[60] B. Keimer *et al.*, Phys. Rev. B **46**, 14034 (1992).

[61] Y. Endoh *et al.*, Phys. Rev. B **37**, 7443 (1988).

[62] J. M. Tranquada *et al.*, Phys. Rev. B **38**, 2477 (1988).

[63] R. J. Birgeneau *et al.*, *Antiferromagnetic spin correlations in insulating, metallic, and superconducting* $La_{2-x}Sr_xCuO_4$, Phys. Rev. B **38**, 6614 (1988).

[64] T. Thio *et al.*, Phys. Rev. B **38**, 905 (1988).

[65] J. M. Tranquada *et al.*, *Neutron-scattering study of the dynamical spin susceptibility in* $YBa_2Cu_3O_{6.6}$, Phys. Rev. B **46**, 5561 (1992).

[66] N. D. Mermin and H. Wagner, Phys. Rev. Lett. **17**, 1133 (1966).

[67] M. Guvitch and A. T. Fiory, Phys. Rev. Lett. **70**, 3995 (1987).

[68] G. Burns, *High-Temperature Superconductivity* (Academic, New York, 1992).

[69] H. Zimmermann *et al.*, J. Less Comm. Met. **164-165**, 138 (1990).

[70] J. Rossat-Mignod *et al.*, Physica **185-189C**, 6 (1991).

[71] M. T *et al.*, Physica B (1998), Proc. SCES98 Conf. (Paris).

[72] N. Fujiwara *et al.*, **90**, 137001 (2003).

[73] N. Nücker, J. Fink, J. C. Fuggle, P. J. Durham, and W. M. Temmerman, *Evidence for holes on oxygen sites in the high-Tc superconductors* $La_{2-x}Sr_xCuO_4$ *and* $YBa_2Cu_3O_{7-y}$, Phys. Rev. B **37**, 5158 (1988).

[74] F. Mila, Phys. Rev. B **38**, 11358 (1988).

[75] N. Motoyama *et al.*, *Effect of Ca substitution and pressure on the transport and magnetic properties of* $Sr_{14}Cu_{24}O_{41}$ *with doped two-leg Cu-O ladders*, Phys. Rev. B **55**, R3386 (1997).

[76] T. Osafune, N. Motoyama, H. Eisaki, and S. Uchida, Phys. Rev. Lett. **78**, 1980 (1997).

[77] N. Nücker *et al.*, Phys. Rev. B **62**, 14384 (2000).

[78] F. C. Zhang and T. M. Rice, *Validity of the* $t-J$ *model*, Phys. Rev. B **41**, 7243 (1990).

[79] A. Ramšak and P. Prelošek, *Comparison of effective models for* CuO_2 *layers in oxide superconductors*, Phys. Rev. B **40**, 2239 (1989).

[80] H. Bethe, Z. Physik **71**, 205 (1931).

[81] F. D. M. Haldane, Phys. Rev. Lett. **45**, 1358 (1980).

[82] F. D. M. Haldane, in *Two-Dimensional Strongly Correlated Electron Systems*, edited by Z. Z. Gan and Z. B. Su, p. 249, Gordon and Breach, 1988.

[83] G. Morandi, *The Role of Topology in Classical and Quantum Physics* (Springer-Verlag, 1992).

[84] G. Sierra, in *Strongly Correlated Magnetic and Superconducting Systems*, edited by G. Sierra and M. A. Martin-delgado, volume 478 of *Lectures Notes in Physics*, Berlin, 1997, Springer-Verlag, Available as eprint: COND-MAT/9610057.

[85] I. E. Dzyaloshinskii, A. M. Polyakov, and P. B. Wiegmann, Phys. Lett. A **127**, 112 (1988).

[86] A. M. Polyakov, Phys. Lett. B **59**, 79 (1975).

[87] A. Belavin and A. M. Polyakov, JETP Lett. **22**, 245 (1975).

[88] E. Lieb, T. Schultz, and D. Mattis, *Two soluble model of an antiferromagnetic chain*, Ann. Phys. **16**, 407 (1961).

[89] J. des Cloizeaux and J. J. Pearson, *Spin-wave spectrum of the antiferromagnetic linear chain*, Phys. Rev. **128**, 2131 (1962).

[90] I. Affleck, COND-MAT/9802045 (1998).

[91] R. Shankar and N. Read, Nucl. Phys. B **336**, 457 (1990).

[92] W. Marshall, Proc. Roy. Soc. (London) **17**, 7 (1955).

[93] E. Lieb and D. Mattis, *Ordering of energy levels of interacting spin stystem*, J. Math. Phys. **3**, 749 (1962).

[94] I. Affleck and E. Lieb, Lett. Math. Phys. **12**, 57 (1986).

[95] I. Affleck, Phys. Rev. B **37**, 5186 (1988).

[96] S. R. White and R. M.Noack, Phys. Rev. Lett. **73**, 886 (1994).

[97] V. N. Popov, *Functional integrals and collective excitations* (Cambridge Univesity Press, 1987).

[98] M. Ogata, M. U. Luchini, S. Sorella, and F. F. Assaad, *Phase diagram of the one-dimensional $t-J$ model*, Phys. Rev. Lett. **66**, 2388 (1991).

[99] M. Nakamura, K. Nomura, and A. Kitazawa, *Renormalization group analysis of the spin-gap phase in the one-dimensional $t-J$ model*, Phys. Rev. Lett. **79**, 3214 (1997).

[100] S. R. White and D. J. Scalapino, *Ground-state properties of the doped three-leg $t-J$ ladder*, Phys. Rev. B **57**, 3031 (1998).

[101] C. Kübert and A. Muramatsu, *Fermions in an antiferromagnet with generalized berry phases*, Phys. Rev. B **47**, 787 (1993).

[102] C. Kübert and A. Muramatsu, Int. J. Mod. Phys. B **28**, 3807 (1996).

[103] A. E. Sikkema, I. Affleck, and S. R. White, *Spin gap in a doped kondo chain*, Phys. Rev. Lett. **79**, 929 (1997).

[104] P. Pieri, *Un contributo allo studio del magnetismo nei sistemi fortemente correlati*, PhD thesis, Univeristy of Bologna, Italy, 1996.

[105] A. Angelucci and G. Jug, Int. Jour. Mod. Phys B **3**, 1069 (1989).

[106] M. D. Stasio *et al.*, *Effective action and adiabatic expansion for the 1-D and 2-D Hubbard models at half filling*, Int. Jour. Mod. Phys B **3**, 1391 (1994).

[107] A. Auerbach, *Interacting Electrons and Quantum Magnetism* (Springer-Verlag, 1994).

[108] T. Dombre and N. Read, Phys. Rev. B **38**, 7181 (1988).

[109] S. R. White and D. A. Huse, Phys. Rev. B **48**, 3844 (1993).

[110] L. C. Venuti, Antiferromagneti quantistici a basse dimensioni, Master's thesis, Università di Bologna, 1997.

[111] U. Schollwöck, O. Golinelli, and T. Jolicoeur, *S=2 antiferromagnetic quantum spin chain*, Phys. Rev. B **54**, 4038 (1996).

[112] G. Xu *et al.*, *Holes in a quantum spin liquid*, Science **289**, 419 (2000).

[113] S. Kobayashi and K. Nomizu, *Foundation of differential geometry, vol II* (Interscience, New York, 1969).

[114] E. Fradkin, *Field Theories of Condensed Matter Systems* (Addison Wesley, 1991).

[115] A. D'Adda, M. Lüscher, and P. D. Vecchia, Nucl. Phys. B **146**, 63.

[116] A. D'Adda, M. Lüscher, and P. D. Vecchia, Nucl. Phys. B **152**, 125.

[117] X. G. Wen, *Effective lagrangian for holes in the spin-liquid state*, Phys. Rev. B **39**, 7223 (1989).

[118] B. I. Shraiman and E. D. Siggia, *Mobile vacancies in a quantum heisenberg antiferromagnet*, Phys. Rev. Lett. **61**, 467 (1988).

[119] B. I. Shraiman and E. D. Siggia, *Mobile vacancies in a quantum antiferromagnet: Effective hamiltonian*, Phys. Rev. B **42**, 2485 (1990).

[120] G. Sierra, J. Phys. A: Math. Gen **29**, 3299 (1996).

[121] A. Hutter, Spin-gap in quasi-eindimensionalen kupraten, Master's thesis, Univeristy of Stuttgart, 1999.

[122] A. M. Tsvelik, *Semiclassical solution of one dimensional model of kondo insulator*, Phys. Rev. Lett. **72**, 1048 (1994).

[123] A. B. Zamolodchikov and A. B. Zamolodchikov, Ann. Phys. **120**, 253 (1979).

[124] S. Katano, T. Nagata, J. Akimitsu, M. Nishi, and K. Kakurai, Phys. Rev. Lett. **82**, 636 (1999).

[125] H. Tsunetsugu, M. Troyer, and T. M. Rice, Phys. Rev. B **49**, 16078 (1994).

[126] M. Troyer, H. Tsunetsugu, and T. M. Rice, *Properties of lightly doped $t-J$ two-leg ladders*, Phys. Rev. B **53**, 251 (1996).

[127] M. Sigrist, T. M. Rice, and F. C. Zhang, Phys. Rev. B **49**, 12058 (1994).

[128] Y. L. Lee, Y. W. Lee, and C.-Y. Mou, Phys. Rev. B **60**, 13418 (1999).

[129] S. Chakravarty, B. I. Halperin, and D. R. Nelson, Phys. Rev. Lett. **60**, 1057 (1988).

[130] A. Muramatsu and R. Zeyher, Nucl. Phys. B **346**, 387 (1990).

[131] M. Veltman, Nucl. Phys. B **319**, 253 (1989).

[132] T. Takahashi *et al.*, Phys. Rev. B **56**, 7870 (1997).

[133] N. Nücker, J. Fink, J. C. Fuggle, P. J. Durham, and W. M. Temmerman, Phys. Rev. B **37**, 5158 (1988).

[134] R. R. P. Singh *et al.*, Phys. Rev. Lett. **62**, 2736 (1989).

[135] M. S. Hybersten, M. Schlüter, and N. E. Christensen, Phys. Rev. B **39**, 9028 (1989).

[136] J. Oitmaa, C. J. Hamer, and Z. Weihong, Phys. Rev. B **60**, 16364 (1999).

[137] M. Brunner, S. Capponi, F. F. Assaad, and A. Muramatsu, *Single hole dynamics in the $t-J$ model on two- and three-leg ladders*, Phys. Rev. B **63**, R180511 (2001).

[138] E. Brezin and J. Zinn-Justin, Phys. Rev. B **14**, 3110 (1976).

[139] S. Gopalan, T. M. Rice, and M. Sigrist, Phys. Rev. B **49**, 8901 (1994).

[140] M. Reigrotzki, H. Tsunetsugu, and T. M. Rice, J. Phys.: Condens. Matter **6**, 9235 (1994).

[141] J. Voit, Phys. Rev. B **47**, 6740 (1993).

[142] V. Meden and K. Schönhammer, Phys. Rev. B **46**, 15753 (1992).

[143] H. J. Schulz, *Metal-insulator transition in the two-chain model of correlated fermions*, Phys. Rev. B **59**, R2471 (1999).

[144] M. Fabrizio, Phys. Rev. B **48**, 15838 (1993).

[145] H. J. Schulz, Phys. Rev. B **53**, R2959 (1996).

[146] L. Balents and M. P. A. Fisher, Phys. Rev. B **53**, 12133 (1996).

[147] V. A. Kashurnikov, N. V. Prokof'ev, B. V. Svistunov, and M. Troyer, Phys. Rev. B **59**, 1162 (1999).

[148] A. M. Polyakov, *Gauge Fields and Strings* (Harwood Academic Publisher, 1987).

Curriculum Vitae

Personal Details

Surname:	Campos Venuti
First name:	Lorenzo
Nationality:	Italian
Date of Birth:	April 15$^{\text{th}}$, 1972
Place of Birth:	Bologna, Italy
Marital status:	Unmarried
Military service:	Exemption from military service due to civil service at the *Sovraintendenza ai Beni Culturali di Bologna*

Education

1978-1983	Primary school *Scuola Elementare Statale "G. Pascoli"*, Bologna
1983-1986	Middle school *Scuola Media Statale "G. Carducci"*, Bologna
1986-1991	Secondary school *Liceo Scientifico Statale "A. B. Sabin"*, Bologna
1991-1998	Università di Bologna,Corso di Laurea in Fisica, Bologna
1995-1996	Univesity College Dublin, Dublin, Ireland. Seven month within the Erasmus Project. Reference professor. Prof. J. Pulè
1999-2003	PhD work at Universität Stuttgart with title *Spin gap in doped ladder system* Supervisors: Prof. Dr A. Muramatsu and Prof. Dr. G. Mahler